January 2015

Synchrophasor Technology And Applications: Benefits Over Conventional Measurements

Andrew Michael Berg

SYNCHROPHASOR TECHNOLOGY AND APPLICATIONS: BENEFITS OVER CONVENTIONAL MEASUREMENTS

by

Andrew Berg
Bachelor of Science, South Dakota School of Mines and Technology, 2010

A Thesis

Submitted to the Graduate Faculty

of the

University of North Dakota

In partial fulfillment of the requirements

for the degree of

Master of Science

Grand Forks, North Dakota

May
2015

This thesis, submitted by Andrew Berg in partial fulfillment of the requirements for the Degree of Master of Science from the University of North Dakota, has been read by the Faculty Advisory Committee under whom the work has been done and is hereby approved.

Hossein Salehfar, Ph.D., Chairperson

Prakash Ranganathan, Ph.D.

Michael Mann, Ph.D.

Arash Nejadpak, Ph.D.

This thesis is being submitted by the appointed advisory committee as having met all of the requirements of the School of Graduate Studies at the University of North Dakota and is hereby approved.

Dr. Wayne Swisher
Dean of the School of Graduate Studies

May 7, 2015
Date

PERMISSION

Title: Synchrophasor Technology and Applications: Benefits over Conventional Measurements

Department: Electrical Engineering

Degree: Master of Science

In presenting this thesis in partial fulfillment of the requirements for a graduate degree from the University of North Dakota, I agree that the library of this University shall make it freely available for inspection. I further agree that permission for extensive copying for scholarly purposes may be granted by the professor who supervised my thesis work or, in his absence, by the Chairperson of the department or the dean of the School of Graduate Studies. It is understood that any copying or publication or other use of this thesis or part thereof for financial gain shall not be allowed without my written permission. It is also understood that due recognition shall be given to me and the University of North Dakota in any scholarly use which may be made of any material in my thesis.

Andrew Berg

May 2015

TABLE OF CONTENTS

LIST OF FIGURES

LIST OF ACRONYMS

Acronym	Definition of the Acronym
AGC	Automatic Generation Control
ATVE	Alternative Total Vector Error
CEII	Critical Energy Infrastructure Information
CRC	Cyclic Redundancy Checking
CT	Current Transformer
DER	Distributed Energy Resources
DSP	Digital Signal Processing
EMS	Energy Management System
FERC	Federal Electric Regulatory Commission
FFT	Fast Fourier Transform
GPA	Grid Protection Alliance
GPS	Global Positioning System
IED	Intelligent Electronic Device
IEEE	Institute of Electrical and Electronic Engineers
LAN	Local Area Network
NERC	North American Electric Reliability Corporation
PDC	Phasor Data Concentrator
PMU	Phasor Measurement Unit
PT	Potential Transformer
ROCOF	Rate of Change of Frequency
RTU	Remote Terminal Unit

SCADA.....Supervisory Control and Data Acquisition

SEL .....Schweitzer Engineering Laboratories

TCP .....Transmission Control Protocol

TVE.....Total Vector Error

UART.....Universal Asynchronous Receiver/Transmitter

USB.....Universal Serial Bus

VT .....Voltage Transformer

WAMS .....Wide-Area Monitoring System

ABSTRACT

The purpose of this thesis is to investigate the benefits of synchrophasor technology in bulk power system measurements. To accomplish this task, multiple methods of investigation and analysis have been conducted. First, a better understanding of the synchrophasor power measurement systems was achieved through a literature review. The review provided some perspective on the differences between these systems and the conventional systems of power measurements.

Then, some utility grade data was acquired and analyzed. In this process, there were some aspects of confidentiality, and that required an added layer of discretion. However, the process made it possible to analyze a variety of authentic measurements from the power system. This analysis provides novelty to the utility industry, but the experience of physical implementation wasn't available through this process. Finally, efforts were directed toward a physical demonstration of a synchrophasor measurement system. A test bed system was configured, and measurements were obtained from the system through phasor measurement units (PMUs). In an attempt to extent this demonstration effort, simulation options were investigated as well. Unfortunately, there are some limitations with the available equipment. Overall, this provided novelty to academia through a physical implementation of this technology. With changing demand, transmission, desires for efficiency, and an evolving generation fleet, extensive grid knowledge is important for maintaining a reliable power system.

CHAPTER I

INTRODUCTION

In recent years, the complexity of the electric power system has increased due to changing load characteristics (e.g. total demand and demand peaks), limited transmission paths, reliability and security improvement, efficiency concerns (e.g. optimal use of aging assets), renewable generation integration, emission reductions, and varying types of other distributed generation resources (DERs) [1][9]. These complex variables require better monitoring and system awareness of the electric power grid. The use of synchrophasors provides the ability to measure phase angles with absolute time references, and this characteristic presents a potential solution for improving system monitoring and awareness [10].

The purpose of this introduction is to describe the concept, infrastructure, and operation of synchrophasor technology in comparison to the conventional power measurement scheme. The conventional power measurement scheme utilizes technology that has performed well for the life of our electrical power grid. However, as reliability, efficiency, and economics have become more dynamic in the electric power system, sophisticated grid monitoring and awareness have become vital needs. The system for monitoring the grid over large regions, also known as the wide area monitoring system (WAMS), can be improved with the use of new technologies. This is shown conceptually in Figure 1. Synchrophasors provide the ability to measure

phase angles with absolute time references, and this characteristic presents a potential solution for improving system dynamics for quick and accurate grid monitoring.

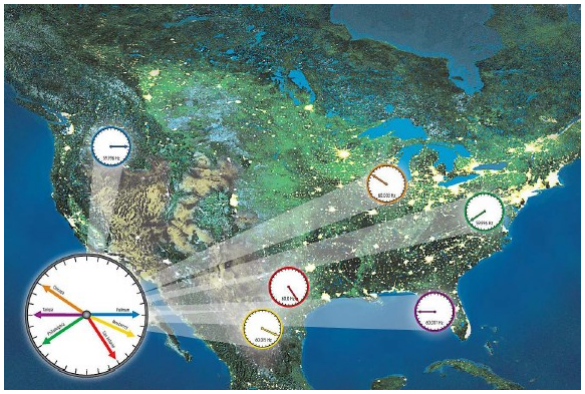

Figure 1. Conceptual Wide Area Monitoring System using Synchrophasors [10].

Measurement Concepts Defined

Conventional power measurements can gather information on bus voltages, transmission line current flows, energy outputs at generation interconnections, line loads, and general interconnection status information [11]. Although the conventional power measurement methods have been effective, the information that the technology provides is limited. The data comes in at an interval of 2-10 seconds per scan, and it relies heavily on calculations that correspond to the information [5]. For example, stress on transmission lines due to changing resources and load are hard to monitor with conventional power measurements. These events can only be monitored through calculations using assumptions about the system's characteristics. Generally, estimates are computationally intensive over large areas, and assumptions can be unreliable.

New power measurements usually imply the use of synchrophasor data from phasor measurement units (PMUs). A synchrophasor is a phasor measurement with respect to an absolute time reference. With this measurement, we can determine the

absolute phase relationship between phase quantities at different locations on the power system [10]. Therefore, the addition of PMUs introduces the dynamic of phase angle measurements with absolute time references. The data comes in at a rate of 60 scans per second, and it relieves some dependence on calculations [5]. For example, stress on transmission lines due to changing resources and load are improved with the phase shift on the lines. These events can be monitored with synchrophasor measurements because of the reactive component derived from the phasors. This is shown conceptually in Figure 2. This alleviates the systems reliance on computationally intensive action and system assumptions that may become unreliable.

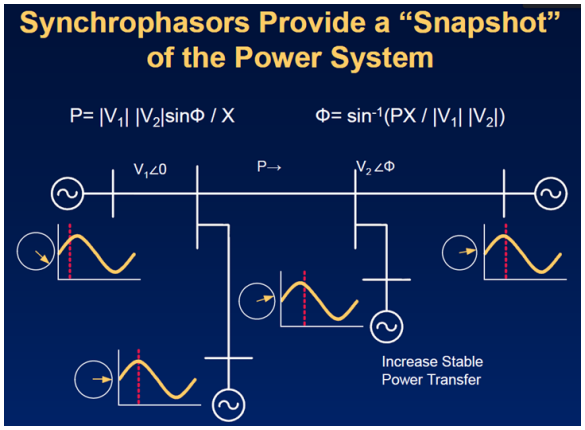

Figure 2. Conceptual Synchrophasor Measurement on a Transmission Line [10].

In order to understand the difference between conventional power measurement and synchrophasor measurement, the differences in concept should be identified [9].

- Conventional Power Measurements:
  - Non-Synchronous
  - Slower Sample Rates
    - 1 scan per 2-10 seconds
  - Intermittently Streamed
- Synchrophasor Power Measurements:
  - Time-Synchronous
  - Faster Sample Rates
    - 60 scans per second
  - Continuously Streamed

In Figure 3, the typical accuracies with synchrophasor measurements are shown [1]. It specifically refers to timestamp, angle, current transformer (CT), and voltage transformer accuracies (VT). VTs are also referred to as potential transformers (PTs).

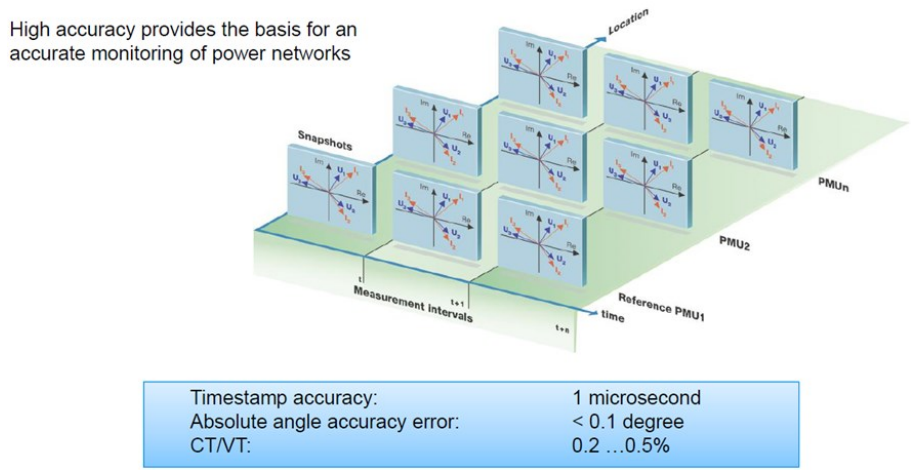

Figure 3. The Concept of Synchrophasor Measurements over Time and Distance [1].

In addition to the differences in the measurement concepts, the actual data obtained from the different measurement types should also be identified [9][11].

- Conventional Power Measurements:
  - Bus Voltage [Real]
  - Line Current [Real]
  - Frequency
  - Line Loading [Real]
  - Status Information
- Synchrophasor Power Measurements:
  - Bus Voltage [Phasor]
  - Line Current [Phasor]
  - Frequency and df/dt
  - Line Loading [Phasor]
  - Status Information

The primary feature of synchrophasor measurement that gives the system increased performance is the measurement of reactive power characteristics. The reactive components of the power system can be inferred by the phasor combinations across certain parts of the grid infrastructure. In a simple power calculation, the following information could be obtained directly from the measurements [4].

$$P = \frac{|V_1||V_2| \sin \Phi}{X} \quad \Longrightarrow \quad \Phi = \sin^{-1}\left(\frac{PX}{|V_1||V_2|}\right) \quad \{V_1, V_2, and\ \Phi\ are\ measured\}$$

$Where$:

$P = Line\ Flow$ $\qquad$ $\Phi = Phase\ Difference\ Across\ the\ line$

$V_1 = Votage\ Magnitude\ at\ One\ End$ $\quad$ $V_2 = Votage\ Magnitude\ at\ Other\ End$

$X = Line\ Reactance$

The problem with this calculation is that the line impedance is still a predetermined parameter. The characteristic is relative to the power loss, but it simply will require some prior knowledge of the system such as transmission line impedance ($resistance, etc$ ...), length, and other integrated elements.

Measurement Infrastructure Types Described

In Figure 4, the conventional power measurement system topology referred to in this report is shown. As shown in Figure 4, this system is driven by remote terminal units (RTUs) and intelligent electrical devices (IEDs) such as real-time protection relays [2].

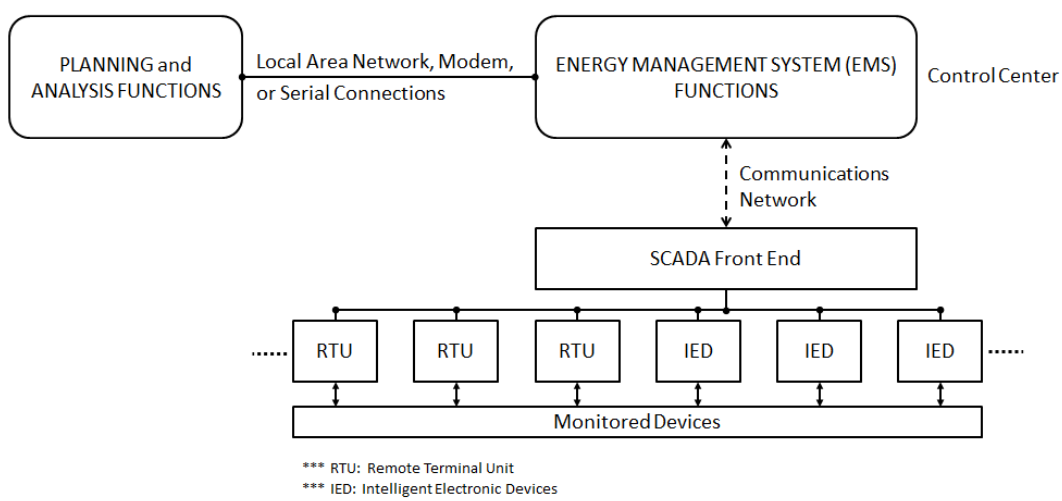

Figure 4. Conventional Power Measurement System Topology [2].

In Figure 5, the new power measurement system topology referred to in this report is shown. In addition to the conventional measurement units, it is driven by the use of PMUs.

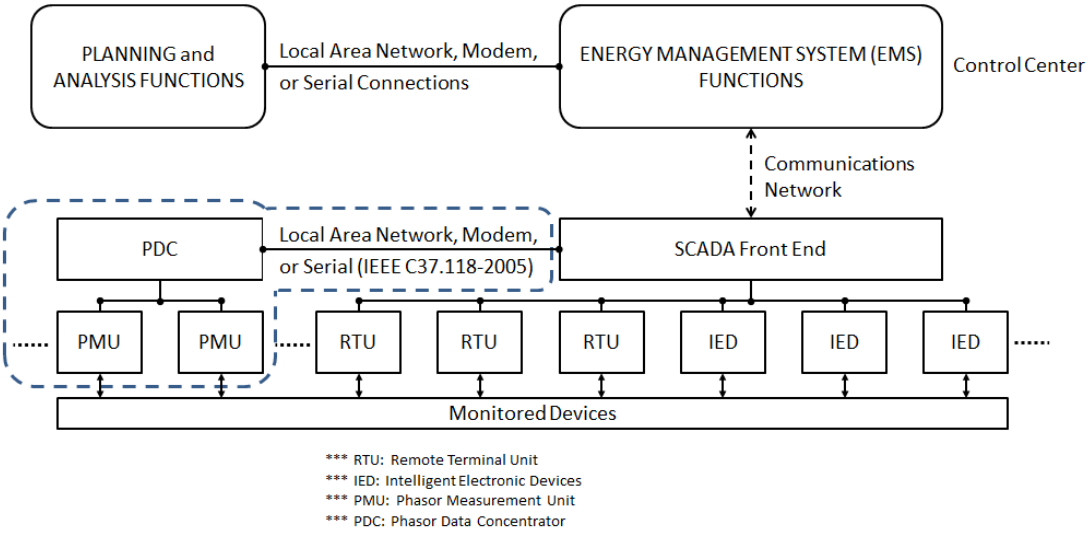

Figure 5. Power Measurement System Topology Utilizing Synchrophasor Technology [2].

Now that the components involved and the corresponding schematics have been identified, it's necessary to understand the operation of each system type.

Measurement Operations Described

The primary destination for the measurement information is the energy management system (EMS), also referred to as the control center. There may be more than one EMS involved in the system, but the same data is being utilized at each level of these control centers. Before this data arrives at the EMS, the data makes a stop at the supervisory control and data acquisition (SCADA) system. The operation for the conventional power measurement system involves the following steps [4][11].

- Conventional power measurement systems have been monitored by:
    - Relays that operate as RTUs connected to the grid
        - Control operation and interconnection
    - Data is sent using the IEC60870-5 (-101) standard
        - A standard in remote terminal measurement protocol
        - Transmitted over modem, serial, or local area networks (LAN)
    - The transmission medium used is Transmission Control Protocol (TCP)
        - Protects against any invading packets on LAN
    - The data is archived for situational awareness at the SCADA system

The operation for the synchrophasor measurement system involves the following steps in addition to the conventional power measurement operation [9][10].

- Synchrophasor power measurement systems have been monitored by:
    - Relays that operate as PMUs connected to the grid
        - Control operation and interconnection
        - Measurements are attached to synchronized timestamps
        - Timestamps are synchronized by global positioning systems (GPS)
    - Data is sent using the IEEE C37.118 (-2005) standard
        - A standard in synchrophasor measurement protocol
        - Transmitted over modem, serial, or local area networks (LAN)
    - The transmission medium used is Transmission Control Protocol (TCP)
        - Protects against any invading packets on LAN
    - The data collection site is a phasor data concentrator (PDC)
        - Time-aligns the data according to the GPS timestamps

- Compensates for communication and processing latencies

o PDC data is archived for situational awareness at the SCADA system

The first difference in these two processes is the addition of a GPS timestamp that is time-synchronized to the relay measurement. This is particularly important to the PMU measurement. This characteristic is very important to the concept of the synchrophasor measurement system and the phasor data gained from its use. However, with the conventional measurement system, the timestamp is not a vital characteristic to monitoring magnitudes without phase measurements. The measurements of frequency response and phase are the only areas that it makes a considerable impact.

In Figure 6, the active role of GPS in synchrophasor technology is illustrated. It clearly displays the concept of how the GPS satellite would transmit synchronized timestamps to nearby receivers for PMUs acting on a transmission line (related by positions A and B).

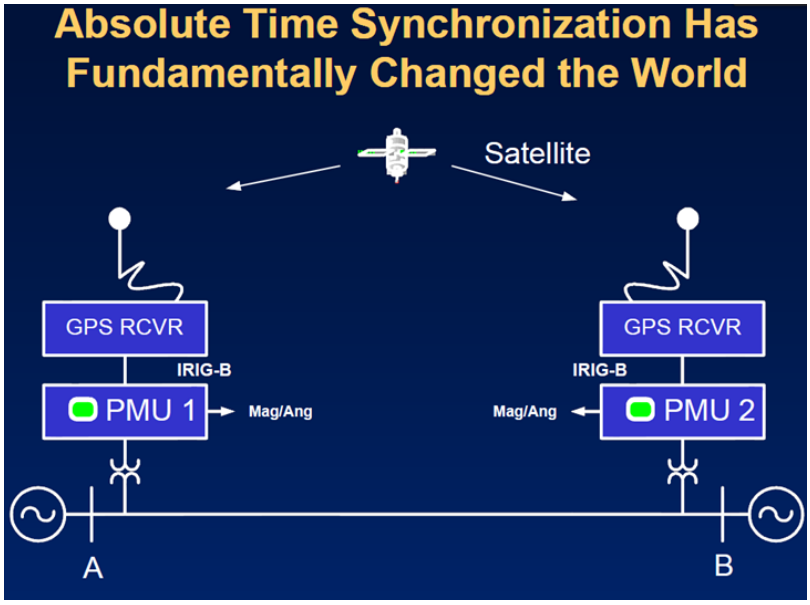

Figure 6. GPS Role in Utilizing Synchrophasor Technology [10].

In Figure 7, the same concept is being illustrated, but it integrates one more step of the time-synchronization process. After each PMU receives its GPS timestamp and connects it to a phasor measurement, the information is sent onto a phasor data concentrator (PDC) to be aligned with its counterparts from other PMUs [9]. The image shows the GPS communication with each PMU (which is equipped with the GPS signal receiver), as well as the transmission of the timestamp/measurement information to the PDC for alignment.

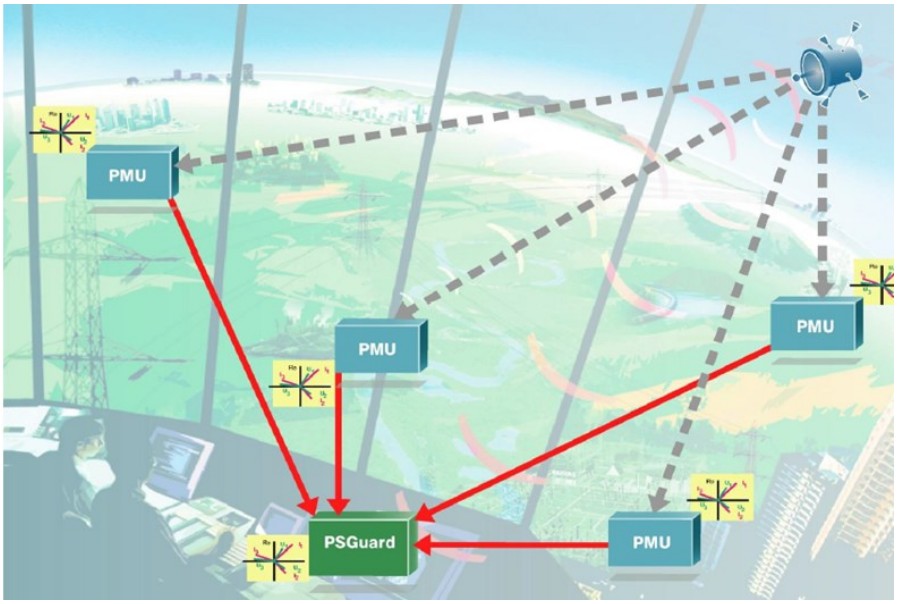

Figure 7. World View of the GPS Role in Utilizing Synchrophasors [1].

The transmission of information between the PMU and PDC units can be analyzed further. In the communication scheme for synchrophasors, the IEEE C37.118 protocol is utilized. In this communication scheme, the data is referenced to as frames. The frames are defined by the following [8].

- Command Frame: Structured, Binary Format
    - Communicates the start and stop commands to and from the PDC
- Header Frame: Unstructured ASCII text
    - Communicates comments or other information
- Configuration Frame #1: Structured, Binary Format
    - Communicates the constant parameters of the PMU configuration
- Configuration Frame #2: Structured, Binary Format
    - Communicates the variable parameters of the PMU configuration
        - A changing number of phasors would fall under this category
- Data Frame: Structured, Binary Format
    - Communicates the real-time PMU phasor data
        - Magnitude, phase angle, frequency, and analog/digital system data

This communication scheme and the flow of these frames are illustrated in Figure 8.

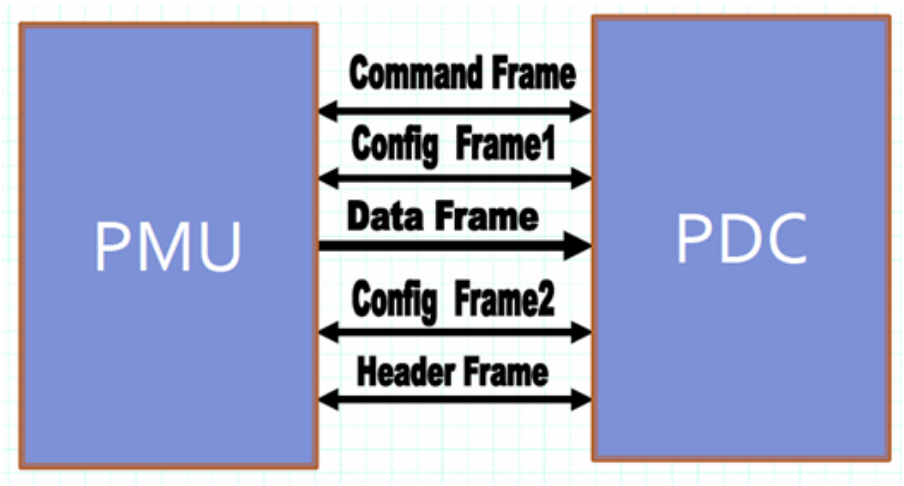

Figure 8. Communication Protocol between a PMU and the PDC [8].

The operating structure that is presented in the IEEE C37.118 protocol also covers the data communication beyond the PDC. To be more specific, it calls for the alignment and communication of the gathered data to the rest of the system. The PDC sends this data to the supervisory control and data acquisition (SCADA) system. The proper format for the information needs to include the header information for each data transmission, the status of each PMU, the phasor data (magnitude and phase angle), the frequency status, the rate of change for that frequency, and any analog/digital system data that coincides with each measurement. With each transmission of data, the communication needs to reflect each PMU within the PDC collection territory as well [8].

In Figure 9, the data structure of the communication between a PDC and the SCADA system is depicted [8]. The last frame is for cyclic redundancy checking.

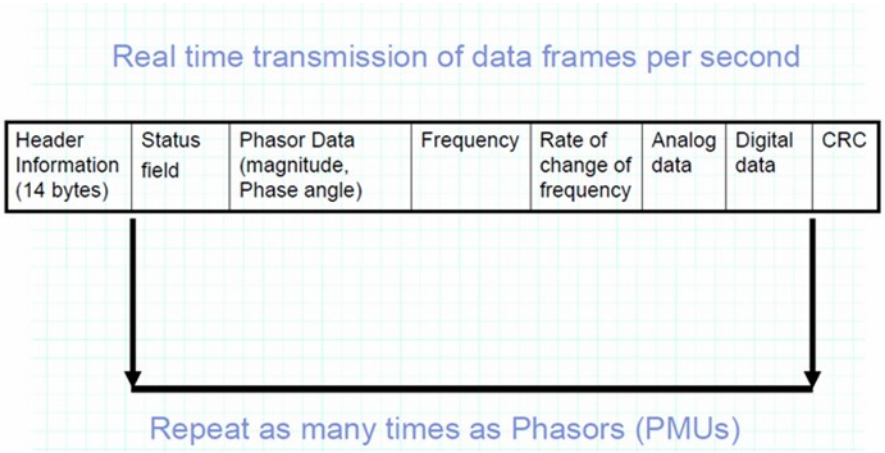

Figure 9. Communication Protocol between a PDC and the SCADA System [8].

In comparison to the conventional power measurement protocol, there is not a large amount of difference. Conventional power measurement uses the IEC60870-5 protocol for transmitting RTU data to the SCADA system. As Figure 10 suggests, the

start and stop frames closely relate to the command and header frames from the IEEE C37.118 protocol. The data unit identifier is very similar to the configuration frames as well. And finally, the information objects of the IEC60870-5 protocol are closely related to the data frame of the IEEE C37.118 protocol. This is all a general reference to the inner workings of each data protocol, but the similarities and differences are truly defined by the way that these binary and text based communications are utilized [8][13].

IEC 101 Frame Format, Variable length		
Data unit	**Name**	**Function**
Start Frame	Start Character	*Indicates start of Frame*
	Length Field (*2)	*Total length of Frame*
	Start Character (repeat)	*Repeat provided for reliability*
	Control Field	*Indicates control functions like message direction*
	Link Address (*0,1 or 2*)	*Normally used as the device / station address*
Data Unit Identifier	Type Identifier	*Defines the data type which contains specific format of information objects*
	Variable Structure Qualifier	*Indicates whether type contains multiple information objects or not*
	COT (*1 or 2*)	*Indicates causes of data transmissions like spontaneous or cyclic*
	ASDU Address (*1 or 2*)	*Denotes separate segments and its address inside a device*
Information Object	Information Object Address (*1 or 2 or 3*)	*Provides address of the information object element*
	Information Elements (n)	*Contains details of the information element depending on the type*
Information Object-2	-----	
-----	-----	
Information Object-m		
Stop Frame	Checksum	*Used for Error checks*
	Stop Char	*Indicates end of a frame*

Figure 10. Communication Protocol between a RTU and the SCADA System [13].

In Figure 11, the overall hierarchy of the synchrophasor power measurement operation is shown. The added details in this diagram emphasize the addition of security gateways and the visualization of phasor data at the EMS and SCADA system level [10]. In Figure 12, another version of the synchrophasor power measurement operation is shown. The details in this diagram emphasize the use of the IEEE C37.118 protocol and alternate connection schemes for the EMS and SCADA system [1].

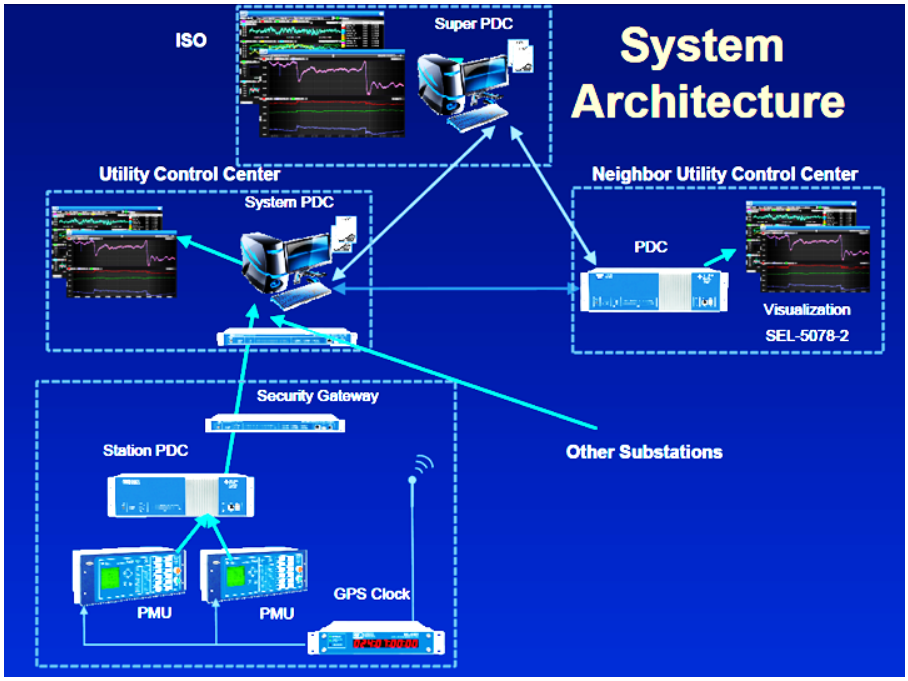

Figure 11. Synchrophasor Power Measurement System Architecture [10].

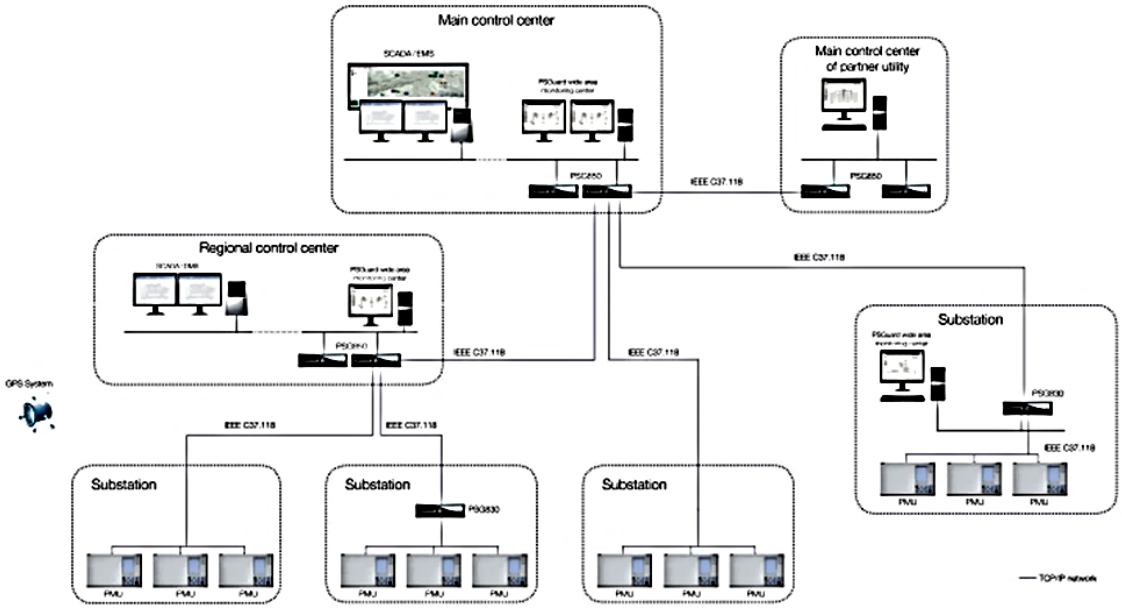

Figure 12. Another Form of the Synchrophasor Architecture [1].

Limitations of Previous Research

The concept of synchrophasors was first put into motion in the early 1990s. The earliest PMU prototype was built at Virginia Tech, and a company called Macrodyne was credited with the first industry grade product in 1992 [12]. In the first ten years of the technology's existence, there was limited circulation of the measurement system. However, with major grid events like that of the Northeast blackout of 2003, the technology has become more popular in response to reliability concerns. Synchrophasor technology has been perceived as a solution for better wide area monitoring and system awareness. Taking that into consideration, this technology has been truly utilized for around ten years. Even with higher circulation of synchrophasor devices, they have been used in limited capacity. The reasons vary, but it is primarily due to the difficulties of implementation, financial viability, and continued reliability and security concerns within associated transitions.

In recent history, two things have changed. First, the technology has improved and has become more affordable as a result of the progress made in semiconductor design. Second, the initiatives of different regulatory authorities have aided the penetration of synchrophasor devices into the power industry. As the technology has improved and become more affordable, it appears to have found a more prevalent existence in some areas of the electric power system. Now that the devices are installed in higher numbers, the new task is proper utilization. That aspect poses some challenges in state estimator design and visualization. Industry professionals are working toward this goal, but development is difficult to achieve with the limited

workforce available. The academic community can provide valuable assistance in this area, but there are some new difficulties in that process as well.

In the electric power industry, there are many concerns with the security of the electric power system. Those concerns relate to the engineering, vulnerability, and detailed design information pertaining to the infrastructure used to support reliable power delivery. Any information under that description is referred to as Critical Energy Infrastructure Information (CEII). The industry has identified that there are instances in which this information could be used to coordinate a malicious attack on the electric power system. In response to that risk, new regulations have come to fruition. As a result, the utilities have less flexibility in sharing data. To enter into a cooperative research effort, utilities are forced to establish non-disclosure agreements and other protective measures with whom they agree to provide sensitive information. It is a level of protection that is usually hard to coordinate, but it is the only way to truly evaluate the usefulness of synchrophasor data to the system that it is monitoring. An academic researcher could use other measurement methods that are developed independent of the utility, but those will be limited by the technology available, as well as the system representation that is monitoring.

The Current Study

Although there are industry professionals working in this area, their availability is limited by other obligations. There are also cooperative agreements in some academic settings, but they are limited in number and their level of development.

Synchrophasor technology is beginning to overtake the conventional measurement devices, but there are many utilities that still operate under the

conventional measurement schemes. With research arrangements, like that used in this thesis, academic studies can further the use of synchrophasor data in state estimation schemes and visualization. The research arrangements used in this thesis are described in Chapter II. The only way to encourage the adoption of synchrophasor data into state estimation and visualization is by presenting benefits in clear and concise manner. By analyzing and categorizing the benefits available through this technology, it is much more likely to get utilities invested in synchrophasor technologies.

CHAPTER II

DATA ANALYSIS

In the conventional measurement schemes, state estimation is dependent on magnitude measurements, power metering, low resolution data, and physical estimates of grid facilities, such as transmission lines. The bulk electric power system is composed of 211,000 miles of transmission and over 10,000 power plants. It is not difficult to see that physical estimates of this expansive system can dramatically impact the accuracy of system monitoring. Data analysis, simulation, and mathematical concepts are all potential methods for evaluation, but in this research, data analysis and mathematical concepts will be the primary methods. Measures for the evaluation may involve: 1) frequency response, 2) error measurements, and 3) interference identification. All of these measurements have been explored. In the Fourier analysis performed, it has been found that frequency can be directly linked to fault events. Also, the total vector error (TVE) of the synchrophasor data with respect to the conventional state estimations is near the compliant level of 1% for sufficient error tolerance. Although this is not a complete success, it does suggest that a synchrophasor-based state estimator scheme may very well support the compliance of the data. If the state estimator was supported by the high-resolution phasor measurements, this would conceivably satisfy the goals set forth by industry standards. Lastly, interference from storm conditions has also been analyzed, and some significant voltage disturbances

were observed. These quick, detailed grid measurements could alleviate issues that have resulted from growing power system complexity. Synchrophasor technology has real potential for wide-area monitoring and system awareness.

Data Masking and Narrative for Analysis

In order to perform data analysis that benefits the bulk power system, some synchrophasor data (PMU data) and complementary conventional data (RTU data and SCADA calculations) is required. Due to a number of factors, this was a difficult task in this research.

Measurements that represent the bulk power system are not readily available to the common researcher. The electric power system is extremely large in its scale, and that complexity is difficult to conceptualize in simple demonstration efforts. The construction of the bulk power system is an ongoing process that is shared among the numerous transmission owners, generation owners, and load serving entities that oversee their respective infrastructure. Building a system prototype is a staggering task for any individual person or group of persons. An authentic measurement of the electric power system is the best approach to making an evaluation. Representative systems are being built in many research settings, but this requires some high level understanding of the representative system and its limitations compared to the full-scale power system.

Additionally, the recovery of bulk power system measurements requires some high levels of access. The bulk power system is regulated by many compliance standards, and these compliance standards are developed to protect the reliability, security, and economic standing of the bulk power system. In response to these

regulations, utilities and other entities within the system are held to certain standards for personnel, knowledge, facilities, programs, and other qualifications to carry out important responsibilities. One specific part of those responsibilities involves the confidentiality of vital information.

Critical energy information infrastructure (CEII) has been a large topic of the Federal Energy Regulatory Commission (FERC) and North American Energy Reliability Corporation (NERC) throughout the past 15 years. This topic has been investigated, and policies have been written to protect information that describes the bulk power system. In most cases, power system information is subject to non-disclosure agreements that are established between participating entities. This provides some security to the bulk power system and its customers, but it adds a layer of difficulty to the research efforts that are needed for technological advancement. The individuals that have access to the information are extremely qualified in the tasks of advancing technology, but the regular tasks of operation, planning, and reliability force limitations on their resources and time. In the area of academics, researchers have the potential to aid in this task, but the regulated access creates a profound limitation.

To solve this problem, a form of representative data was created. To do this, some fields of data were masked by an anonymous entity. Real measurements were assigned a random name and timestamp that were not associated with the point of measurement or measurement timeframe, respectively. In essence, some real plot points were provided, but the data was not attributed to a real location or time. This pseudonym and non-representative timestamp has little impact to the functional analytics being performed, but it opens the opportunity for outside entities to evaluate

and report of the functionality of one data type versus the other (PMU data versus RTU data).

Using this information, some data analysis and mathematical concepts were used. The results are mathematically sound, but the information remains protected.

Benefits of High-Resolution Synchrophasor Data

To capture the general comparison between synchrophasor data and conventional measurement data, the following plots were constructed. Since the resolution of synchrophasor data is substantially higher that conventional measurement, the conventional measurement trend displays a flatter, stair-step type of trend in comparison to the synchrophasor data. This can be observed in Figure 13. From the plot shown, a couple of characteristics shine through. The fact that synchrophasor data provides higher resolution is clearly shown. As a result, the higher resolution provides transient information that conventional measurements cannot provide.

With the availability of high-resolution frequency data, relevant functions for this information simply become faster and more detailed. In the bulk power system, the frequency is highly important to reliability. Off-nominal frequency can impact system operations and market efficiency [6].

There are four primary ways in which off-nominal frequency can negatively affect the system. It could damage equipment that serves the electric power system, including generation, transmission, transformation, protection devices, and customer loads. It could also degrade the quality of the power delivered. That can cause load devices to malfunction or perform in an unsatisfactory manner. In very extreme cases, off-nominal frequency could lead to a power system collapse. This is usually an event

that is caused by a combination of equipment failure and protective system triggering. And finally, it could result in overloading transmission lines as various generators try to restore system frequency for market efficiency [6].

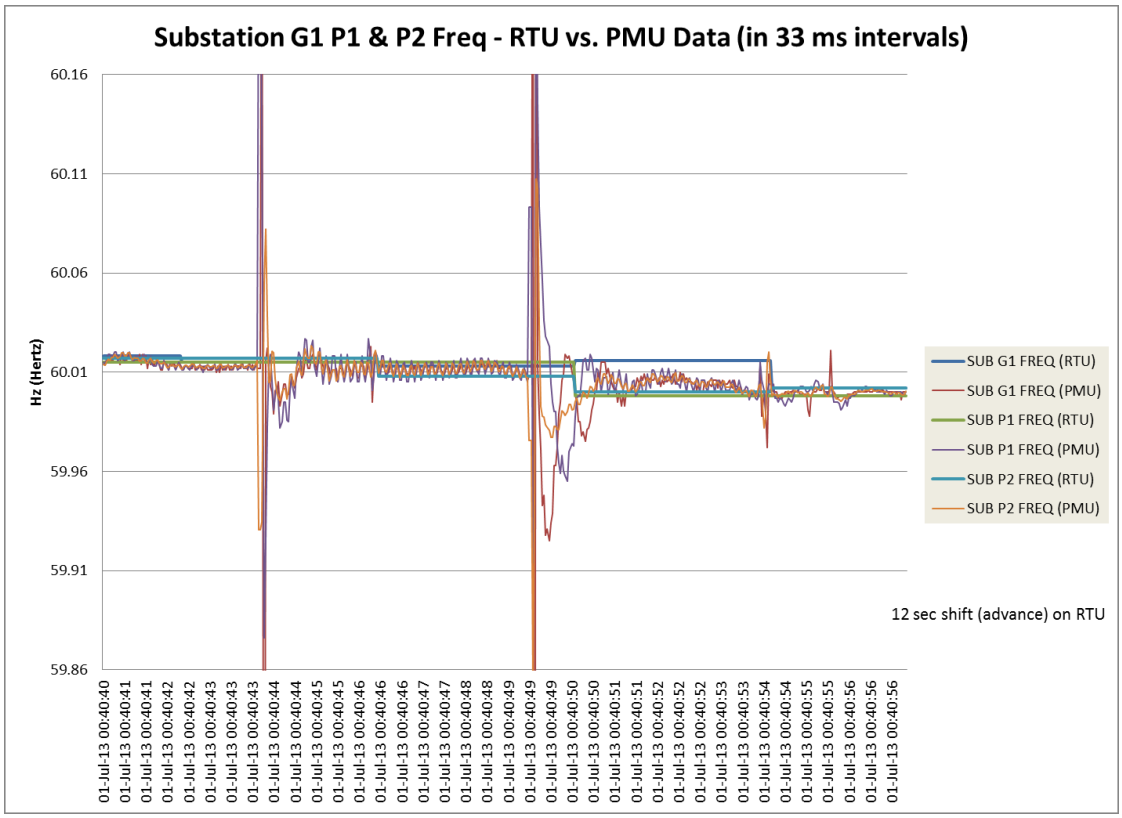

Figure 13. Conventional (RTU) Frequency Data versus Synchrophasor (PMU) Frequency Data.

These scenarios can happen individually or in conjunction with each other. For example, there can be a significant generator outage that creates difficulties in all of these areas. Assuming a substantial generator outage occurs for a few generators during an ice storm. If the storm damages a couple of facilities that are vital to a small fleet, that takes out some vital generation to the area. Also, wind farms may be limited due to the direct impact of icing. As a result, the area experiences a large generation

deficit, and in turn, the system frequency drops below nominal. Assuming that the temperatures are that low, customer heating loads may be high, and that exacerbates the deficit further. With that issue, the power quality is likely to see some degradation [6].

To correct the loss of generation, neighboring sources are dispatched up. The issue that may result from this mitigation relates to transmission capacity. The transmission has limits, and the increased dispatch of neighboring generation can cause overloads under specific contingencies. That can cause protection equipment to trip, or even failures due to unforeseen contingencies or equipment malfunction. If facilities are lost, the events could exacerbate the overall system imbalance. This could result in significant damage, poor load service, system collapse, and market instability [6].

Criteria have been developed for off-nominal frequency deviations for generators and transformers. In Figure 14, IEC 34-1 Voltage-Frequency limits are shown. During system intact operation, frequency may vary between 58.8 and 61.2 Hz for a 60 Hz system (voltage between 0.95 and 1.05 per unit). During contingencies, frequency may vary between 57 and 61.8 Hz (voltage between 0.92 and 1.08 per unit). In addition to the IEC 34-1 limits, a general plot for frequency response is shown [6].

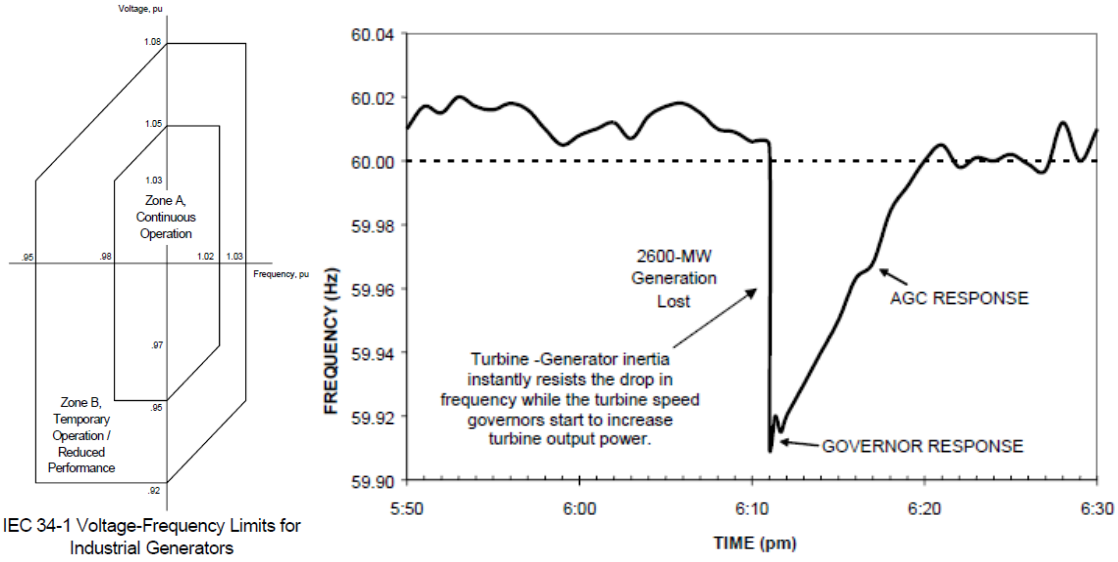

Figure 14. IEC 34-1 Voltage-Frequency Limits / General Frequency Response for an Event [6].

To further describe the three stages of frequency response, the continuum of frequency actions are shown in Figure 15. As shown in Figure 15, the green area on the right describes normal conditions, and this would correspond to the inertia response of the system (while using AGC to balance generation and load in real time). The blue area describes the limits to governor response. This could be interpreted as the outer bounds of normal frequency response. Once the frequency drifts outside of governor response, underfrequency and overfrequency corrections are made to balance generation and load. If that does not work as expected, the system is in danger of experiencing equipment damage. Higher level actions would need to be taken for the contingencies being experienced.

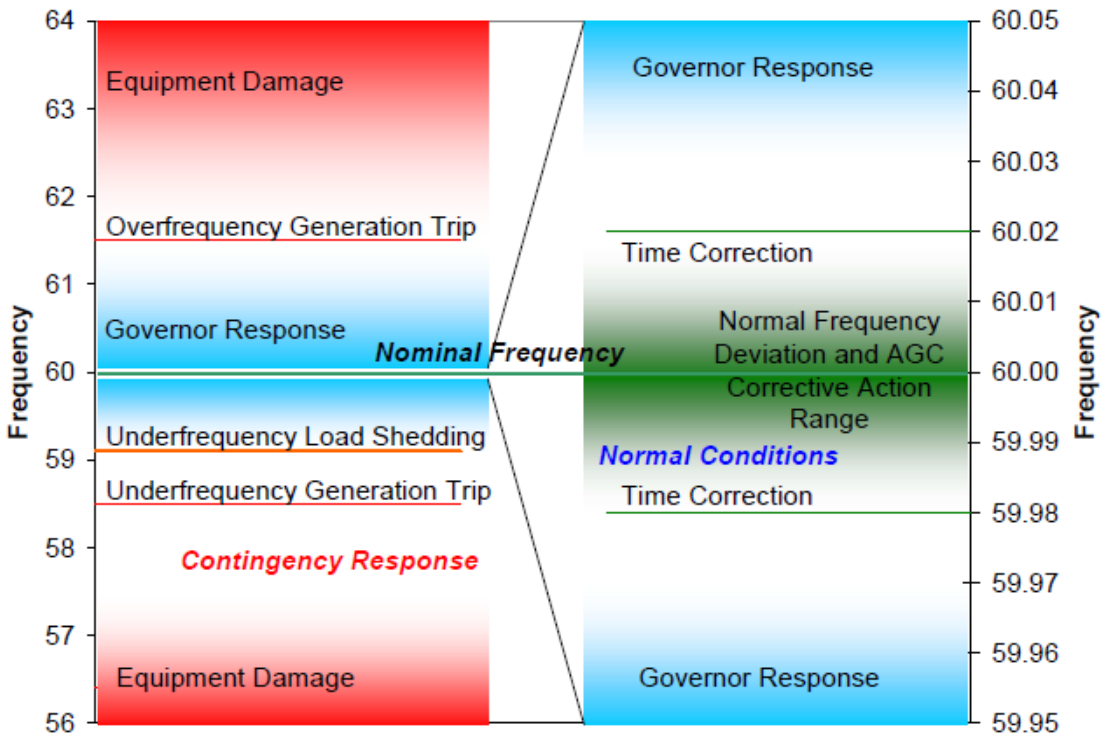

Figure 15. IEC 34-1 Frequency Response Stages [6].

Transmission Line Outage

In the following plots, the data represents an event where a line tripped out that was carrying a significant amount of power flow. PMU data, along with the corresponding RTU (and SCADA) data, from two separate locations was analyzed, and that data is shown in Figures 16 and 17. One of them was at a wind farm, which didn't appear to be producing very much power at the time of the event. The other was from a transmission substation with a heavily loaded transformer. The substation is approximately 50 miles south of the wind farm.

The RTU data clearly misses some transient information that resulted from the line outage. In Figure 16, the entire data sample is shown, and that duration is over a 10 minute timeframe. In Figure 17, the line trip is shown over a 30 second timeframe.

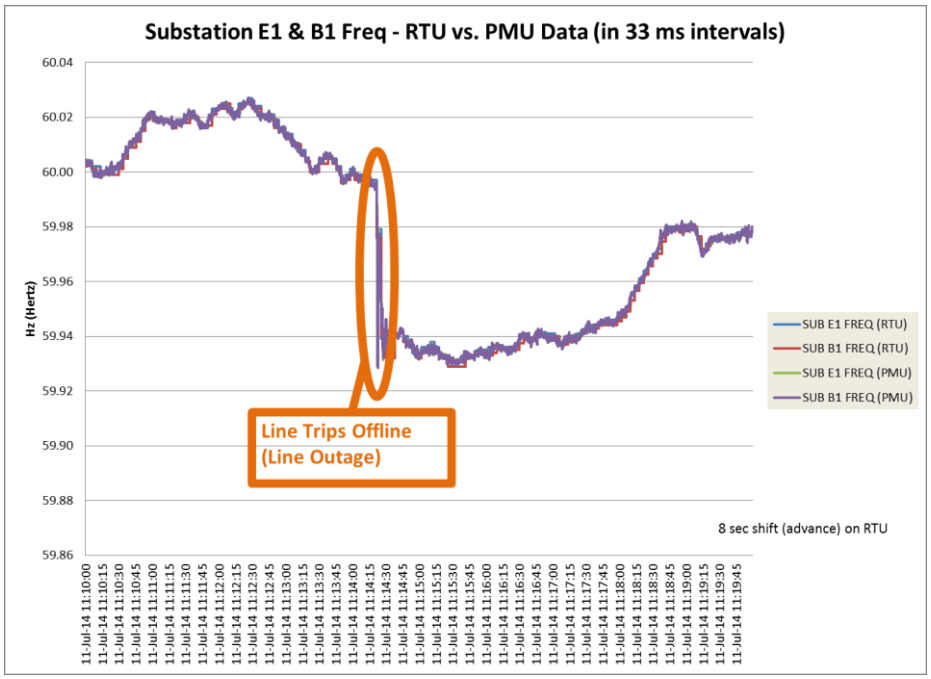

Figure 16. Frequency Data Comparison during a Line Outage – 10 minute timeframe.

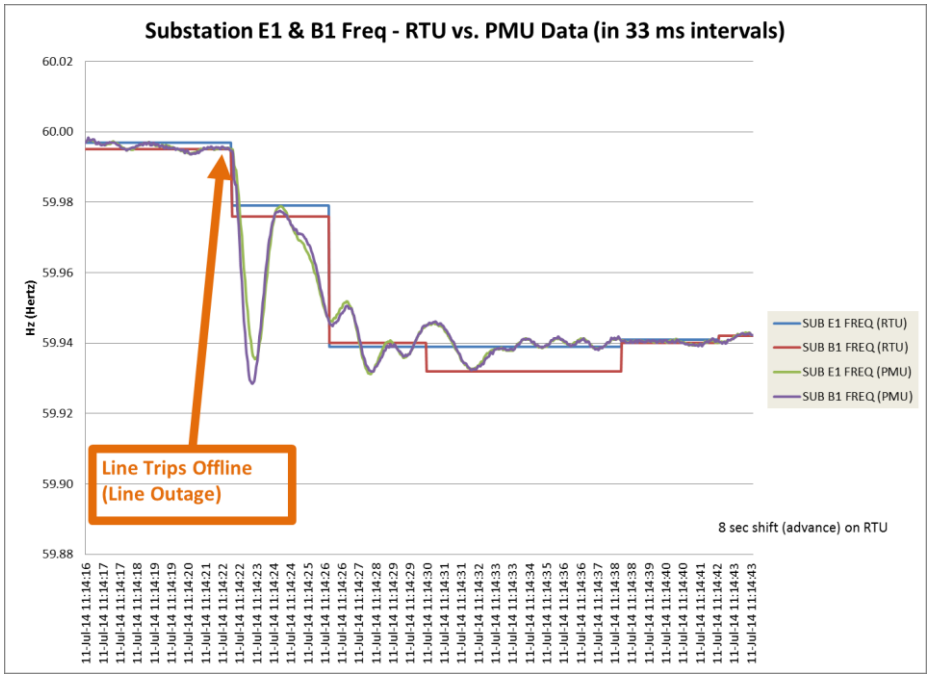

Figure 17. Frequency Data Comparison during a Line Outage – 30 second timeframe.

It might not be anything that directly impacts the reliability of the bulk power system, but it is possible that these transients could continue to ripple over a period of time. And, depending on the time intervals from the RTU data, the ripples could go undetected. In the grand scheme of power system monitoring, the RTU data provides some delayed, yet relatable data in comparison to the PMU data. However, in a more stressed contingency, an observer could certainly see damaging changes with PMU data in a shorter timeframe than that of the conventional measurement techniques. Under the general functions of RTU measurements within SCADA, there could be as much as four seconds of "system blindness" at the control center during damaging events.

The next plot is another interesting representation of the frequency data being measured by PMUs. In Figure 18, the rate of change in the frequency is shown.

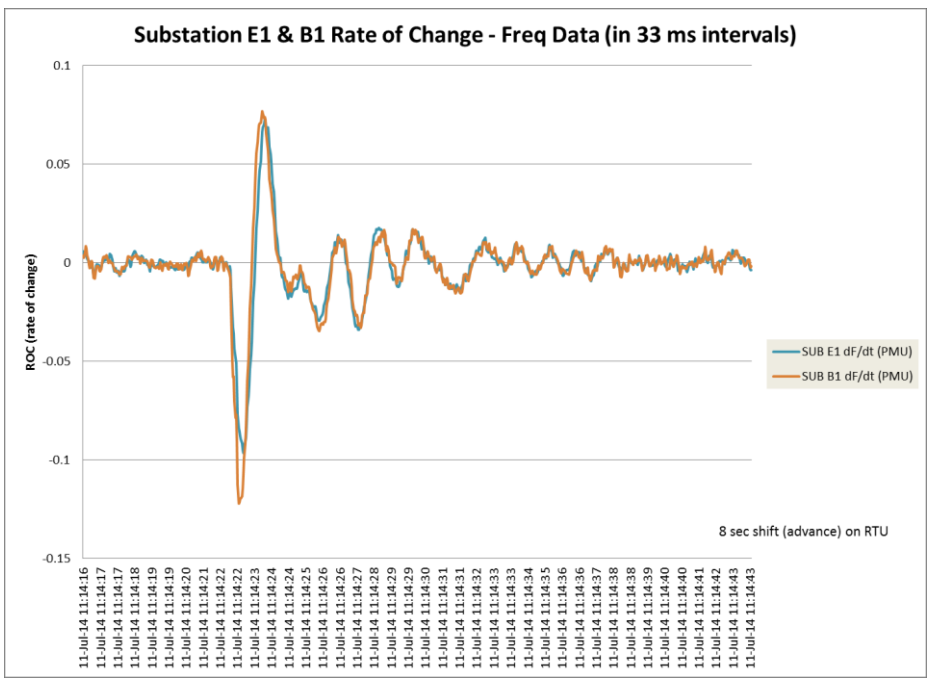

Figure 18. Rate of Change in the Frequency Data from Synchrophasors during a Line Outage.

The simplicity of this information is rather useful in attaining an indication that an event has happened. In normal conditions, the system maintains a fairly constant frequency. That is to be expected in a system intact condition. Any changes in frequency are normally slight in magnitude, and any substantial changes are gradual. In that sense, the frequency might shift within an acceptable range over time. Load service might ramp up or down, and the generation that is dispatched to the load regulates toward that consumption. For that reason, PMU data isn't that interesting during system intact conditions. RTU data satisfies most scenarios when the system is operating according to the plans of balancing authorities. However, when an unexpected event happens, PMU data becomes more appealing in the identification of system changes. The changes can also be characterized by this information.

For the sake of exploration, the power flow at the transmission substation (Substation E1, 50 miles south of the wind farm) was analyzed. The power flow at the other substation (Substation B1) was rather low, and it doesn't appear to provide very much information. However, the transformer located at Substation E1 is carrying significant power flow, and it changes throughout the duration of this event.

In Figures 19 and 20, the real power data is shown for Substation E1. As with the frequency plots, the first plot shows the entire data sample (10 minute timeframe), and the second real power plot shows the specific transition period (30 second timeframe). The plots are oriented in a way that power flow changes are shown in an exaggerated scale. The curve appears to vary drastically, however, the power flow regulates within approximately 35 MW range. The gradual changes correspond to the

variations of the frequency. In general, the real power increases as the frequency increases, and it decreases as the frequency decreases.

The unusual transients, shown in Figure 20, show the real power swings during this line outage. Ultimately, the alternate sources to this substation are working to compensate for the loss. Although the power flow from the line that was lost is no longer supplied, the loading on that transformer still exists. In response to that system change, the generation on the system begins to regulate the service to this area. First, the flows on the alternate lines begin to respond (governor response). Then, the generation begins to dispatch to the load (AGC response). This is more clearly shown in the 10 minute timeframe plot of Figure 19. This event seems to represent the stages of frequency response quite well. Even without a system model for the event, the data appears to give reasonable insight toward the benefits of high-resolution PMU data.

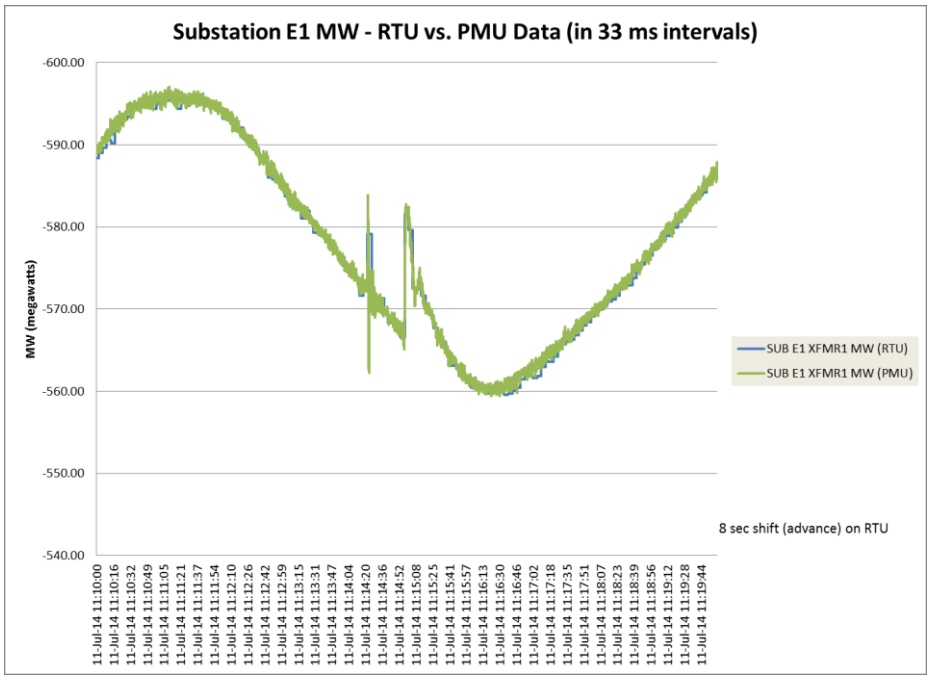

Figure 19. Real Power Data Comparison during a Line Outage – 10 minute timeframe.

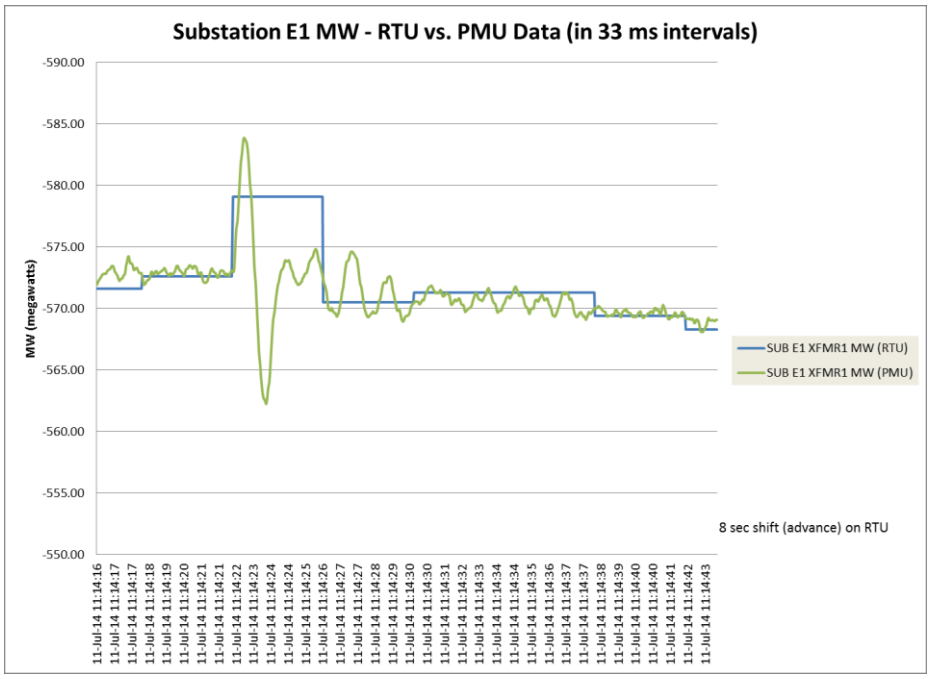

Figure 20. Real Power Data Comparison during a Line Outage – 30 second timeframe.

In Figures 21 and 22, the reactive power data is shown for Substation E1. Two things are immediately noticeable in these plots. First, the magnitudes of the PMU measurement and RTU measurement are not in alignment. There are a number of factors that could impact this data in such a way. The current transformers (CTs) or potential transformers (PTs) could be connected in different locations, or calibrated differently (this is likely the case). It also could be the result of inconsistent calculations. That can be a concern for some conventional measurement techniques.

Second, the gradual changes correspond to the variations of the frequency, but the reactive power consumption is not positively correlated with the frequency. In general, the reactive power increases as the frequency decreases, and it decreases as the frequency increases.

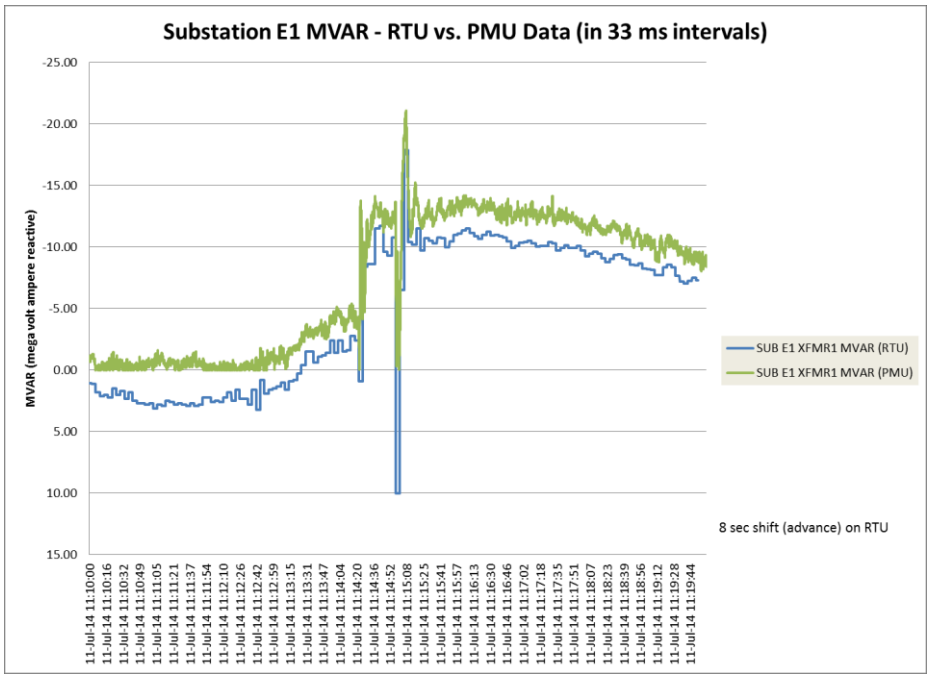

Figure 21. Reactive Power Data Comparison during a Line Outage – 10 minute timeframe.

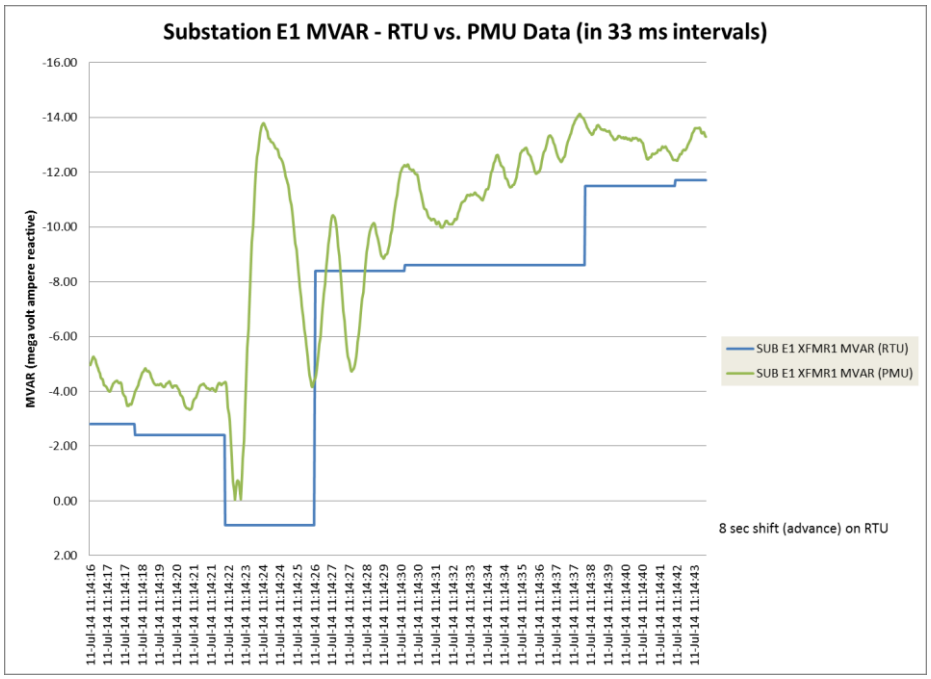

Figure 22. Reactive Power Data Comparison during a Line Outage – 30 second timeframe.

The unusual transients, shown in Figure 22, show the reactive power swings during this line outage. Again, the alternate sources to this substation are working to compensate for the loss. First, the flows on the alternate lines begin to respond (governor response). In terms of the reactive power, an increase in reactive power draw into the area is observed. Then, the generation begins to dispatch to the load (AGC response). The reactive power flow begins to gradually decrease as the frequency returns to nominal. This is more clearly shown in the 10 minute timeframe plot of Figure 21. Again, the stages of frequency response are represented well.

In Figures 23 and 24, the voltage data for both substations is shown, and each plot is comparing the RTU and PMU data. In terms of the Substation E1 data in Figure 23, this clearly shows some evidence for inconsistent connections or calibration.

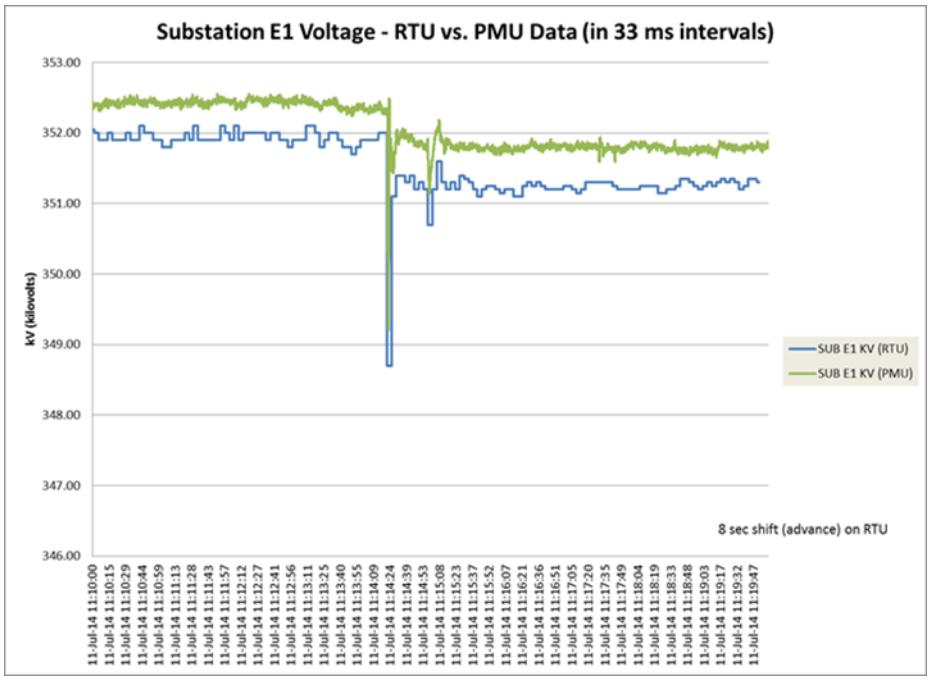

Figure 23. Voltage at Transmission Substation (E1) during a Line Outage – 10 minute timeframe.

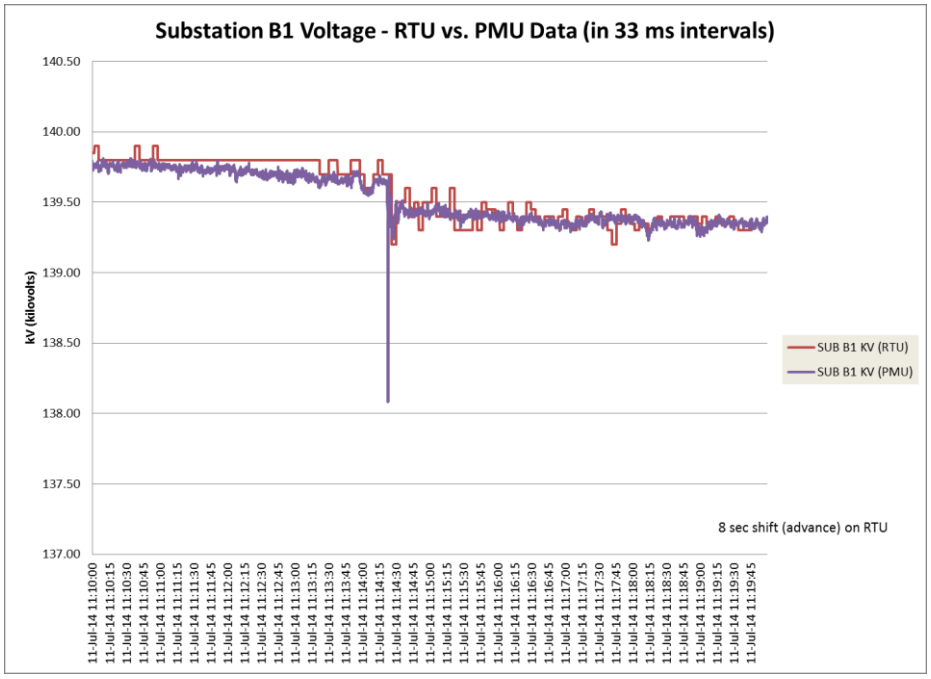

Figure 24. Voltage at Wind Farm Substation (B1) during a Line Outage – 10 minute timeframe.

Baseload Generation Outage

In the following plots, the data represents an event where multiple high voltage line trips occurred during a severe storm. This resulted in a baseload unit tripping offline, and other generation units were left in a state of "rocking" due to the stresses following the lost transmission and generation. Data from three separate locations was analyzed. One of them was at the interconnection line for the generation unit that tripped offline, and the other two were at interconnections of the other generators.

Again, the RTU data misses some transient information. In Figures 25 and 26, frequency data from the PMUs and RTUs is shown. In Figure 25, the entire data sample is shown, and that duration is over a 10 minute timeframe. In Figure 26, the major transition is shown over a 30 second timeframe.

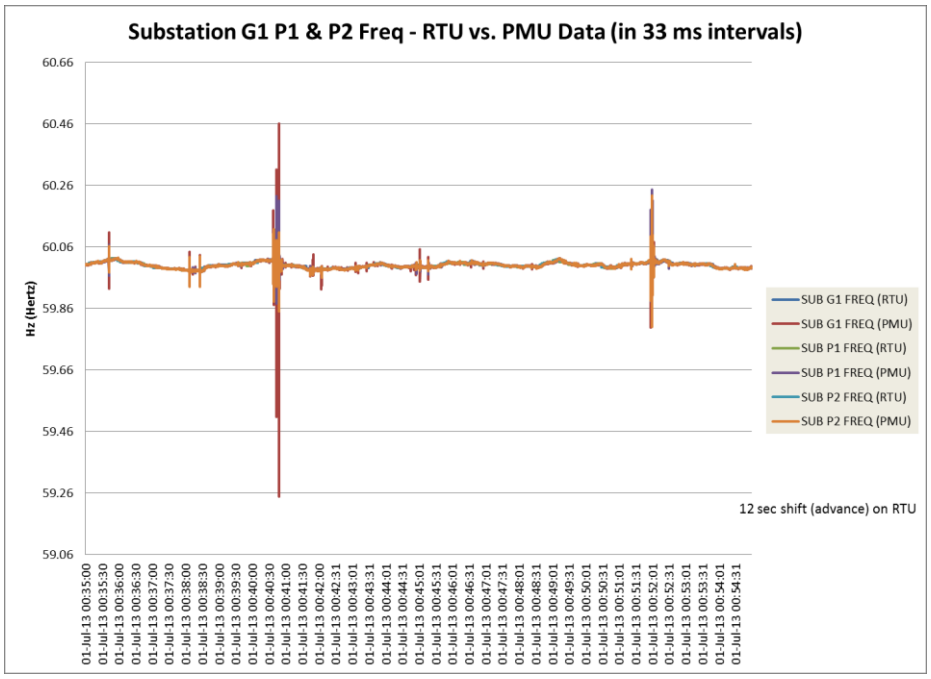

Figure 25. Frequency Data Comparison during a Generation Outage – 10 minute timeframe.

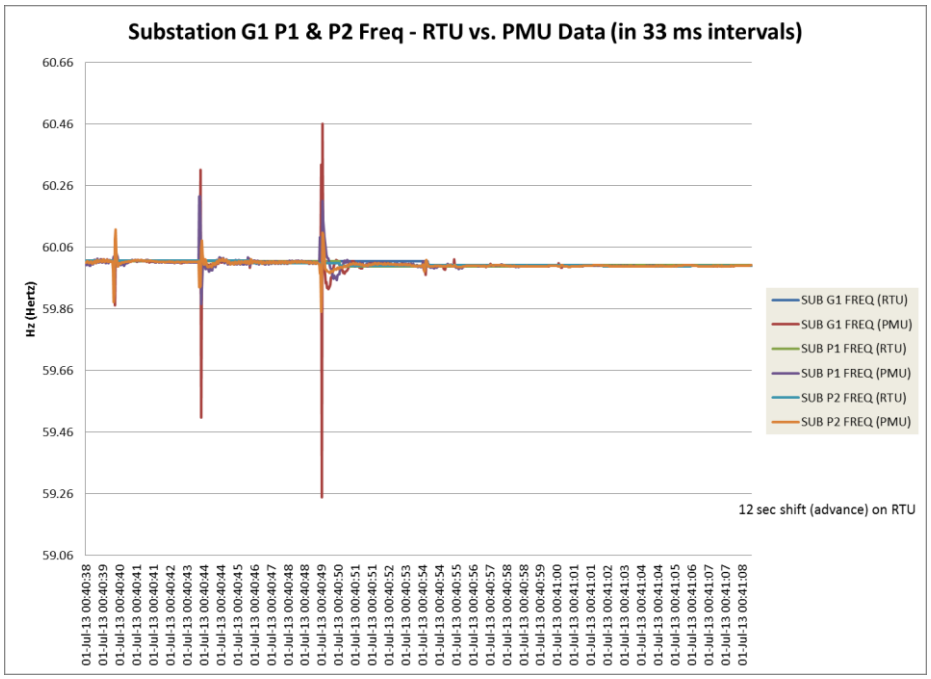

Figure 26. Frequency Data Comparison during a Generation Outage – 30 second timeframe.

As in the case of the line outage, these frequency transients might not directly impacts the reliability of the bulk power system, but the transients do continue to ripple over a period of time. For most of the event, the ripples could go undetected by RTU measurements. The RTU data shows a variation of about 0.05% from nominal, while the PMU data shows variations higher than 1.25% from nominal. In this stressful event, one could certainly see damaging changes with PMU data that is completely lost in conventional measurement. As in the line outage event, there could be as much as four seconds of "system blindness" at the control center during damaging events. Obviously, the frequency stays fairly constant, but the transients are ongoing. The rate of change of frequency (ROCOF) information was unavailable for this event. This event occurred during early implementation of the PMUs, and ROCOF wasn't enabled.

For the sake of exploration, the power flow at each generation interconnection was analyzed. The power flow at all of the "rocking" generation interconnections was fairly consistent throughout the event. The generation interconnection for the unit that tripped offline was carrying about 350 MW of power flow prior to the outage. Following the outage, the transmission line appears to be drawing a small amount of power (about 10 MW). This is probably the generation station's local load service. Outside of the transition that occurs during the outage, power flow is fairly consistent at that location as well. In a sense, the power flow is consistent in two separate stages. First, the generator is producing power (pre-outage) at about 350 MW, and then, the generator is no longer supplying its own station service power (post-outage) of about 10 MW. The other two generation interconnections appear to be producing 1200 MW and 110 MW, and the output is consistent outside of the "rocking" transients.

In Figures 27 and 28, the real power data is shown for the generator that trips offline. The first plot shows the entire data sample (10 minute timeframe), and the second real power plot shows the specific transition period (30 second timeframe). The outage transient, shown in Figure 28, shows the real power swings during this generation trip. First, the output appears to jump slightly. After about 6 seconds, this is followed by the generation outage. The frequency drops slightly at all of the generation interconnections, but the sag in frequency is momentary. The generators quickly regulate the frequency at their interconnections. This is to be expected for transmission that is so closely located to the generation. This is clearly shown in the 30 second timeframe plot of Figure 26. The frequency at generation interconnections shouldn't vary drastically, and this event demonstrates that response quite well.

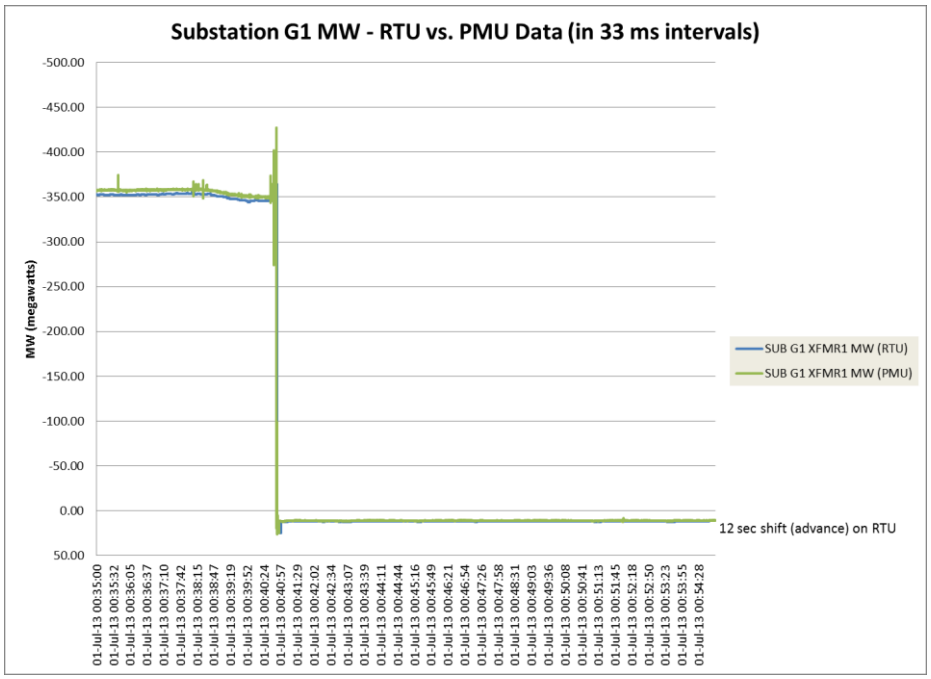

Figure 27. Real Power Data Comparison during a Generation Outage – 10 minute timeframe.

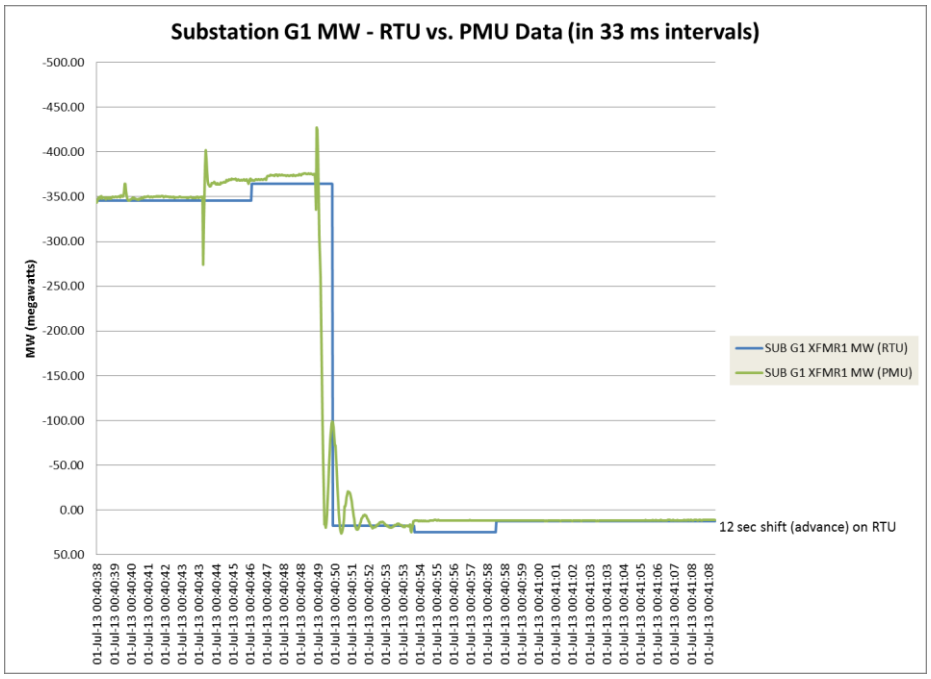

Figure 28. Real Power Data Comparison during a Generation Outage – 30 second timeframe.

In Figures 29 and 30, the reactive power data is shown for the generator that trips offline. Two things are immediately noticeable in these plots. First, the magnitudes of the PMU measurement and RTU measurement are close, but as with the line outage, they are not in alignment. The current transformers (CTs) or potential transformers (PTs) could be connected in different locations. It also could be the result of inconsistent calculations. That can be a concern for some conventional measurement techniques.

Second, the outage doesn't cause a complete loss of reactive power. Even without the generation output, there appears to be some reactive power output from the generation interconnection. This could be the result of many different factors. A couple of factors may include line charging or a shunt capacitor on the transmission.

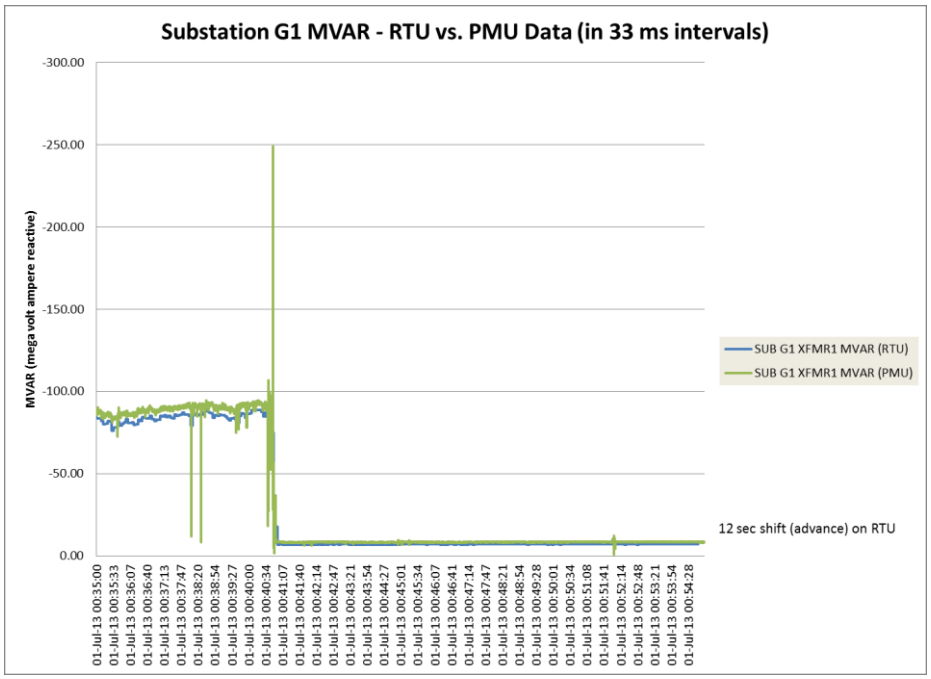

Figure 29. Reactive Power Data Comparison during a Generation Outage – 10 minute timeframe.

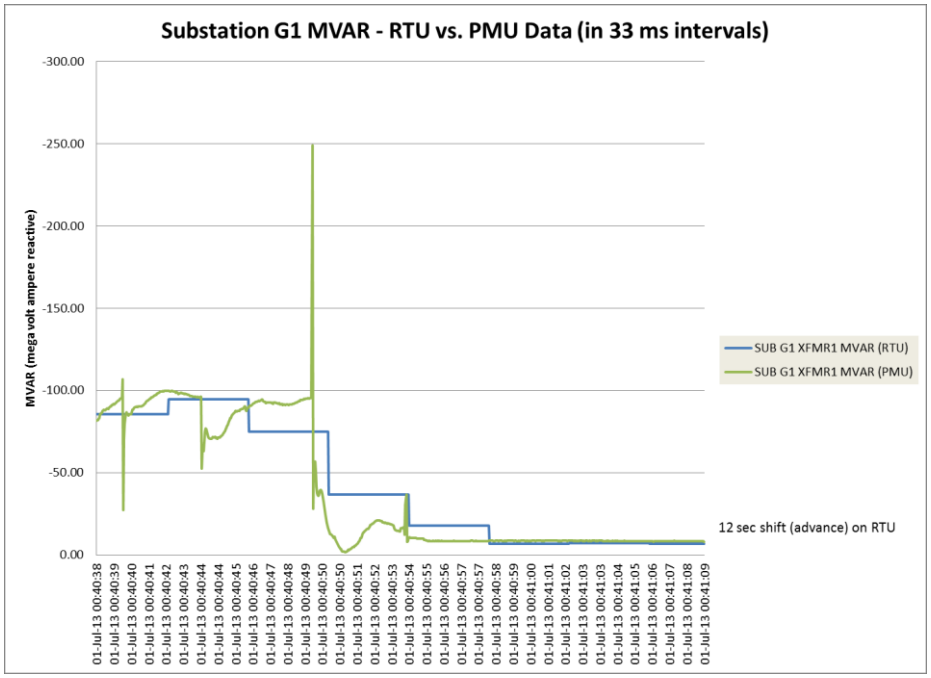

Figure 30. Reactive Power Data Comparison during a Generation Outage – 30 second timeframe.

The unusual transients, shown in Figure 30, show the reactive power swings during this line outage. Again, the reactive power flow on this transmission suggests that there are some other sources of reactive support. Some of it may be completely passive, but there may be some active components (switching capacitors, etc…) that are working against the recent loss. First, the fixed system begins to respond (governor response). Then, the active facilities in the area begin to switch on (and off) to correct voltage and other system characteristics that diminish following the generation loss (corresponding actions that correlate with AGC response).

In Figures 31 through 34, the real and reactive power for the other two generation interconnections is shown. The generator data shows increased reactive power output to compensate for lost generation. Real power stays roughly the same.

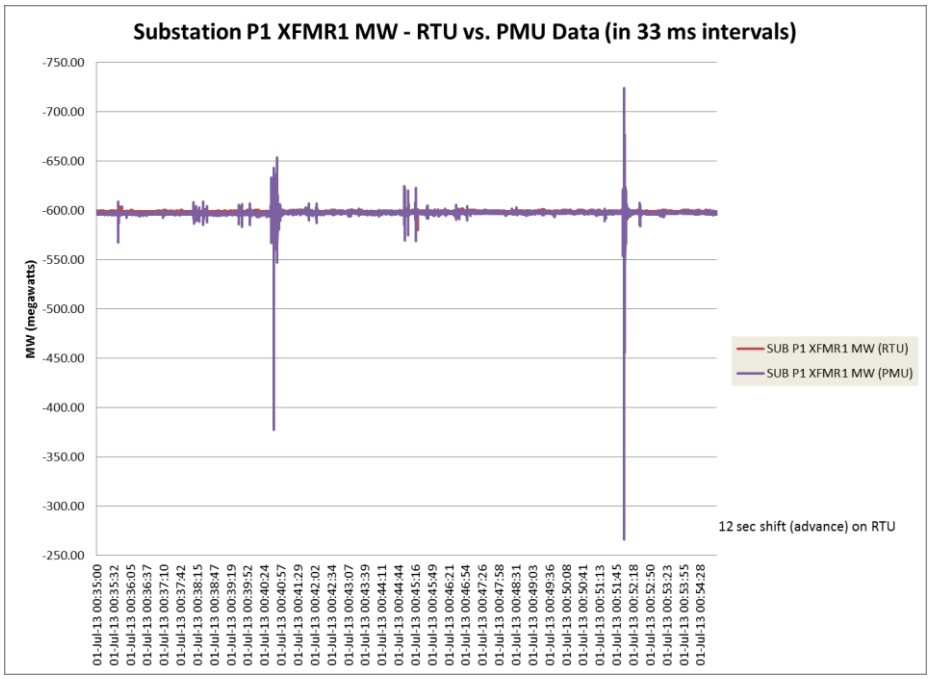

Figure 31. Real Power Data Comparison for the "Rocking" 1200 MW Generator.

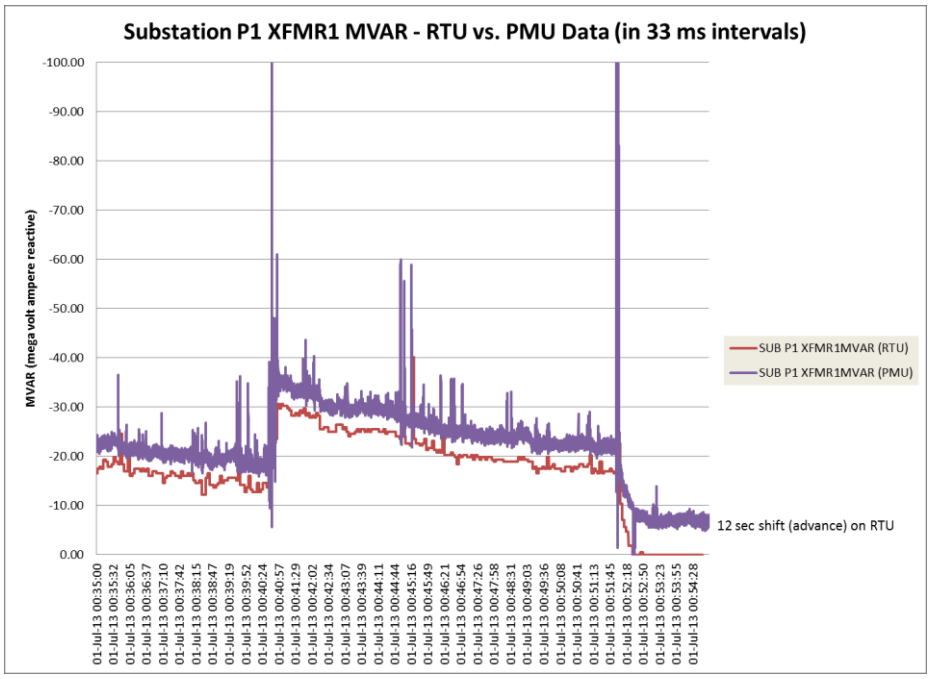

Figure 32. Reactive Power Data Comparison for the "Rocking" 1200 MW Generator.

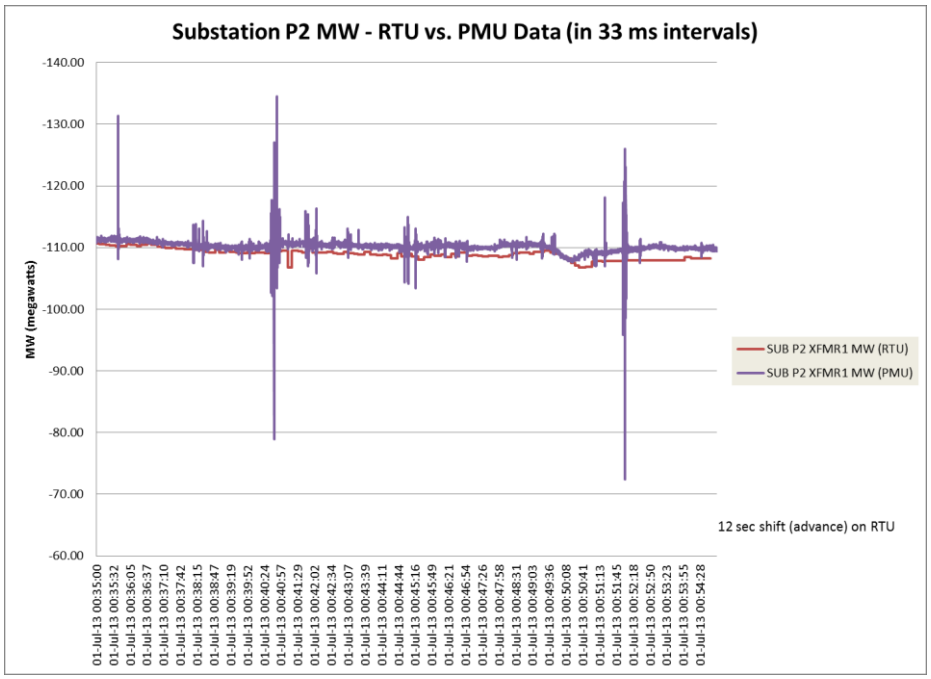

Figure 33. Real Power Data Comparison for the "Rocking" 110 MW Generator.

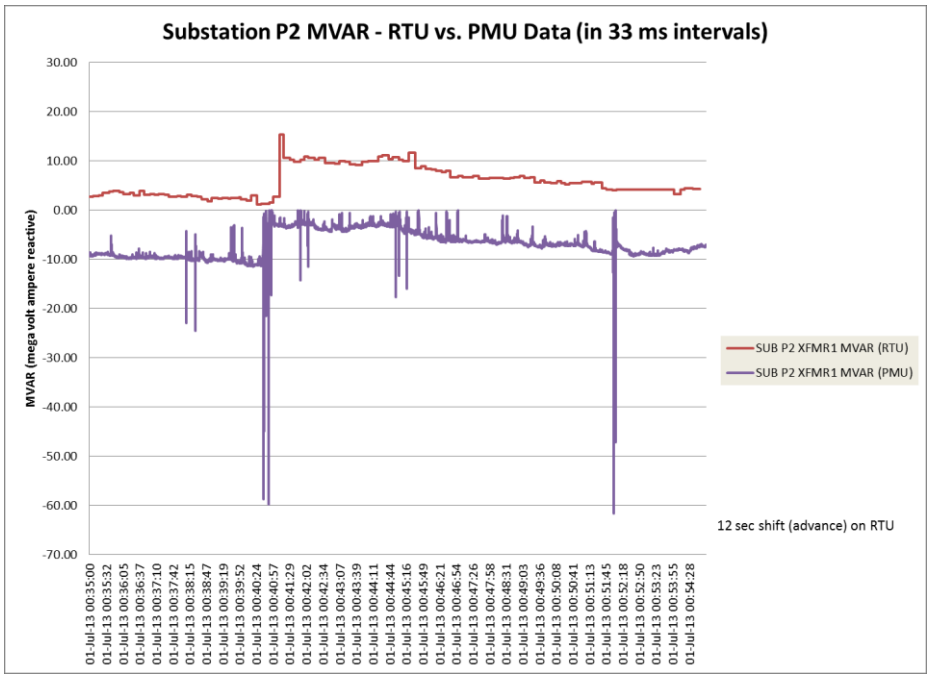

Figure 34. Reactive Power Data Comparison for the "Rocking" 110 MW Generator.

Throughout the event, the generation output appears to be regulating up and down sporadically. This is not normal for the system, and it seems to be present before and after the generation outage. However, it gets extremely obvious after the line outage. The post-outage stresses seem to have a particularly profound impact on the reactive power flow. And again, the magnitudes of the PMU measurement and RTU measurement are not in perfect alignment. This might be another problem with the CTs or PTs, or it could be the result of inconsistent data calculations.

Significant Storm Disturbance

In the following plots, the data represents an event during a severe storm that swept through a metropolitan area during the summer. The plots in this section show the impact of multiple distribution faults during the storm. Numerous small voltage dips associated with the distribution faults prevail during the timeframe of this data.

Within the ten minute timeframe, some insight can be draw from the effects of these distribution outages on the transmission system that supports this metropolitan area. This did not result in any transmission or generation tripping offline, but power quality was certainly in question. Voltage data from four separate locations (within a 50 mile radius) was analyzed. As with the previous events, the RTU data misses some transient information. In Figures 35 through 42, voltage data from the PMUs and RTUs is shown. In the odd numbered figures, the entire data sample is show, and that duration is over a 10 minute timeframe. In even numbered figures, the one minute timeframe that includes the largest voltage dips is shown. Although this information is not extremely revealing, it is useful in the analysis of power quality during customer inquiries. Conventional data that is provided by SCADA falls short in this respect.

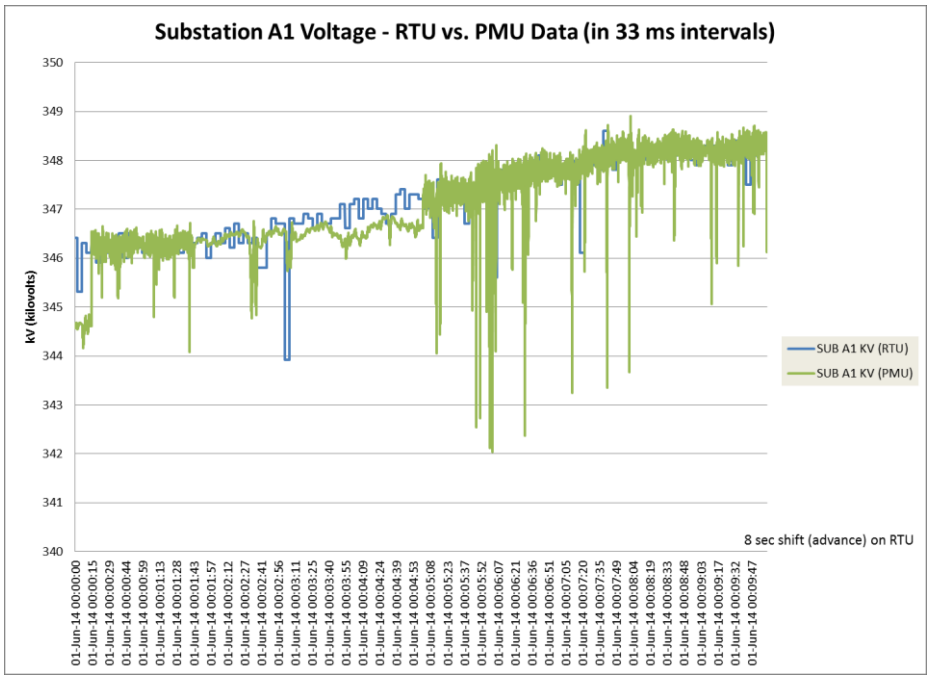

Figure 35. Voltage Data (Substation A1) Comparison during a Storm – 10 minute timeframe.

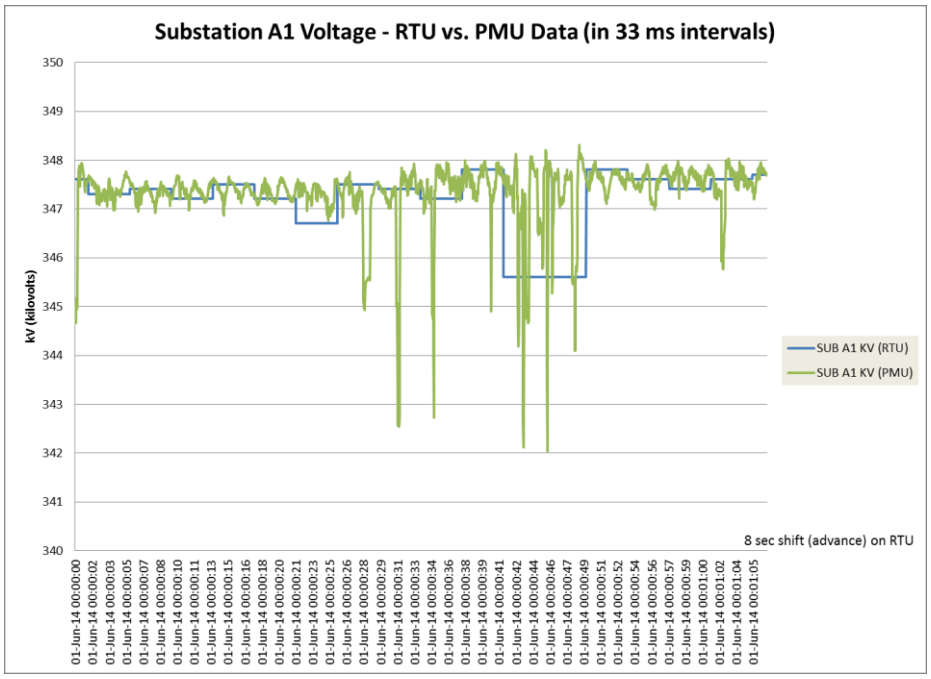

Figure 36. Voltage Data (Substation A1) Comparison during a Storm – 1 minute timeframe.

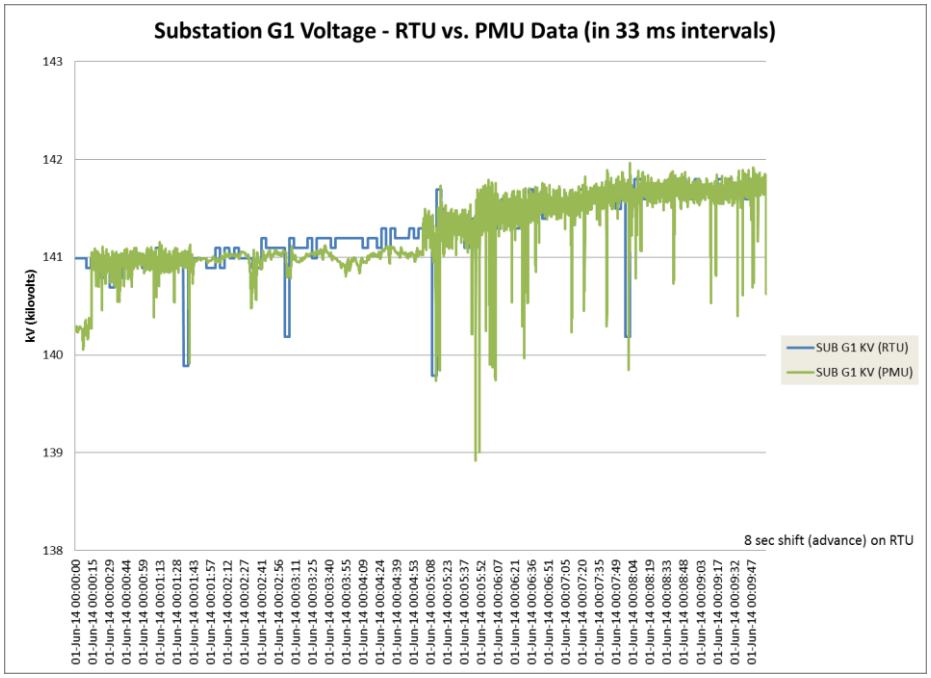

Figure 37. Voltage Data (Substation G1) Comparison during a Storm – 10 minute timeframe.

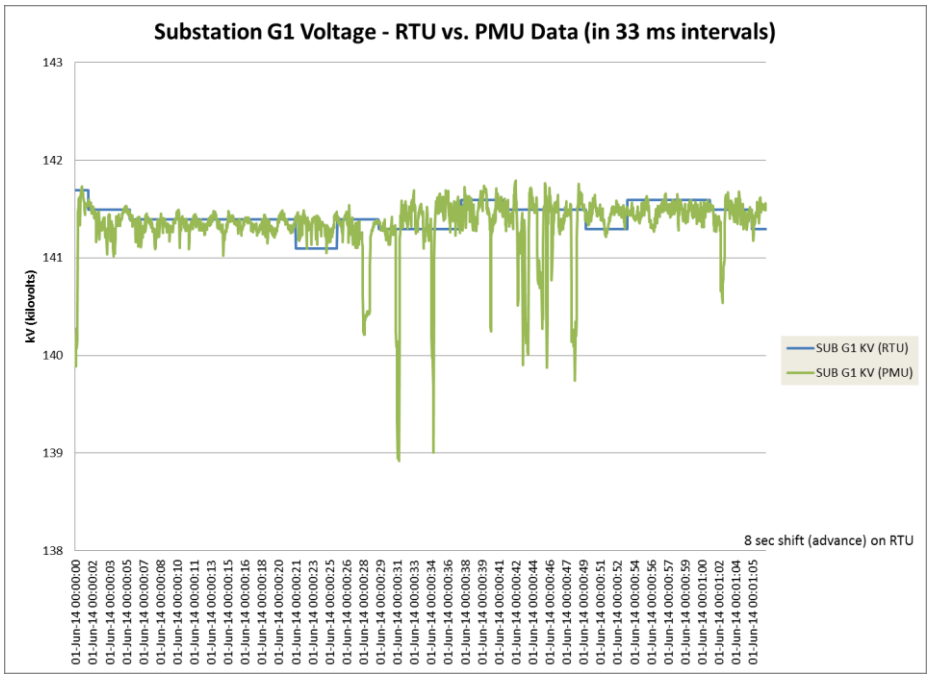

Figure 38. Voltage Data (Substation G1) Comparison during a Storm – 1 minute timeframe.

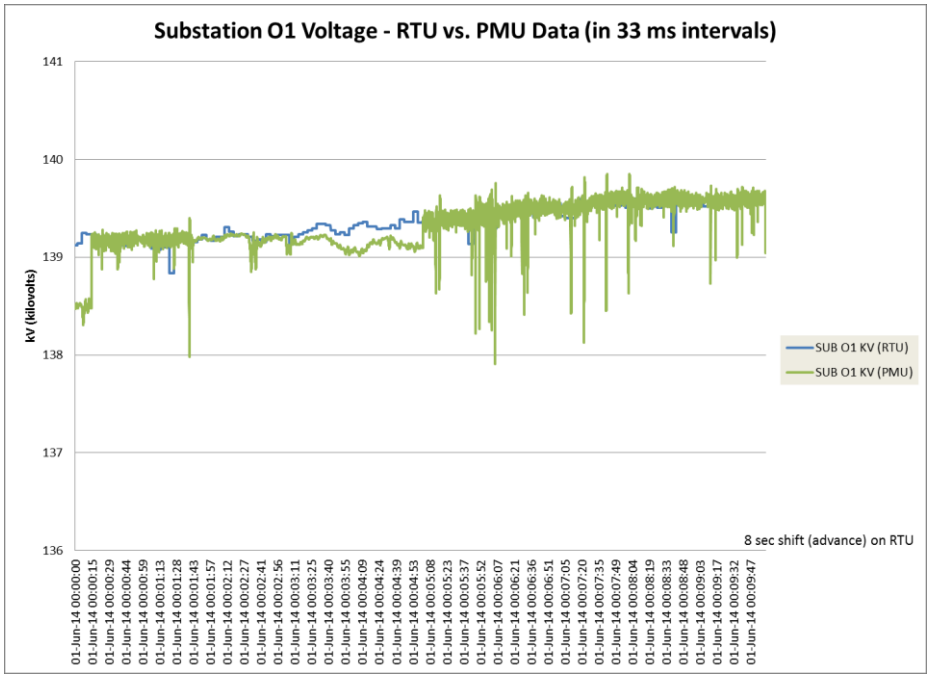

Figure 39. Voltage Data (Substation O1) Comparison during a Storm – 10 minute timeframe.

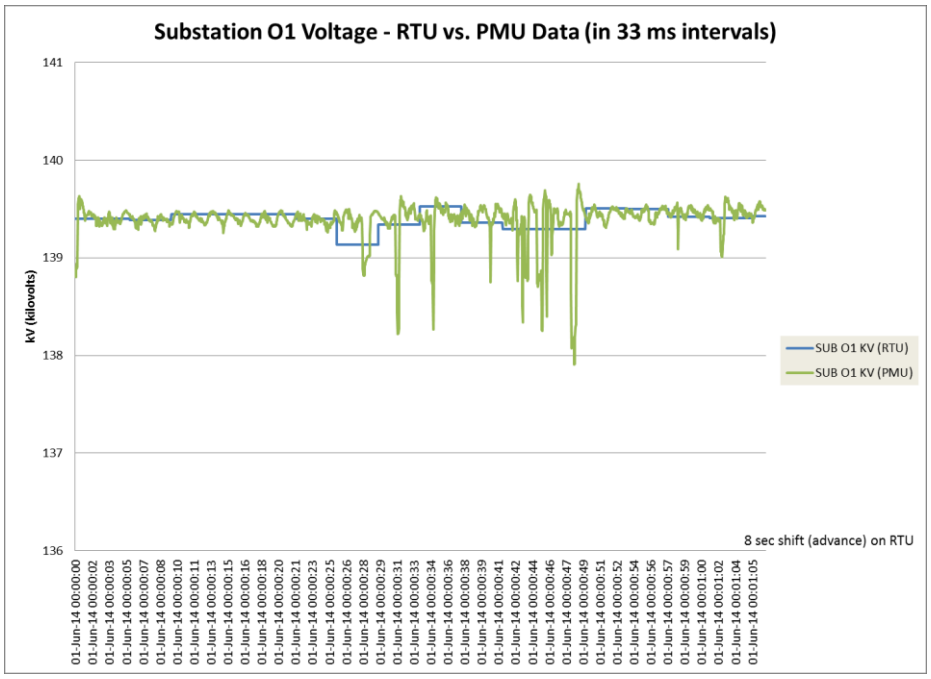

Figure 40. Voltage Data (Substation O1) Comparison during a Storm – 1 minute timeframe.

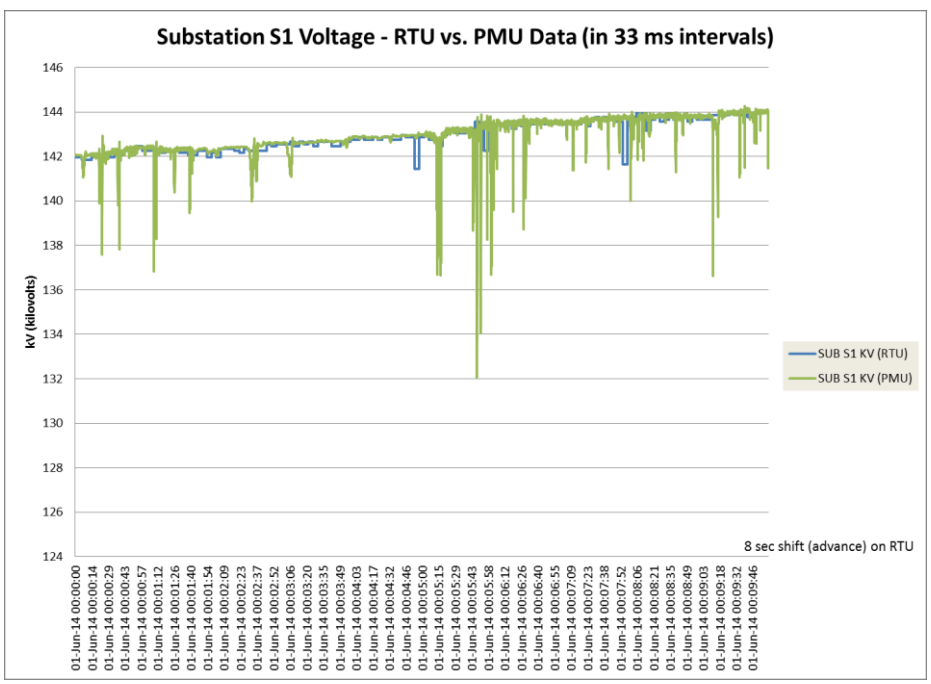

Figure 41. Voltage Data (Substation S1) Comparison during a Storm – 10 minute timeframe.

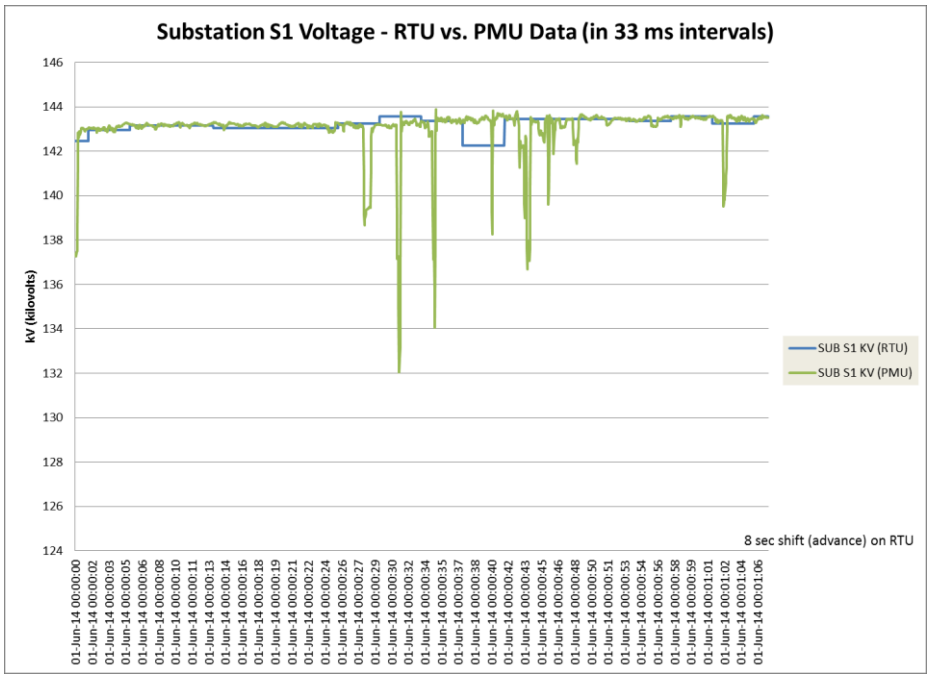

Figure 42. Voltage Data (Substation S1) Comparison during a Storm – 1 minute timeframe.

Catastrophic Fault

In the following plots, the data represents an event during a distribution transformer fault. The plots in this section show the impact of this transformer fault upon the 69 kV transmission that services the area. The distribution fault hangs on for a substantial amount of time (nearly three minutes). During the event, the transformer experienced some significant arcing that resulted in it being destroyed. In this particular event, only PMU data was made available. There were two nearby PMUs on the 69 kV system. In looking at the phase angle data, large spikes of phase angle separation occur in the data. At certain points during the event, the voltages come completely out of phase as well. This data from the two nearby locations was analyzed.

This event occurred over an extensive period of time, and it is likely that the failure was unavoidable. However, further damages to the substation may have been

avoided under the right conditions. The use of PMU data for SCADA functions probably wouldn't have avoided the event. However, PMU data may become useful for identifying the characteristics of a catastrophic fault to a transmission facility.

In Figures 43 and 44, voltage magnitude data from the PMUs is shown. In Figure 43, the entire data sample is show (10 minute timeframe). In Figure 44, the three minute duration in which the fault occurs is shown. The magnitude plots clearly show a loss of voltage to the area as the transformer begins to burn up. Afterward, the voltage shows a dramatic increase before settling down to nominal. In Figures 45 and 46, the voltage angle difference between the two PMUs is shown. In Figure 45, the entire data sample is show (10 minute timeframe). In Figure 46, the three minute duration in which the fault occurs is shown. Noise after the fault is easily observed.

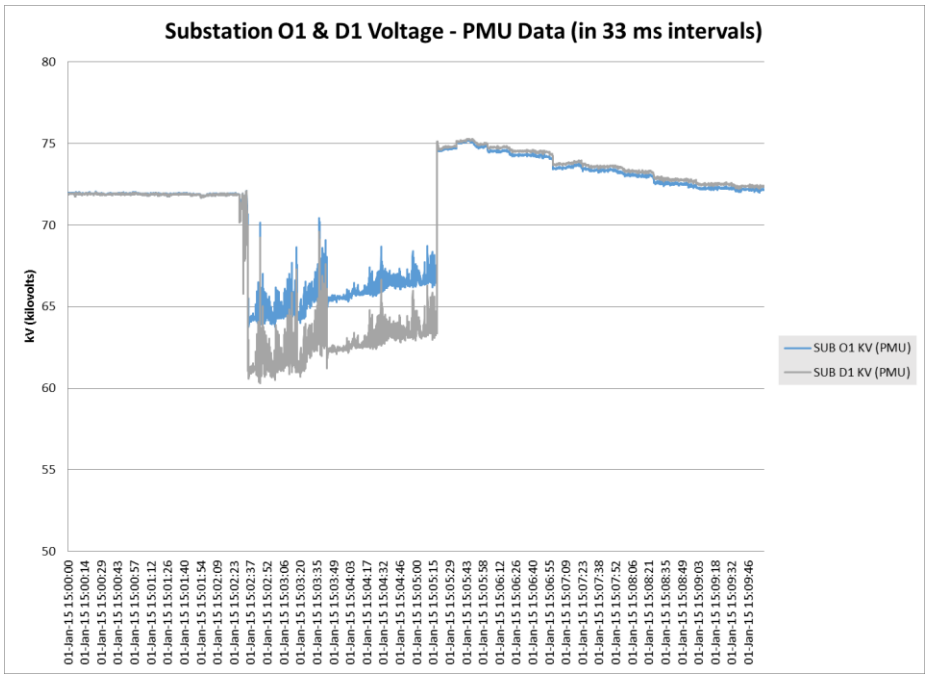

Figure 43. Voltage Magnitude Measurements during a Transformer Fault – 10 minute timeframe.

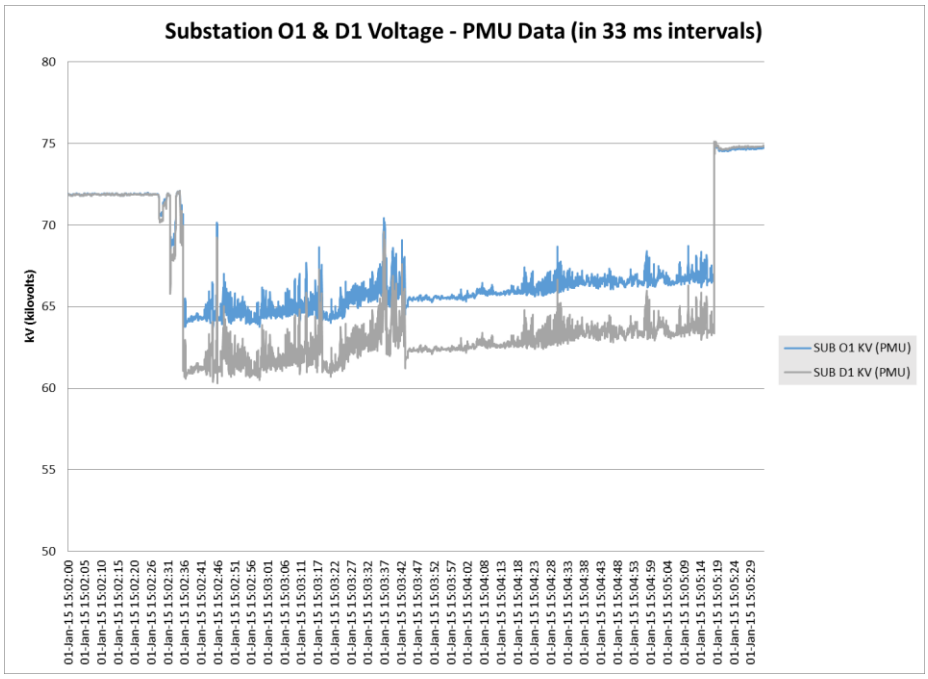

Figure 44. Voltage Magnitude Measurements during a Transformer Fault – 3 minute timeframe.

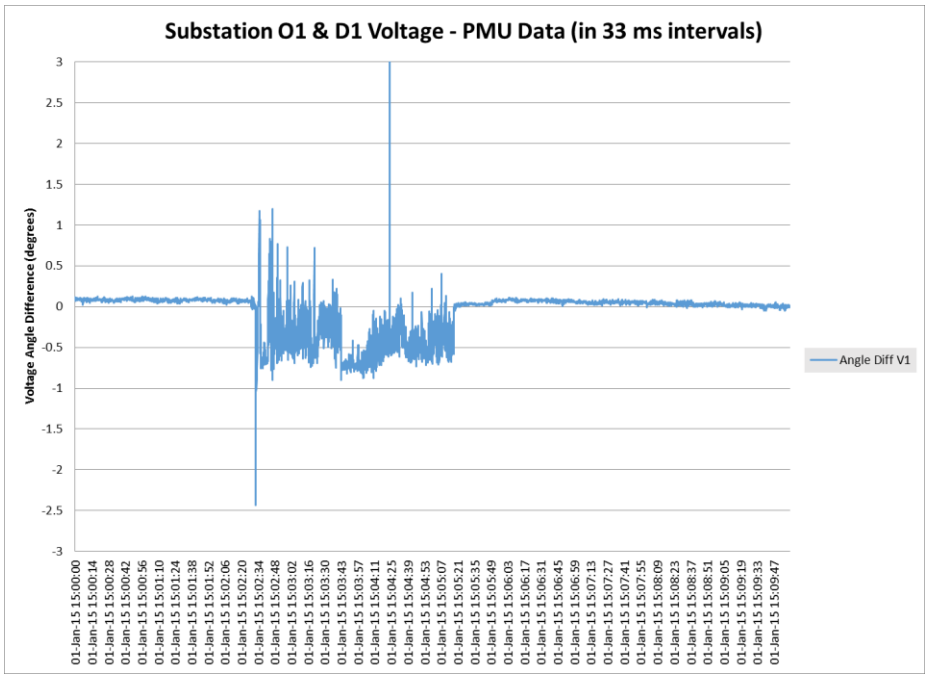

Figure 45. Voltage Angle Difference (between Substation O1 and D1) during a Transformer Fault – 10 minute timeframe.

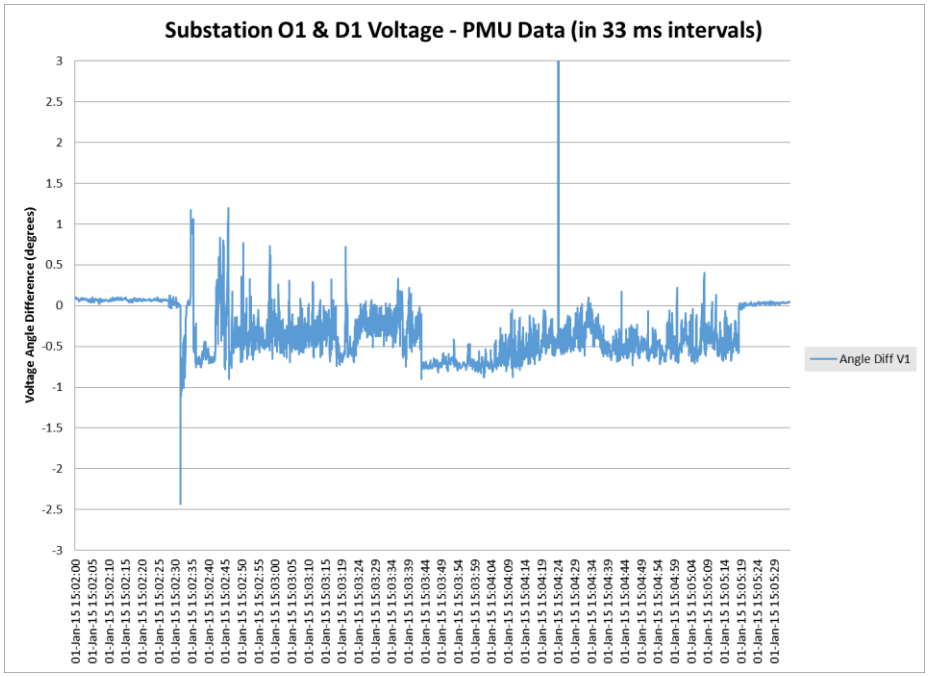

Figure 46. Voltage Angle Difference (between Substation O1 and D1) during a Transformer Fault – 3 minute timeframe.

CHAPTER III

DEMONSTRATION

To add value to the understanding of this technology, some demonstration projects were devised to further investigate the functionality of synchrophasor equipment. The earlier chapters investigate the uses of the resulting data, but that data was provided by a utility. The utility procured the synchrophasor equipment, installed it, calibrated it, integrated the system, and acquired the system measurements. There are some valuable lessons to be learned throughout that process.

One particular aspect concerns communication. Transmitting this information requires some very specific consideration of the data transfer. For each parameter that is desired, there is a burden on communication. Additionally, the level of precision for those desired parameters determines the level of that burden. Although there are different communication mediums that are capable of massive data transfer, the cost of constructing, maintaining, and operating such mediums creates the need for balance. The communication medium and data requirements must be prudently coordinated.

Another specific consideration concerns the acquisition of the GPS clock. In order to have reliable synchrophasor data, the reception of three satellite signals is important for proper GPS clock operation. That communication must be consistent.

And finally, the demonstrated system being monitored is not complicated; however, the bulk power system is complicated. There are simulation schemes that can

approximate some portions of this complex system, but the correct infrastructure must be available for proper demonstration. Many things contribute to the acquisition of these measurements, and some of the demonstration efforts require some mid-level power measurements conveyed through analog devices.

Laboratory Demonstration of a Single Phase System

The University of North Dakota is a recent recipient of some synchrophasor equipment. Schweitzer Engineering Laboratories (SEL) donated two phasor measurement units (both are model SEL-351A PMUs), a GPS clock (SEL-2407), and a bullet antenna for the GPS clock's satellite communication. The appropriate documentation and cables were also provided. In response to this generous donation, the department has begun the process of planning a laboratory-based power system project. In the project, an electric power system has been proposed for academic research. This undertaking is a gradual process, and it requires some exhaustive research to plan it correctly. However, the equipment requires some preliminary investigation and testing. In order to do that, a demonstration has been performed as a part of the research work reported in this thesis.

In this demonstration, a simple power system was constructed within a university laboratory. The primary concerns with the construction of this simple power system involve the voltage and current measurement specifications. The voltage input for the PMUs requires a range of nominal voltage between 67 and 120 V_{rms} (with a 173 V_{rms} continuous limit). The current input for the PMUs requires a range of nominal current between 0 and 5 A_{rms} (with a 15 A_{rms} continuous limit).

Due to some facility limitations, it was determined that a standard wall outlet system should be sufficient. The voltage for a standard wall outlet is $120\ V_{rms}$, and the current for a standard circuit breaker is $15\ A_{rms}$. The load that was selected for this demonstration was an incandescent light bulb (40 W) with a dimmer switch. That means that the current should be between 0 and $0.34\ A_{rms}$. Therefore, the voltage and current should be roughly within the nominal range (and below the continuous ratings). Figure 47 shows part of the schematic of this laboratory setup.

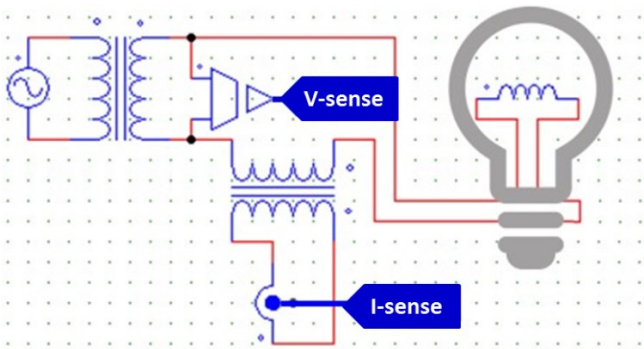

Figure 47. Single Phase Power System Schematic for the Laboratory Demonstration Setup.

First, an isolation transformer is used to supply the power to this system. This was done purely for system separation, and it also creates a buffer for the equipment. In Figure 48, the isolation transformer-to-system connection is shown.

Figure 48. Isolation Transformer used for System Separation and Equipment Protection.

In this demonstration, it was determined that some transients would be more interesting for the analysis than simply powering the load. To do that, the system would need a switch to simulate the event of an open breaker during a fault. To satisfy this need, a simple light switch was connected in series. In Figure 49, the switch equipment that was used to simulate a fault is shown.

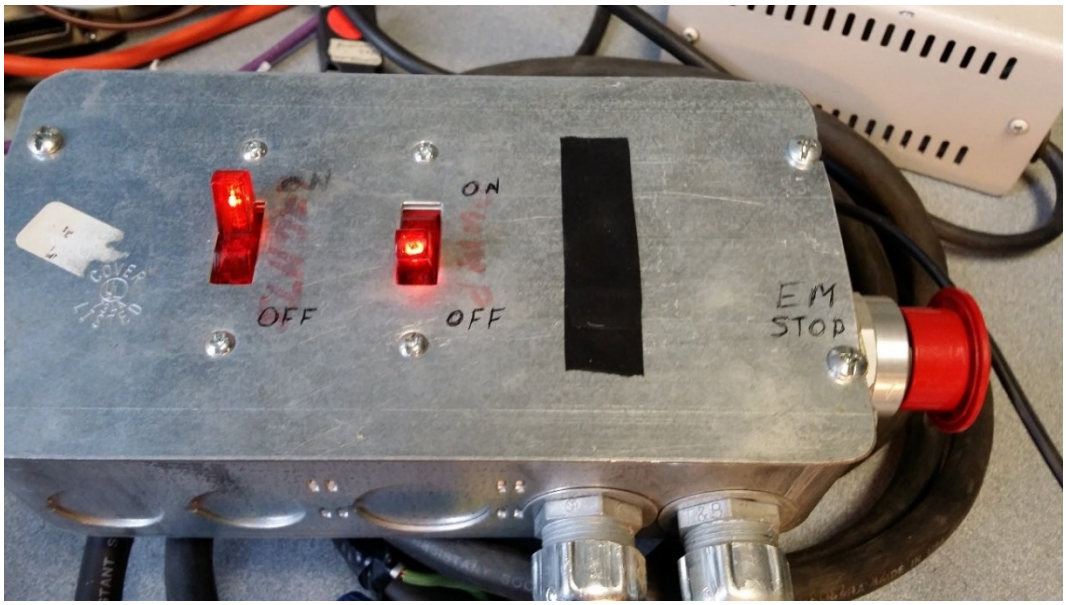

Figure 49. Switch Equipment for Simulating an Open Breaker during a Fault.

The next part of the system is a bit more complex. A small "bus system" was constructed for two uses, and is shown in Figure 50. Since the system voltages are the same as the PMU measurement voltages, the same "bus system" was capable of both functions. In an actual power system where these voltage levels do not correspond, these systems are kept far from each other. The voltage measurement is taken from the hot and neutral lines coming from the switch equipment. Fuses have been added for additional protection to the PMU voltage measurement terminals (1 A glass cartridge fuses).

Then, the current measurements are taken from a small transformer. The transformer is connected in series with the load, and this transformer is used to isolate the demonstration system from the PMU current measurement terminals. This is similar to the use of the current transformer, or CT, that is used in an actual power system. This transformer does not have a 1:1 ratio from primary to secondary, but the ratio is known. It has a primary-to-secondary ratio of 20:10.8. This is used to adjust the current measurements to the actual values (similar to the methods used for CTs).

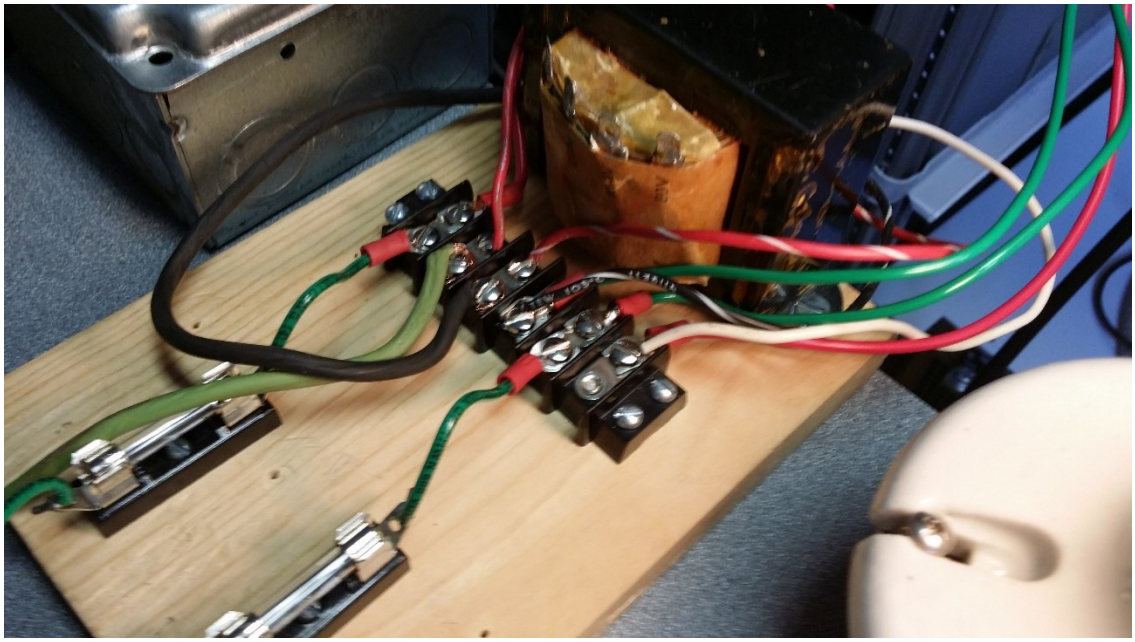

Figure 50. “Bus System” for the System Voltages and PMU Measurement Voltages.

After taking measurements at the “bus system” for the PMU, the hot line and the neutral line (via the transformer used for current measurement) is connected to an outlet box that serves the load, as shown in Figure 51. The outlet box is used for a convenient connection to the light load. And finally, the light load is plugged into the outlet box. The light load has a dimmer switch on the side that can be used to regulate different load levels, as shown in Figure 52.

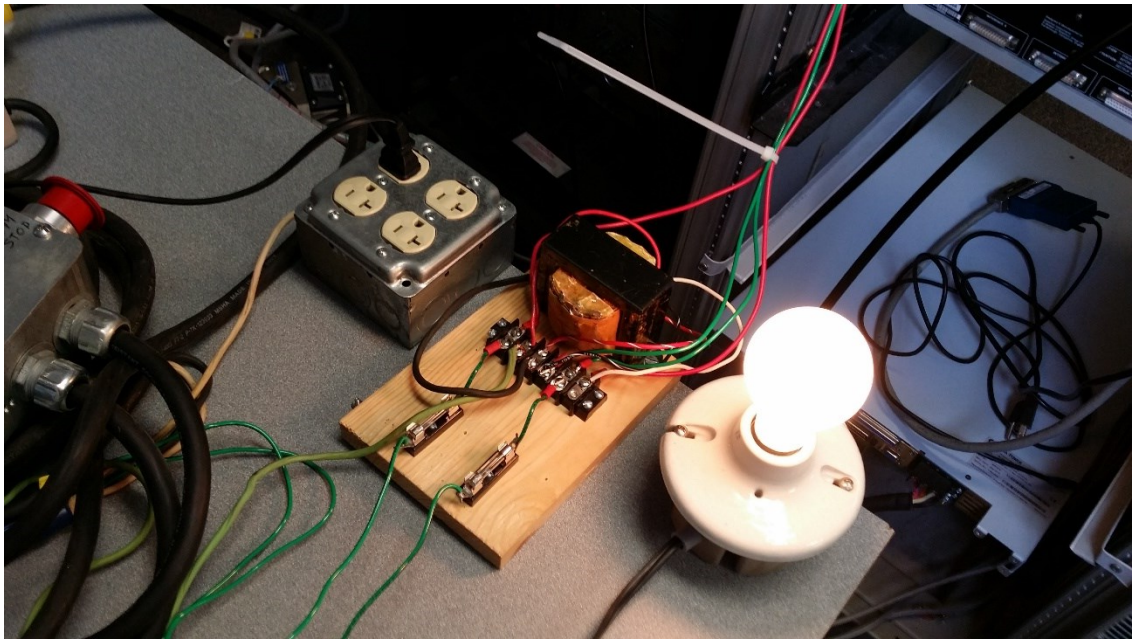

Figure 51. Outlet Box and Light Load for the Demonstration Setup.

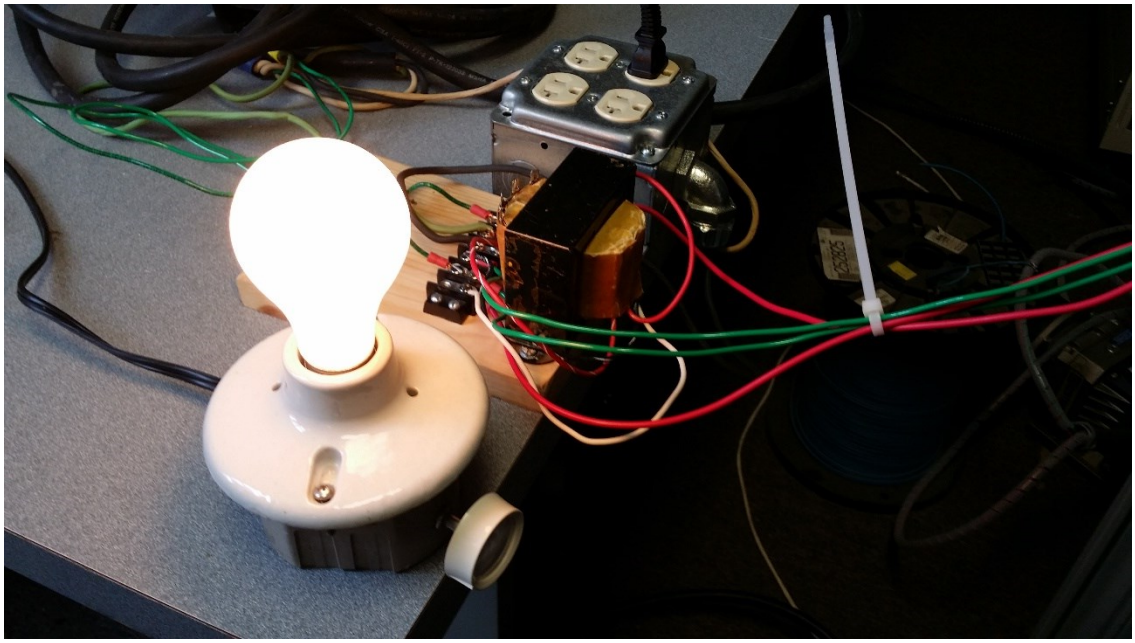

Figure 52. Outlet Box and Light Load for the Demonstration Setup – Dimmer Switch.

In Figure 53, the back of the PMU used for this demonstration is shown. Toward the lower left corner of the PMU, the current measurement wires are connected to Phase A (terminal block) for current. Toward the middle, the voltage measurement wires are connected to Phase A (terminal block) for voltage. The coaxial cables are used for transmitting the GPS clock time information to the PMUs. The UART cable is the data transfer cable, and it is connected to the laboratory computer for data capture and archiving.

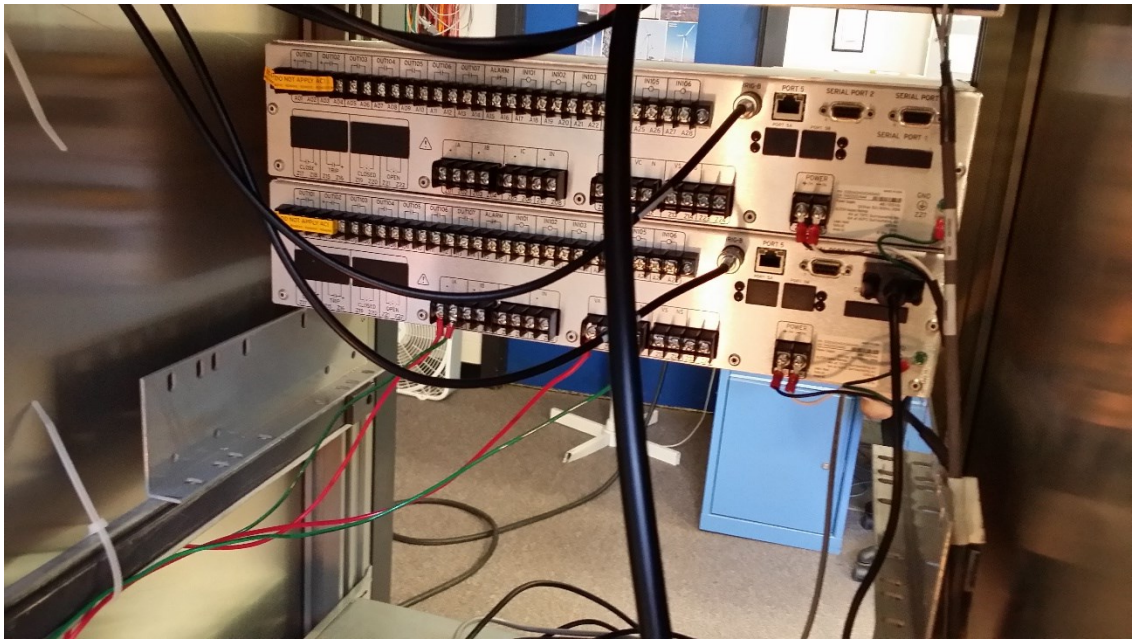

Figure 53. Rear View of the PMU Equipment.

The GPS clock is responsible for tracking time for the PMUs, but the GPS clock doesn't perform this task on its own. It depends upon satellite signals to verify its time tracking, and it receives the signals through an antenna, and the antenna is intended to be mounted outside. To avoid mounting the antenna outside, the antenna was mounted near a window without the bullet cap attached. This is shown in Figure 54.

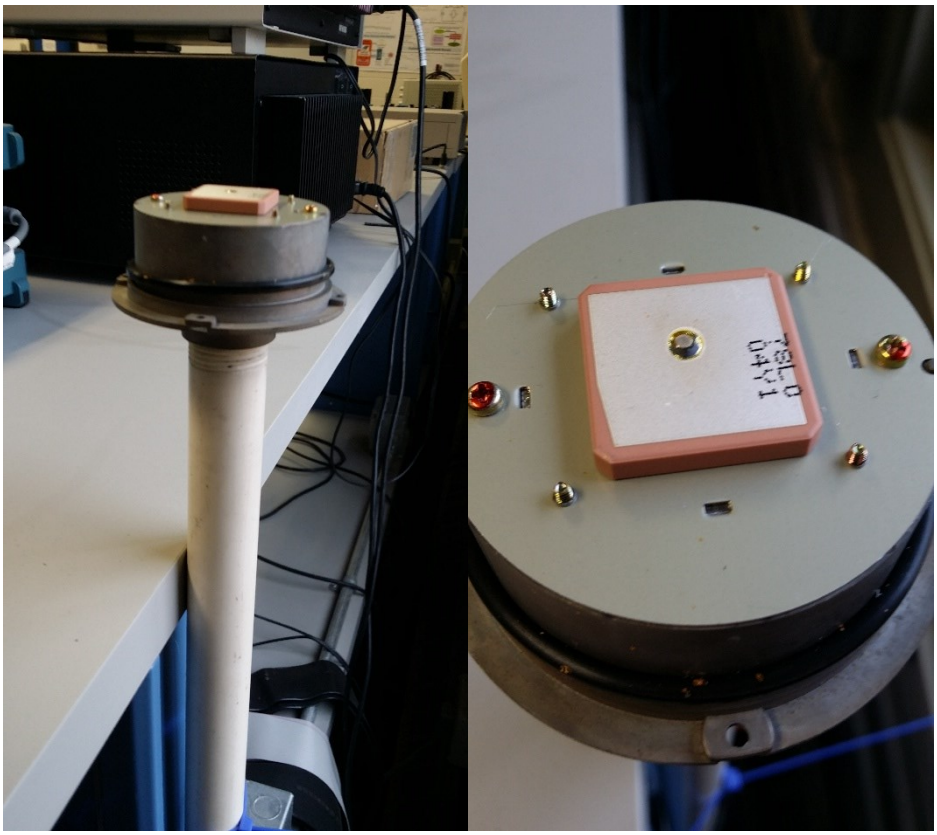

Figure 54. Bullet Antenna for Satellite Signal Reception.

When the GPS clock is receiving a consistent feed of information from the antenna, the GPS clock has a higher level of certainty concerning its time information. If the antenna has bad reception, the GPS clock is working purely from its internal time tracking. Any amount of error could stack up over time. If the feedback from the antenna was lost for a substantial amount of time, the GPS clock goes into a state of "holdover" until the signal is achieved again. During a full holdover, the red light on the front of the module will light up next to the status label. Occasionally, this will light up as an orange light, but that simply means that the timestamp is at risk. Figure 55 shows the GPS clock in good signal continuity, or satellite lock.

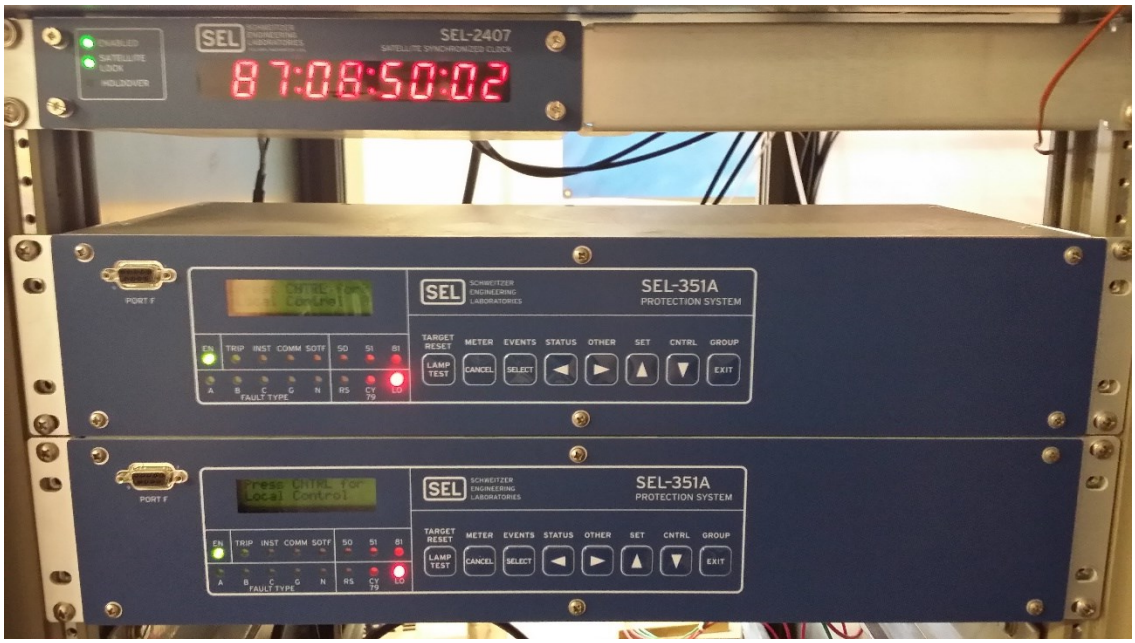

Figure 55. Front View of the PMU Equipment.

The above steps marked the completion of the hardware setup for the demonstration. However, there is a large amount of work involved in software settings. For the PMU relays, the laboratory computer was used for setting up the relay settings. To do this, the SEL Quickset program was used. Three primary groups were involved in the setup of the PMU. First, a number of "Global" settings were changed to correctly identify the operation that was desired. Synchrophasor measurements were enabled, and the measurements required for the demonstration were enabled. Some other settings were also changed to obtain the desired message size, message rate, and PMU identification. Second, a number of Group 1 settings were adjusted to correctly scale the incoming measurements. In a typical system, the measurements are preformed through potential and current transformers. In this demonstration, the voltage doesn't need the adjustment, but the transformer ratio was used for the current.

Finally, the Port 3 settings were configured for data transmission. In order to compare the data with the analysis from earlier sections, the message rate was set to 30 msg/sec. Figure 56 outlines the message size and baud rate for this message rate.

Message Description	Bits (Integer)	Bits (Float)
SYNC	16	16
FRAME SIZE	16	16
ID CODE	16	16
SOC (Timestamp)	32	32
FRACSEC (Fraction)	32	32
STAT	16	16
FREQ	32	32
DFREQ	32	32
ANALOG	0	0
DIGITAL	0	0
CHECK	16	16
VS	32	64
VA	32	64
VB	0	0
VC	0	0
IN	0	0
IA	32	64
IB	0	0
IC	0	0
Positive Seq Voltage	32	64
Positive Seq Current	32	64

Bit Total	368	528
Byte Total	46	66

MRATE 30 mesgs per second

Baud Rate	11040	15840

Figure 56. Message Size Calculation for the Configuration used in the Demonstration.

Ultimately, the baud rate chosen for the computer's USB port and the baud rate for Port 3 (UART) on the PMU was set to 57600. Some odd characteristics resulted from lower settings that were available (19200 and 38400 baud rate settings). Once the settings were finished, the visual tools were configured.

With the PMU configured and transmitting data, some interfaces were needed to display and archive the measurements being made. To do this, two software platforms were used. The primary platform used was the PMU Connection Tester software from the Grid Protection Alliance (GPA). This software is capable of reading PMU data in real-time, recording the data, and archiving the data. It is not a SEL product, but it works sufficiently with the standard IEEE C37.118-2005 data being provided. SEL has software available for the same function, but the product isn't freely available. Figure 57 shows a screen shot of the PMU Connection Tester software.

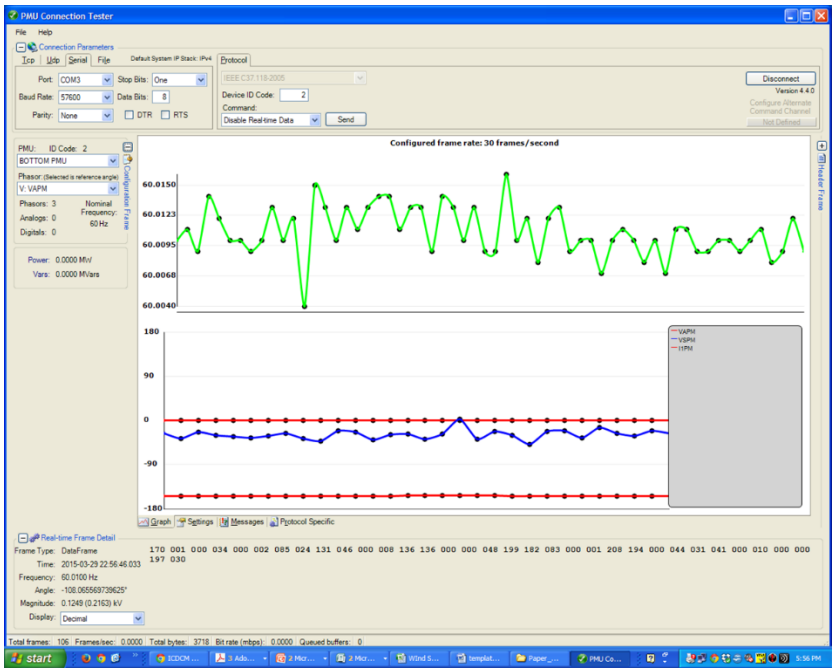

Figure 57. Visual Display of the PMU Connection Tester Software.

In Figure 57, the top graph is a display for frequency measurements. The bottom graph is a display for phase measurements. In that graph, there are three traces, and only two are displaying actual measurements. The red line that is at the zero axis is a floating voltage being used for reference (Phase Voltage VS). The blue trace is the measured voltage of the power system. The other red line toward the bottom of the graph is the measured current of the power system. The dialog box at the bottom describes the real-time message, or real-time data frame, details. This section can be used to monitor the magnitudes of the voltage and current.

The other software platform used to display the synchrophasor data was the SEL Quickset software. It has an application called the Human-Machine Interface, or HMI. In Figure 58, a sample of the displays available is shown. This display differs from the PMU Connection Tester, and the information is based on a different reference voltage (Phase A).

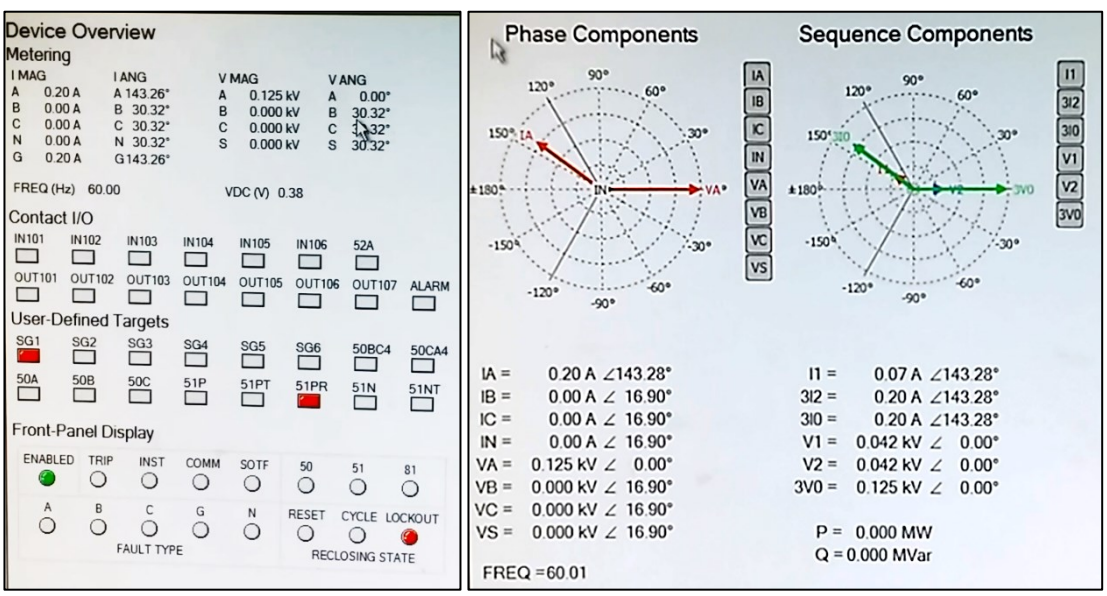

Figure 58. Visual Display of the Human-Machine Interface Application.

The PMU Connection Tester software has the capability to archive data through some additional applications. However, there is a process required to capture some interesting information. To record some measurements, the software was set up and archival was initiated. Then, the demonstration power system needed to be controlled manually. In a normal power system, the loads will change according to customer demand. In addition to those dynamic load changes, faults will naturally occur because of different system disturbances. For this contained system, these events need to be manually created. The load was dynamically changed using the dimmer switch on the light load, and the faults were simulated by the standard switch. Due to the manual effort of this demonstration, the duration of the data is only about a minute and a half. The above process was followed, and PMU data was recorded to a csv file for analysis.

In Figures 59 through 65, the PMU data that was recorded is displayed. There is only one PMU, and it is measuring a single phase (voltage and current). The voltage magnitude measurements are shown in Figure 59, and it clearly shows the "faults" created by turning the switch equipment off and on. Some voltage magnitude variations also took place, and these variations negatively correlate with the changing load. That was controlled with the dimmer switch. This can be better observed in Figure 60. The voltage phase measurements are shown in Figure 61, and it shows how the measurements become sporadic and meaningless after separating from the system. The current magnitude measurements are shown in Figure 62, and it also shows the "faults." It also shows that the current magnitude variations positively correlate with the changing load. The phase data is shown in Figure 63, and since current is used to regulate the load, the phase measurements of the current vary with changes in load.

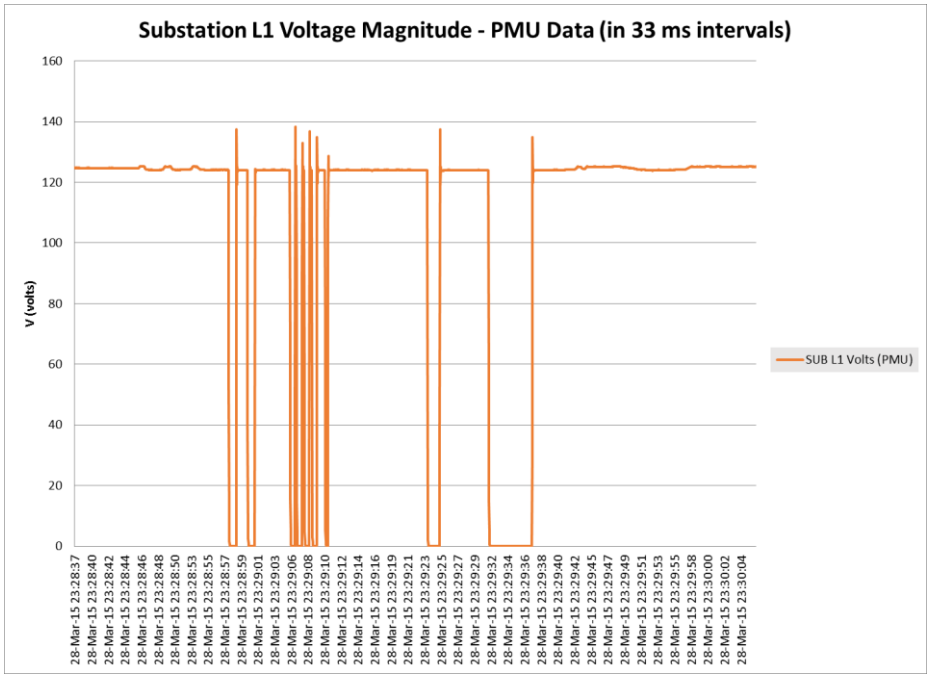

Figure 59. Voltage Magnitude at the Light Load during Random Load Changes and Faults.

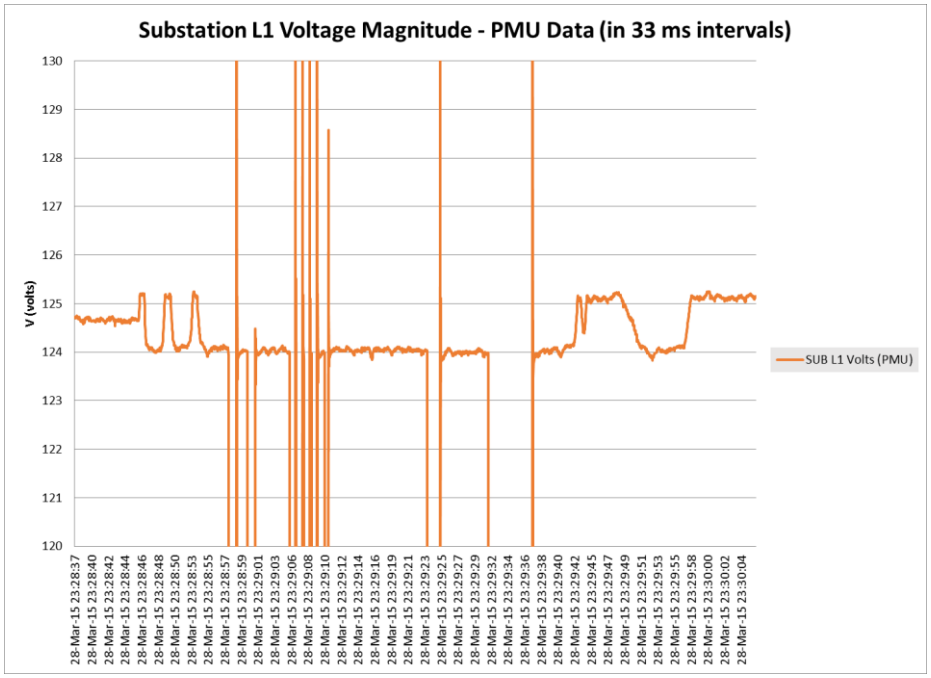

Figure 60. Voltage Magnitude at the Light Load during Random Load Changes and Faults (Zoom).

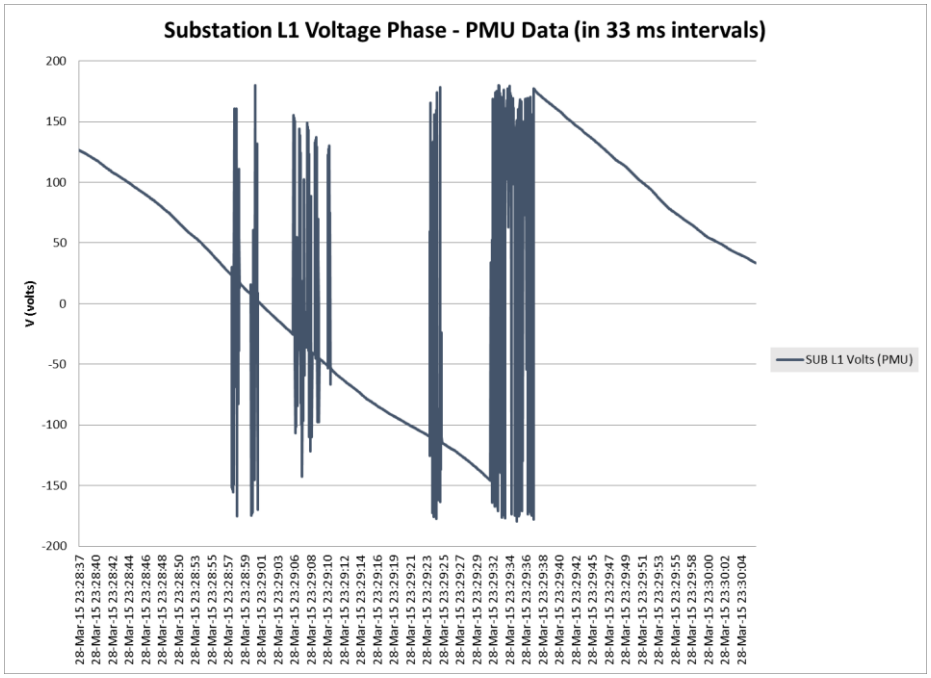

Figure 61. Voltage Phase at the Light Load during Random Load Changes and Faults.

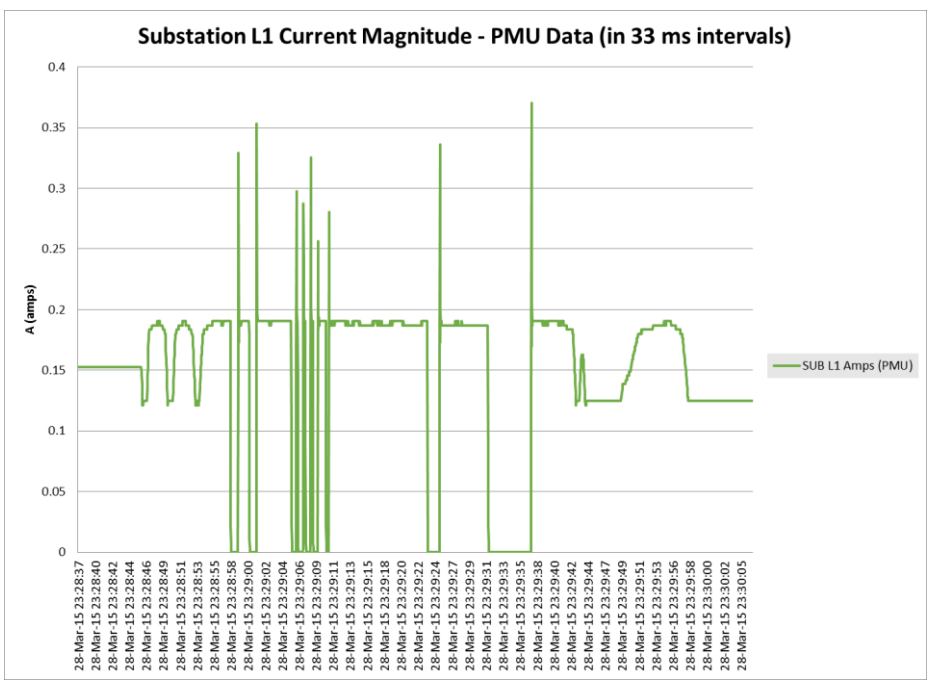

Figure 62. Current Magnitude at the Light Load during Random Load Changes and Faults.

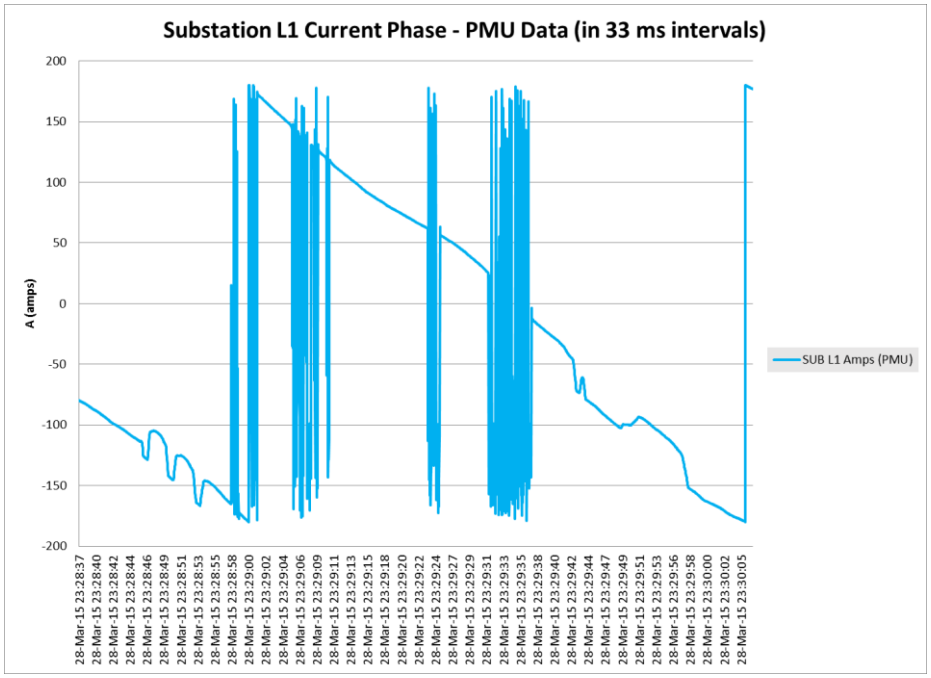

Figure 63. Current Phase at the Light Load during Random Load Changes and Faults.

The voltage magnitude data was approximately 125 V_{rms} when the system was intact, and the "fault" transients were approximately 140 V_{rms} at peak. Therefore, the measurements were close to the nominal measurement range, and the peaks were well within the continuous limit. The current magnitude data was approximately 0.20 A_{rms} when the system was intact, and the "fault" transients were approximately 0.37 A_{rms} at peak. Therefore, the measurements were within the nominal measurement range, and the peaks were well within the continuous limit. The current magnitude and phase were positively correlated with load level, and the voltage magnitude and phase were negatively correlated with the load level. In Figure 64, the frequency data is shown. In Figure 65, the rate of change in frequency is shown. Both figures show significant frequency transients corresponding to "fault" occurrences and loss of power to the load.

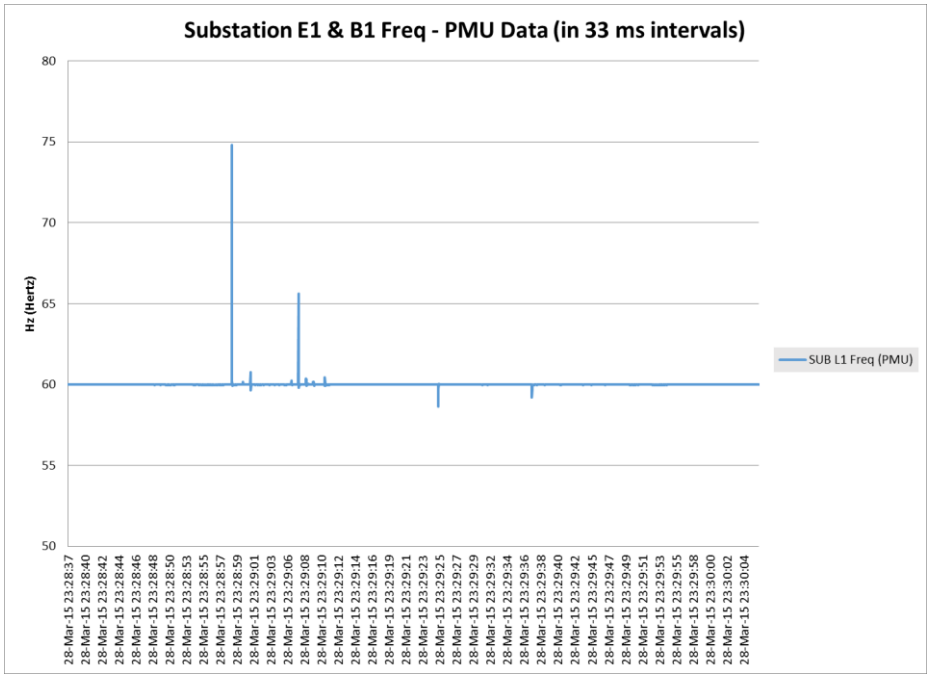

Figure 64. Frequency at the Light Load during Random Load Changes and Faults.

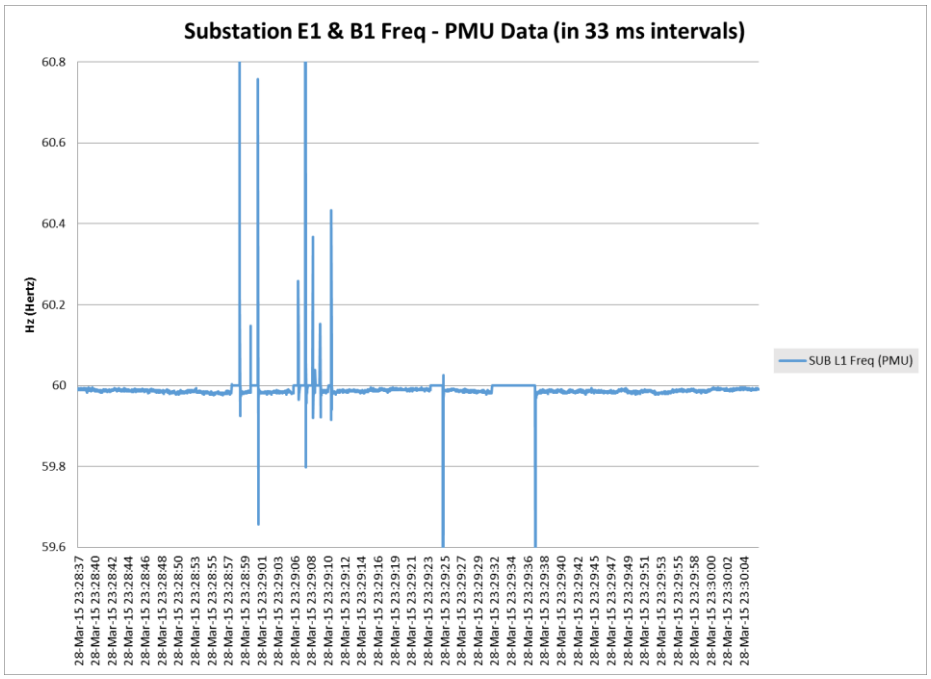

Figure 65. Frequency at the Light Load during Random Load Changes and Faults (Zoom).

MATLAB Simulink and dSPACE Investigation

In addition to the laboratory demonstration of a single phase system, the concept of power system simulation was discussed. The premise of this demonstration was to model a power system, convert it to a programmable board, and send the outputs of that model to PMU. The model would replace the laboratory demonstration's power system in this scheme. However, some problems were discovered in exploring this process. In the beginning of this investigation, an IEEE 14 bus system was imported into Simulink using the SimPowerSystems blocks. Figure 66 shows the model of the 14 bus power system.

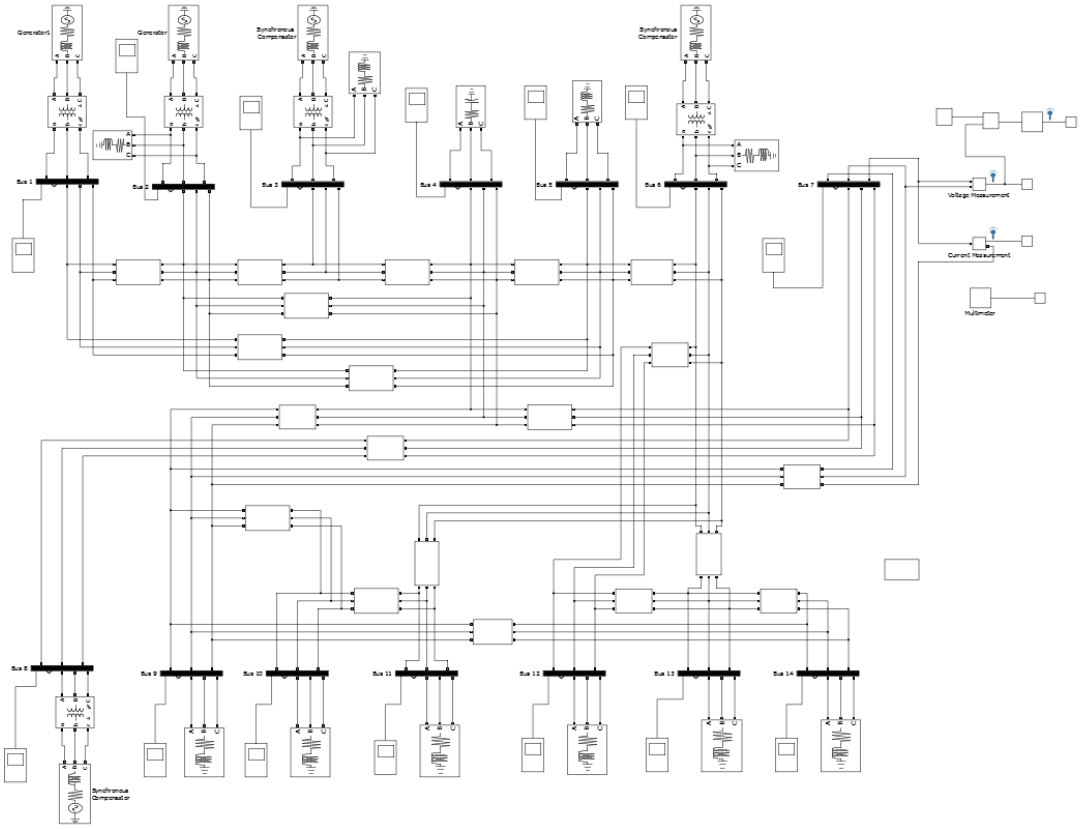

Figure 66. IEEE 14 Bus Power System Model in MATLAB Simulink.

The Simulink-based system compiles and runs as expected, and that is demonstrated by the voltage measurement shown in Figure 67. The model could potentially be configured for both synchrophasor and conventional RTU measurements. To satisfy that approach, the measurements could be set up to measure magnitude and phase at a high resolution (30 samples per second or faster), or the measurements could be set up to measure magnitude at a low resolution (a sample every two seconds). Different plots and other calculated measurements could be displayed through the Simulation Data Inspector and other applications. However, there are issues when implementing this model through a programmable dSP board.

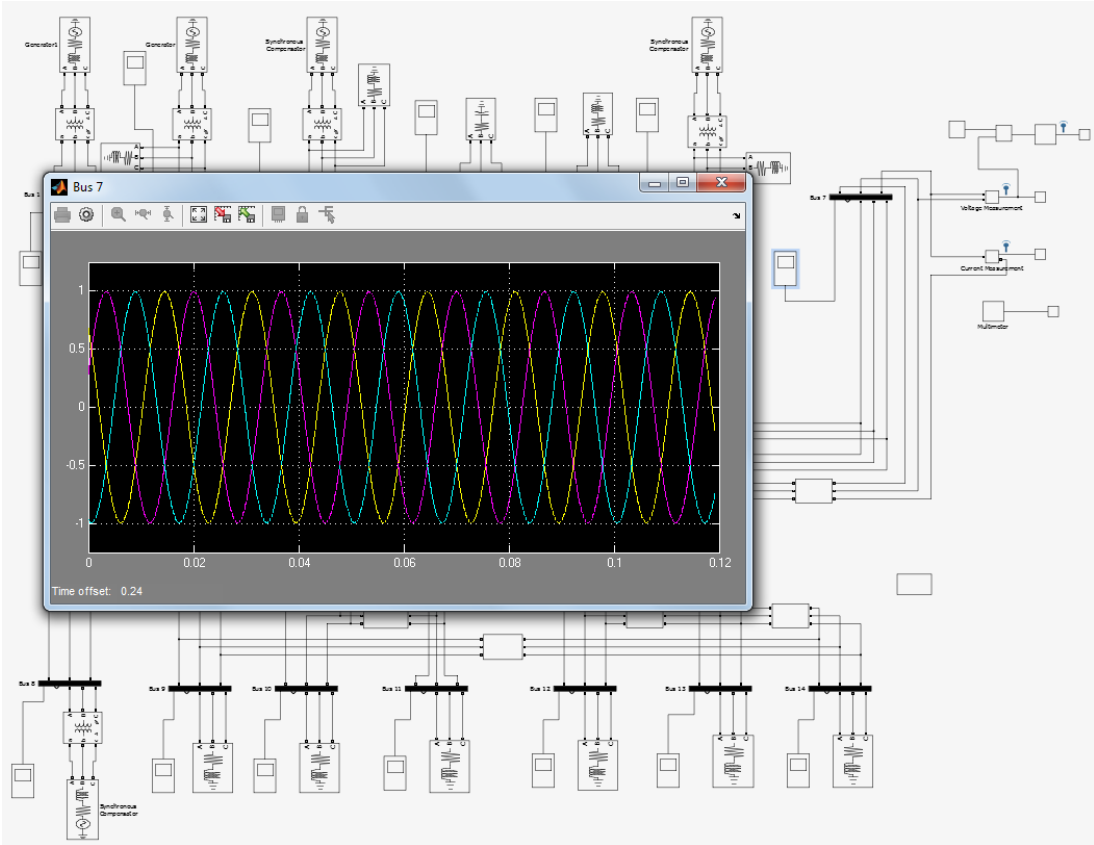

Figure 67. Voltage Measurement of the IEEE 14 Bus Power System Model at Bus 7.

In the dSP board available through dSPACE, models can be imported from MATLAB Simulink, but it can only accept certain blocks from the Simulink library. The models from the SimPowerSystems library are not allowed in the dSPACE architecture. So, an alternative approach was investigated. The new method was to create a Simulink model that simply uses some "From Workspace" blocks to cycle some previously recorded PMU data through the dSPACE as shown in Figure 68. This method does work, but the transmission of that data from the I/O board is difficult to do. The outputs on that board are typically for digital communication and PWM signals. Voltage measurements and current measurements that are passed to the PMU need to be analog in nature. This creates an issue when trying to utilize the dSPACE for PMU measurement.

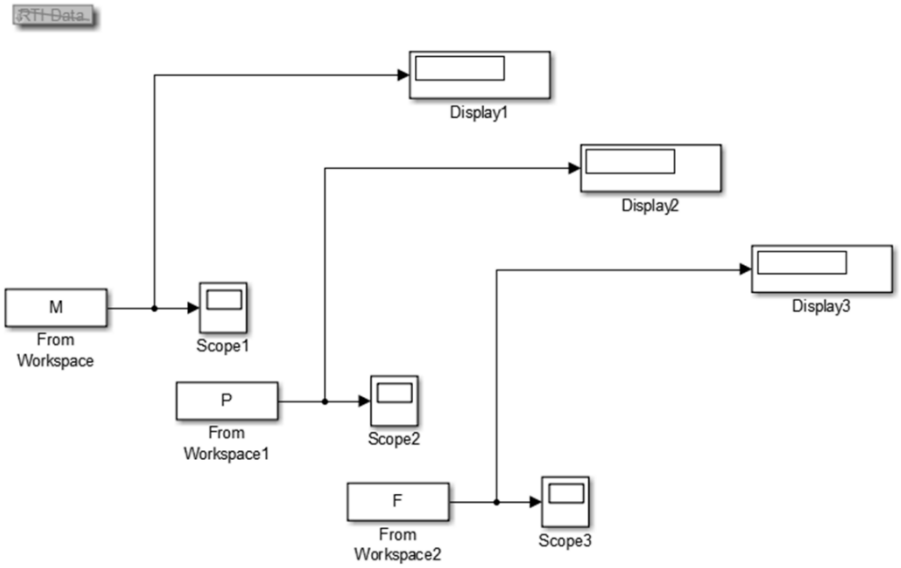

Figure 68. MATLAB Simulink Model that Utilizes the "From Workspace" Blocks for PMU Data.

In summary, the correct equipment may allow such a system to be created and used for demonstration, but the dSPACE system is incapable of this operation in its current form. The standard method for creating a power system model in Simulink is incompatible with the dSP board, and the voltage of the dSPACE outputs is incompatible with the requirements of the PMU measurement inputs. The alternate model method shows promise for bypassing the Simulink model issues, but the output of the dSPACE system would require some more electronics to support the measurement requirements for the PMUs.

The PMUs perform quite well when a physical model is available, and future efforts at the University of North Dakota could benefit from this foundational work. If a physical power system was available to the Department of Electrical Engineering, such a system would be a very clear application for this equipment. In addition to that opportunity, some electronics could be developed for the output of the dSPACE I/O board. With a compatible converter to match the dSPACE outputs with the PMU inputs, a MATLAB Simulink model could be simulated, and PMU measurements could be taken by using a hardware-in-the-loop scheme. This may prove to be more useful for a range of simulations that cover a variety of events. The specific details describing this simulated system would also be available, and that information would allow for additional investigation such as state estimation, stability analysis, contingency analysis, and other analysis types.

CHAPTER IV

RESULTS

To demonstrate the value of synchrophasors, some higher level analysis can be used. Data analysis, simulation, and mathematical concepts are all potential methods for evaluation, but in this research, data analysis and mathematical concepts were the primary methods. Chapter III had an extensive display of measurement data comparisons, and the narratives of these events were described. By doing that, the data analysis portion of the evaluation was performed. However, mathematical concepts are yet to be addressed. In this chapter, the emphasis is directed toward some mathematical concepts that may be employed with synchrophasor measurements.

Measures for this mathematical evaluation include frequency response for event (and interference) identification, frequency response for generation loss identification, and total vector error. In the analysis performed, it has been found that frequency can be directly linked to certain fault events. If the right system information is available, it can also be connected with the loss of generation. In terms of total vector error (TVE), it also requires the use of system information. This presents a problem under the constraints of this research. TVE is typically a measure of error that compares the synchrophasor measurements with a state estimator. To create a state estimator, an intimate knowledge of the electric power system is required. This information is

sensitive, and cannot be provided to personnel outside of the utility or regional planning/operational entities. As an alternative, synchrophasor measurements were compared to the conventional measurements instead (alternative TVE, or ATVE).

Frequency Response for Event Identification

In the next couple of plots, the data represents Fourier analysis of the line outage event described in Chapter II. In this event, a line tripped out that was carrying a significant amount of power flow. PMU data from two separate locations was analyzed. One of them was at a wind farm with low output power at the time of the event. The other was from a transmission substation with a heavily loaded transformer. The substation is approximately 50 miles south of the wind farm.

In Figures 69 and 70, Fourier analysis of the frequency data from the PMUs is shown. In Figure 69, the Fourier analysis of the transmission substation voltage data from the PMUs is show. In Figure 70, the Fourier analysis of the wind farm voltage is shown. The timeframe displayed in these figures corresponds to 4096 (2^{12}) samples. This sample was chosen for ease of calculation with the format of Fourier analysis chosen (Microsoft® Excel's Data Analysis Toolbox). Those samples include the 30 second timeframe that was referenced in the Line Outage section of Chapter II (that 30 seconds corresponds to an approximately 910 samples).

In both figures, the Fourier analysis clearly shows three dominant frequencies during the event. Two notable differences can be seen between the two figures. First, the FFT magnitude levels are different, and this is only due to the voltage level differences at each location (345 kV and 138 kV, respectively). Second, the dominant frequencies change order. Regardless, the dominant frequencies are approximately

59.9 (nearly nominal), 60.0 (nominal), and 58.9 Hz. The third frequency component clearly shows a drop in the system frequency, especially when comparing it to the spectrum shown in the figures.

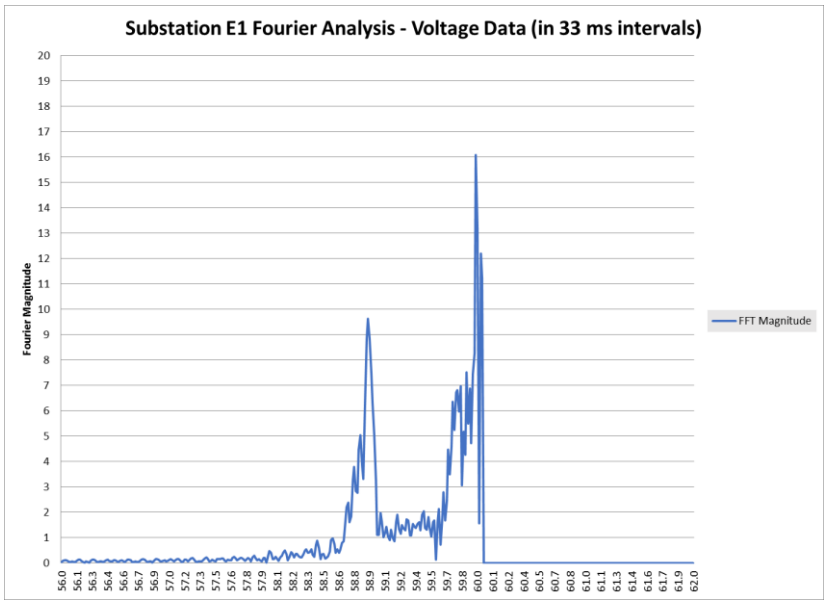

Figure 69. Fourier Analysis of Voltage (Substation E1) during a Line Outage.

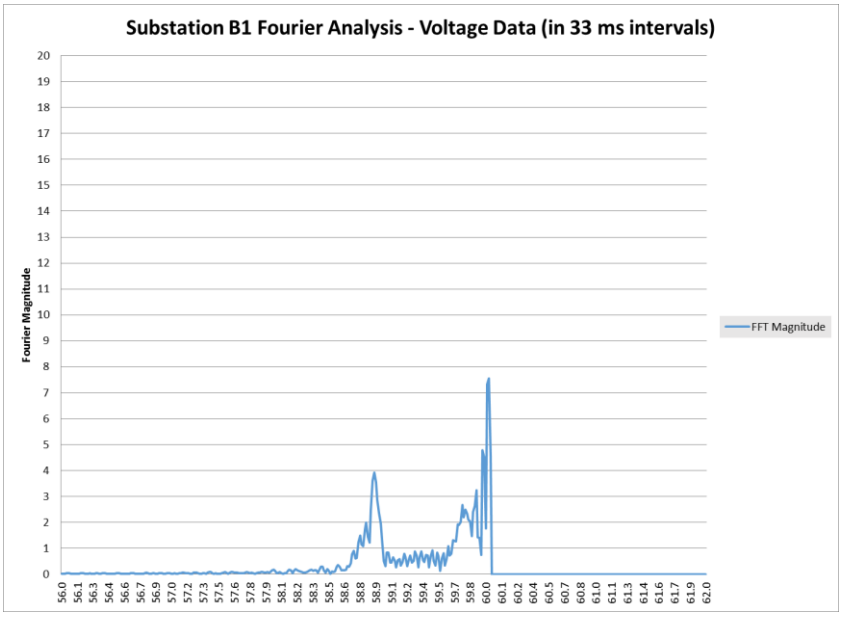

Figure 70. Fourier Analysis of Voltage (Substation B1) during a Line Outage.

In the next couple of plots, the data represents Fourier analysis of the baseload generation outage event described in Chapter II. In this event, multiple high voltage line trips occurred during a severe storm. This resulted in a baseload unit tripping offline, and other generation units were left in a state of "rocking" due to the stresses following the lost transmission and generation. PMU data from three separate locations was analyzed. One of them was at the interconnection line for the generation unit that tripped offline, and the other two were at interconnections of the other generators that are left in a state of "rocking" as a result of the stresses.

In Figures 71 through 73, Fourier analysis of the frequency data from the PMUs is shown. In Figure 71, the Fourier analysis of the baseload generation (the unit that tripped offline) voltage is shown. In Figures 72 and 73, the Fourier analysis of the "rocking" generation voltage is shown. The timeframe displayed in these figures corresponds to 4096 (2^{12}) samples. Those samples include the 30 second timeframe that was referenced in the Baseload Generation Outage section of Chapter II (that 30 seconds corresponds to an approximately 910 samples).

In these figures, the Fourier analysis reveals a range of dominant frequencies during the event. Although the FFT magnitude levels are different, this is due to the voltage level differences at each location (345 kV, 345 kV, and 138 kV, respectively). The dominant frequencies range from 59.7 Hz to 60.0 Hz. The frequencies are nominal (or nearly nominal) frequency components of the system. This would imply that there is no real issue. However, the frequency components are all significant in terms of the spectrum. The figures show a fairly compelling range of variation on the system frequency. This implies that the "rocking" may negatively impact system equipment.

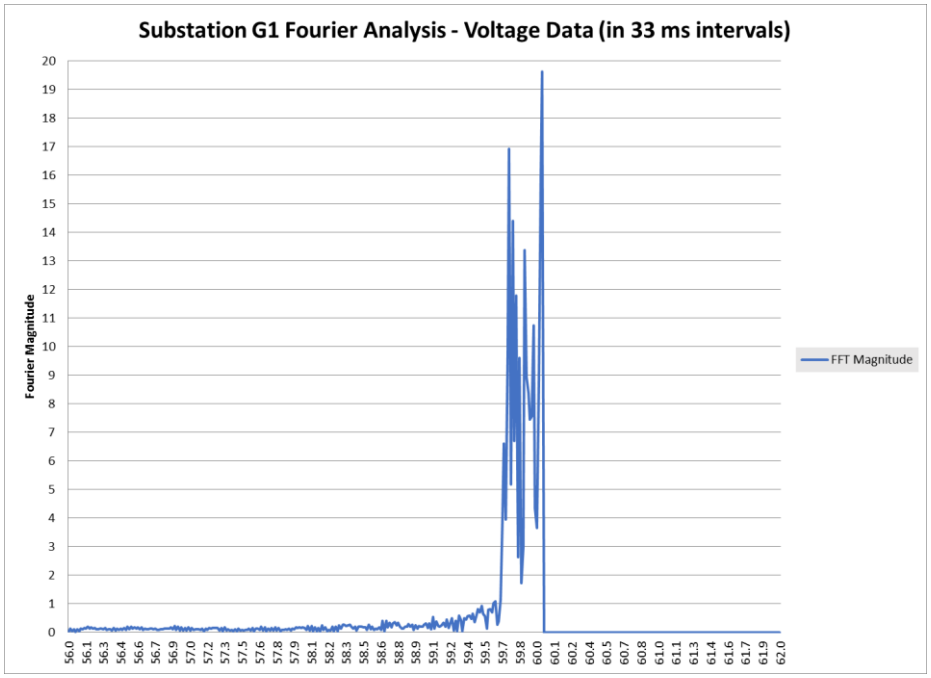

Figure 71. Fourier Analysis of Voltage (Substation G1) during a Generation Outage.

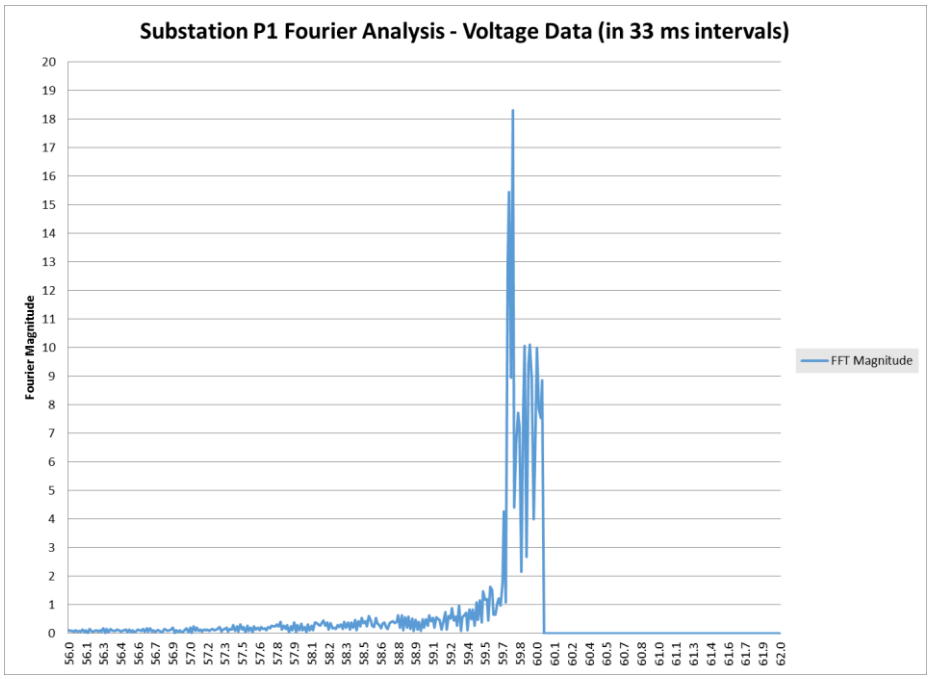

Figure 72. Fourier Analysis of Voltage (Substation P1) during a Generation Outage.

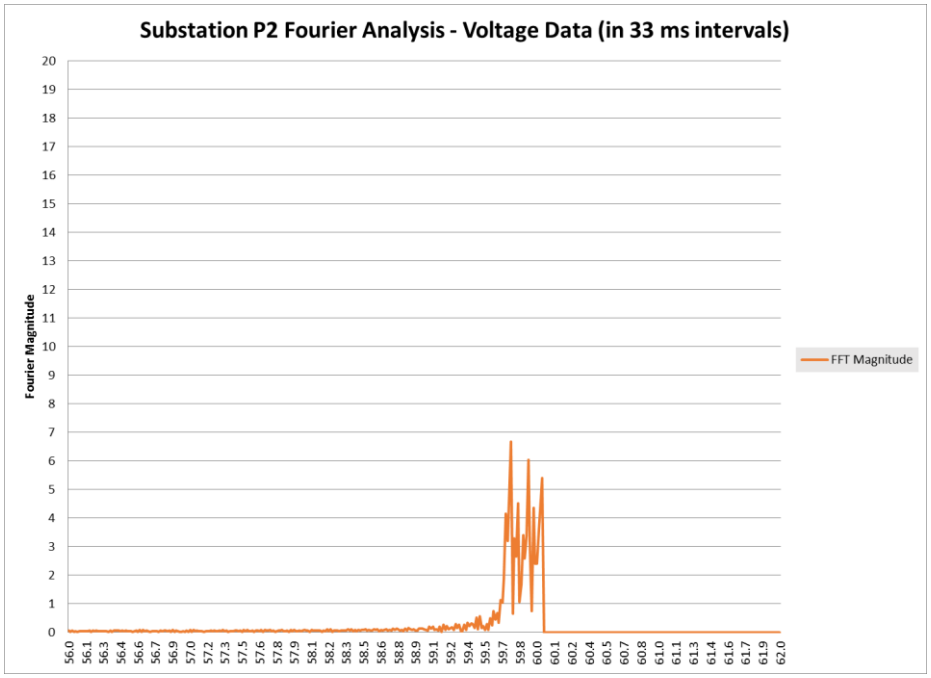

Figure 73. Fourier Analysis of Voltage (Substation P2) during a Generation Outage.

Overall, the Fourier analysis reveals that access to the entire signal and its characteristic can provide insight into the frequency spectrum being experienced by the bulk electric power system. With convention measurement, magnitude measurements and frequency measurements are available, but the two cannot be combined to recover the entire signal characteristic. With synchrophasor measurements, the phase measurements are also available, and that makes it possible to monitor all characteristics of the signal (at higher resolution). That allows more flexibility in terms of Fourier analysis. When the Fourier analysis is performed, some dominant frequencies are identified over time. In the line outage, it clearly impacted the standing frequency for an extended period of time. In the generation outage, the frequency became erratic, even though the standing frequency stayed reasonably close to nominal.

Frequency Response for Generation Loss Identification

In this analysis, the Baseload Generation Outage event from Chapter II is being considered. In this event, multiple high voltage line trips occurred during a severe storm. This resulted in a baseload unit tripping offline, and other generation units were left in a state of "rocking" due to the stresses following the lost transmission and generation. PMU data from three separate locations was analyzed. One of them was at the interconnection line for the generation unit that tripped offline, and the other two were at interconnections of the other generators.

In order to analyze the frequency response after a generation loss, information about system inertia and other system parameters is required. As shown in the equation below, the inertia constant (H) of the power system is related to the system's baseload level, frequency, and power imbalance (mechanical power versus electrical power). This equation is derived from mathematical representations of a synchronous generator.

$$H = \frac{(P_m - P_e) \cdot f}{\left(2 \cdot \frac{df}{dt} \cdot MW_{base}\right)} \qquad (1)$$

This analysis is difficult to perform under the confidentiality constraints that are in place. Under the current arrangement, masked data and narratives that describe a variety of events have been provided. However, the exchange of critical information that describes the system is prohibited. So, some general information was recovered from publicly available data concerning the region. Specifically, the baseload level for the region being analyzed is roughly 18 GW at peak. In this off-peak scenario, it is reasonable to estimate that the load is about 65% of the peak (11.7 GW). All of the other information is available (frequency is 60 Hz and power imbalance is 350 MW).

Some of the other information requires some higher level understanding of the event. For the moment following the event, the change in frequency needs to be understood. In order to do that, the minimum frequency following the event and the frequency leading up to it must be taken. Figure 74 shows the basis of this information.

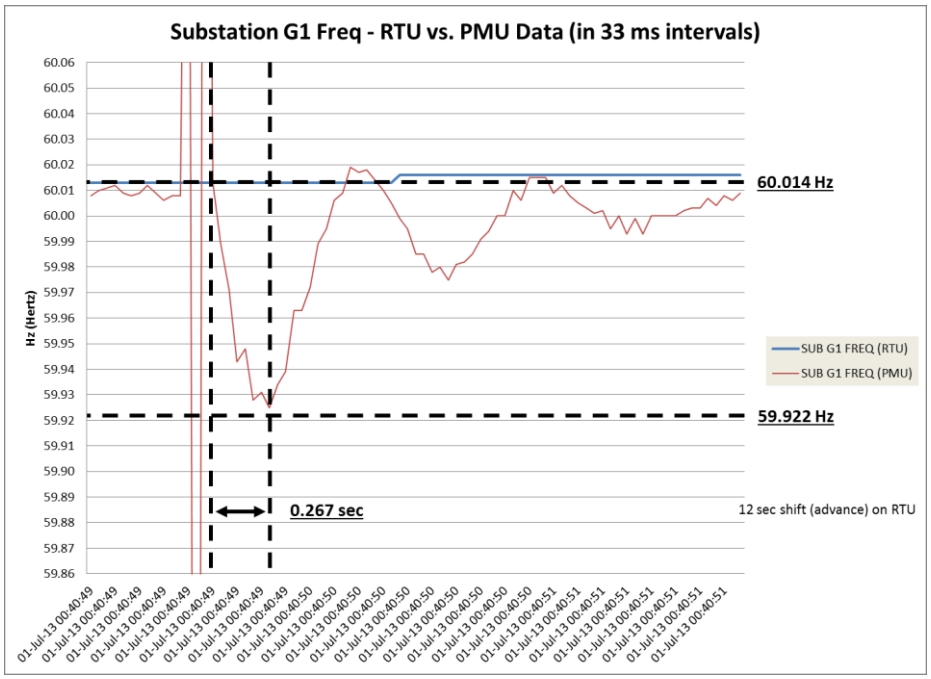

Figure 74. Change in Frequency over Time during Governor Response after a Generation Outage.

In addition to that, the time that passes between those two frequencies must also be taken. This time refers to the governor response. The result of that extraction of information is the change in frequency over time, or df/dt.

$$\frac{df}{dt} = \frac{(59.922 - 60.014)Hz}{(0.267)sec} \approx -\frac{11}{32}\ Hz\ per\ second \qquad (2)$$

The time that it takes for the tripped generation to settle is also required, as shown in Figures 75 and 76. After the outage, the system compensates for the loss. Other generation is dispatched to the area, resulting in governor and AGC response.

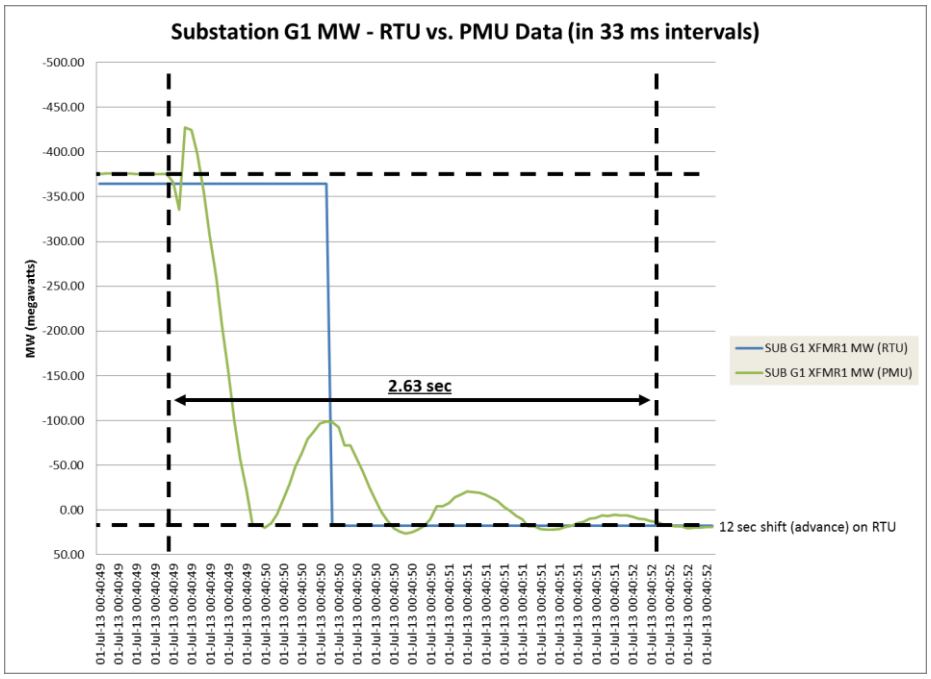

Figure 75. Settling Time during Governor and AGC Responses after a Generation Outage.

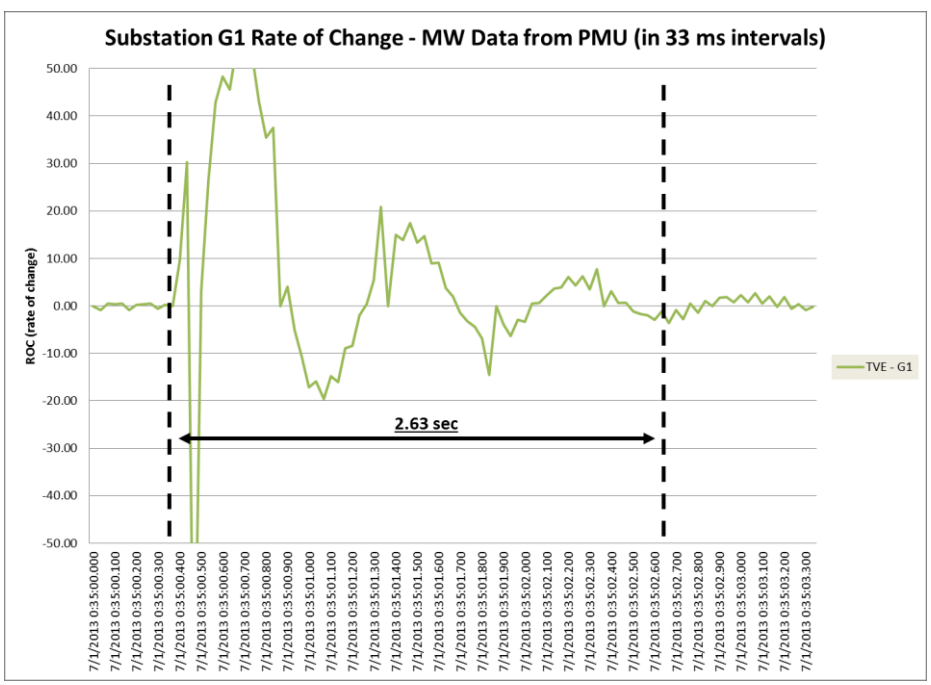

Figure 76. Settling Time after a Generation Outage - Rate of Change of the Real Power.

Using that information, Equation (1) can be used to estimate generation loss according to the frequency response and system characteristics. Although this is information that can be monitored at the generation interconnection itself, this is useful for events where that information is unavailable (e.g. another utility's generation).

$MW_{base} = 11.7\ GW$ $\qquad f = 60\ Hz$ $\qquad \frac{df}{dt} = -\frac{11}{32}\ Hz\ per\ second$

$$H = \frac{(P_m - P_e)\cdot f}{\left(2\cdot\frac{df}{dt}\cdot MW_{base}\right)} = \frac{(P_m - P_e)\cdot(60\ cycles/sec)}{\left(2\cdot\left(-\frac{11}{32}\ cycles/sec^2\right)\cdot(11.7\ GW)\right)} \tag{3}$$

$$H = \frac{(P_m - P_e)\cdot(-7.44\ sec)}{(GW)} \tag{4}$$

$Assuming\ H = 2.63\ seconds\ \ldots$

$$Loss\ of\ Generation = (P_m - P_e) = \frac{H\cdot(GW)}{(-7.44\ sec)} = \frac{(2.63\ sec)\cdot(GW)}{(-7.44\ sec)} \tag{5}$$

$$Loss\ of\ Generation = (P_m - P_e) \approx -0.35\ GW \tag{6}$$

This example appears to be a reasonable method for analyzing the loss of generation to the system. Although there are some assumptions made in this demonstration, they are based on factual information. The assumptions are simply used as a basis for this mathematical operation. This frequency response measure appears to have value if the baseload level of the system is known.

The value of this measure would be most useful for regional dispatch without the availability of power flow information. In conventional generation dispatch, frequency is used in conjunction with power flow information. If power flow information is available, it's well suited for generation dispatch. In the absence of power flow information, frequency can provide some insight during outages.

Alternative Total Vector Error (ATVE)

Total vector error, or TVE, is an industry standard for accuracy on synchrophasor (PMU) measurements. It is described by the IEEE C37.118.1a-2014 standard. It states that the data must be within 1% of error when compared to the estimates of the power system's state estimator. The equation for TVE is shown below.

$$TVE(n) = \sqrt{\frac{\left(\hat{X}_r(n) - X_r(n)\right)^2 + \left(\hat{X}_i(n) - X_i(n)\right)^2}{\left(\left(X_r(n)\right)^2 + \left(X_i(n)\right)^2\right)}} \qquad (7)$$

$\hat{X}_r(n)\ and\ \hat{X}_i(n) = Real\ \&\ Imaginary\ Measurement\ Components\ from\ a\ PMU$

$X_r(n)\ and\ X_i(n) = Real\ \&\ Imaginary\ Estimates\ Components\ from\ a\ State\ Estimator$

The state estimator requires the use of system information. This presents a problem under the constraints of this research. As shown in Equation (7), TVE is a measure of error that compares the synchrophasor measurements with estimates from a state estimator. To create a state estimator, an intimate knowledge of the electric power system is required. This information is sensitive, and cannot be provided to personnel outside of the utility or regional planning/operational entities. Implementing a state estimator is an intensive process that requires substantial investment. Appropriate software, comprehensive system characteristics, and implementation time is required to make a state estimator. That makes it difficult to invest in a state estimator for synchrophasor measurements. That creates a problem for evaluating a new synchrophasor measurement system. However, there may be value in alternative total vector error measures. So, an alternative was used to evaluate synchrophasor (PMU) measurements against conventional (RTU) measurements. As shown in Equation (8), this method will be referred to as the alternative total vector error, or ATVE.

$$ATVE(n) = \sqrt{\frac{\left(\hat{X}_r(n) - \tilde{X}_r(n)\right)^2 + \left(\hat{X}_i(n) - \tilde{X}_i(n)\right)^2}{\left(\left(\tilde{X}_r(n)\right)^2 + \left(\tilde{X}_i(n)\right)^2\right)}} \qquad (8)$$

$\hat{X}_r(n)$ *and* $\hat{X}_i(n)$ = *Real & Imaginary Measurement Components from a PMU*

$\tilde{X}_r(n)$ *and* $\tilde{X}_i(n)$ = *Real & Imaginary Measurement Components from a RTU*

In the next couple of plots, the data represents ATVE analysis of the line outage event described in Chapter II. In Figure 77, the ATVE analysis of apparent power is shown. The transmission substation (Substation E1) with the heavily loaded transformer has a relatively low ATVE (approx. 0.55%) throughout the timeframe. During the line outage, a spike in error can be observed (approx. 3.95%). The wind farm substation (Substation B1) has a relatively high ATVE (approx. 9.55%).

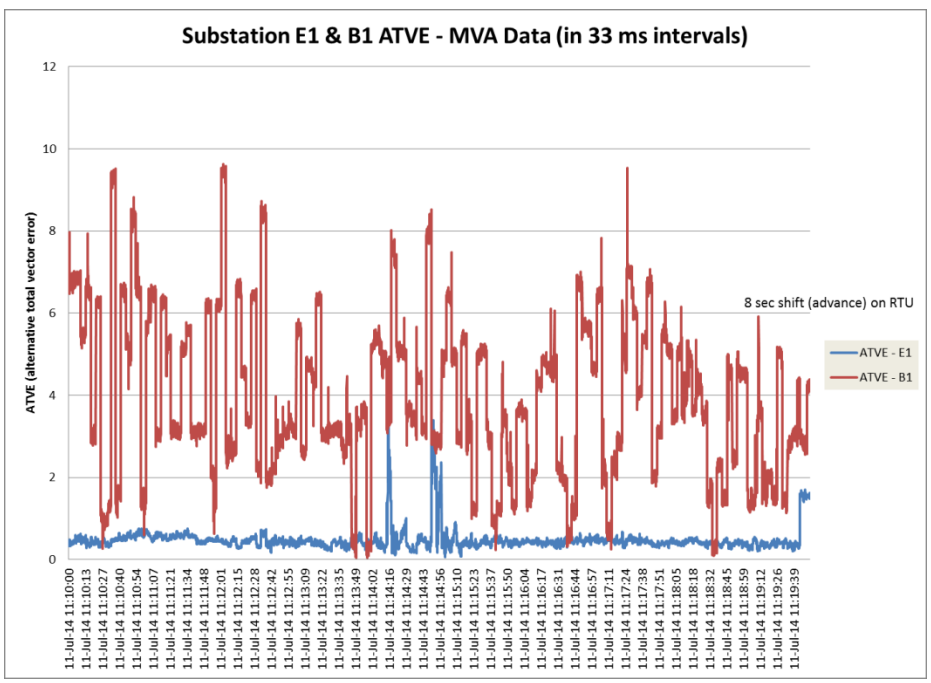

Figure 77. Alternative Total Vector Error of Power Measurement during a Line Outage.

Two notable details can be observed in Figure 77. First, the disparity between Substation E1 and B1 can be described by the power flow experienced at each substation. When the measurements are of high magnitude (Substation E1), the small inaccuracies (calibration, etc…) that impact the measurements do not have a significant impact. However, when the measurements are low (Substation B1), the small inaccuracies at each stage of measurement are capable of significant error implications.

In Figure 78, the ATVE analysis of voltage is shown. In this analysis, both substations have relatively low values of ATVE. The voltage ATVE at Substation E1 is approximately 0.35%, and the voltage ATVE at Substation B1 is approximately 0.22%. During the line outage, a spike in error can be observed at both substations (approx. 1.15%). This is outside of 1% error, but data resolution may have caused it.

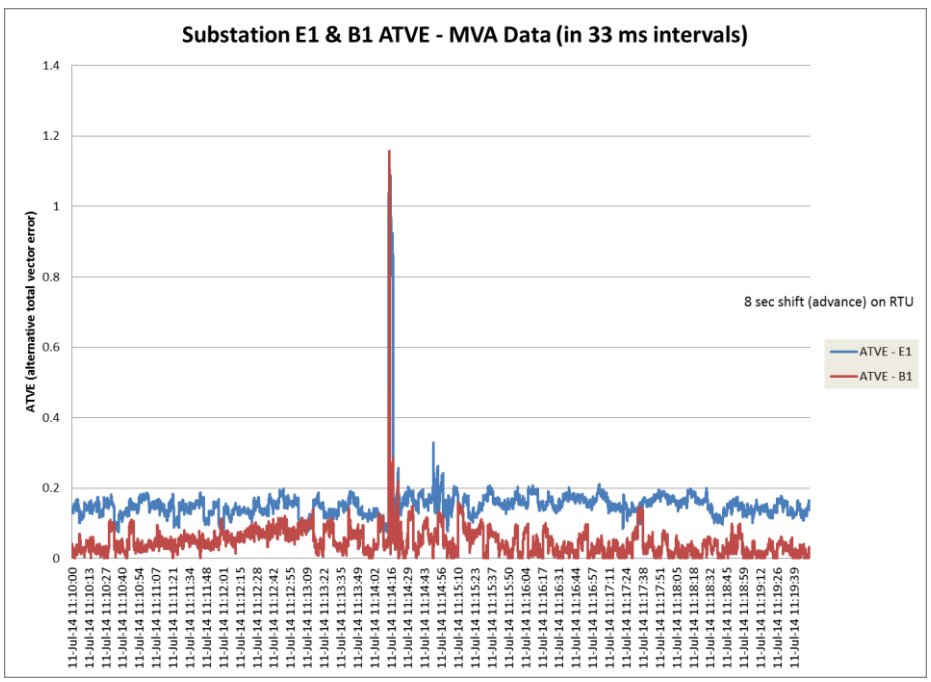

Figure 78. Alternative Total Vector Error of Voltage Measurement during a Line Outage.

In the next couple of plots, the data represents ATVE analysis of the baseload generation outage event described in Chapter II. In Figure 79, the ATVE analysis of apparent power is shown. The interconnection for the generator that trips offline (Substation G1, 350 MW) has an ATVE of approximately 3.25% prior to the outage. During the line outage, an extreme spike in error can be observed, and the error settles out at about 15%. The 1200 MW interconnection (Substation P1) has an ATVE of approximately 2.65%. Although there are some outliers throughout the timeframe, it stays roughly in the range of 2.65%. The 110 MW interconnection (Substation P2) has an ATVE of approximately 13%, consistently (despite some outliers, similar to P1). It appears that the ATVE at these locations is inherently higher. Before this event, the only location that has reasonable error is the 1200 MW interconnection (Substation P1).

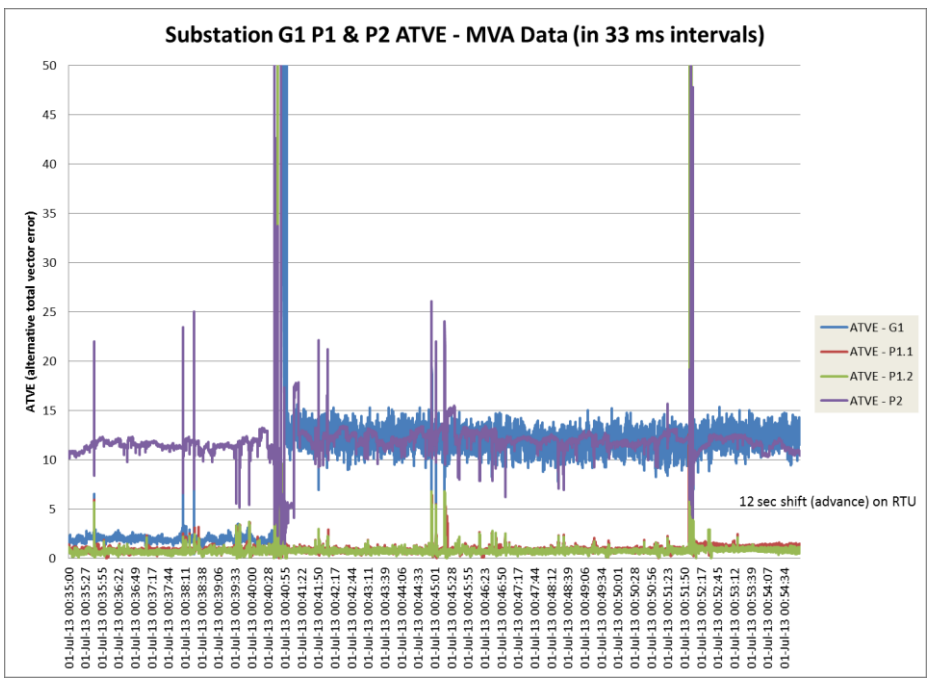

Figure 79. Alternative Total Vector Error of Power Measurement during a Generation Outage.

Three notable details can be observed in Figure 79. First, the 1200 MW interconnection (Substation P1) is the only location where the error is close to 1% throughout the event. That isn't surprising when comparing its size to the other generation. Second, the 350 MW generation that trips offline (Substation G1) has an ATVE that is comparable to Substation P1, but the error is inflated after the outage. As stated earlier, higher measurements aren't significantly affected by small inaccuracies (calibration, etc…). However, lower measurements are affected by small inaccuracies. The ATVE of Substation G1 becomes more comparable with the error of the 110 MW generation (Substation P2). Third, the ATVE of the 110 MW generator is significantly high throughout the event. The primary concern that shows up in this scenario relates to the extremely high error for the 110 MW generator. Upon further investigation, it appears to be a problem with the reactive power flow at the 110 MW generator. Referring back for Figure 34, it clearly displays the inconsistency between conventional and synchrophasor measurements.

In Figure 80, the ATVE analysis of voltage is shown. In this analysis, all of the substations have relatively low values of ATVE. The voltage ATVE at Substation G1 is approximately 0.28% (0.78% after the outage), and the voltage ATVE at Substation P1 and P2 is approximately 0.72%. During the generation outage, many spikes in error can be observed at all substations (approx. 11.40% for most of the spikes and between 30-50% at the instant of the outage). Outside of the irregular spikes in error, the voltage ATVE is within 1% error. Again, the spikes may have been a product of incompatible data resolution. At the error spikes, the synchrophasor data may not be in alignment with updated measurements taken from conventional technology.

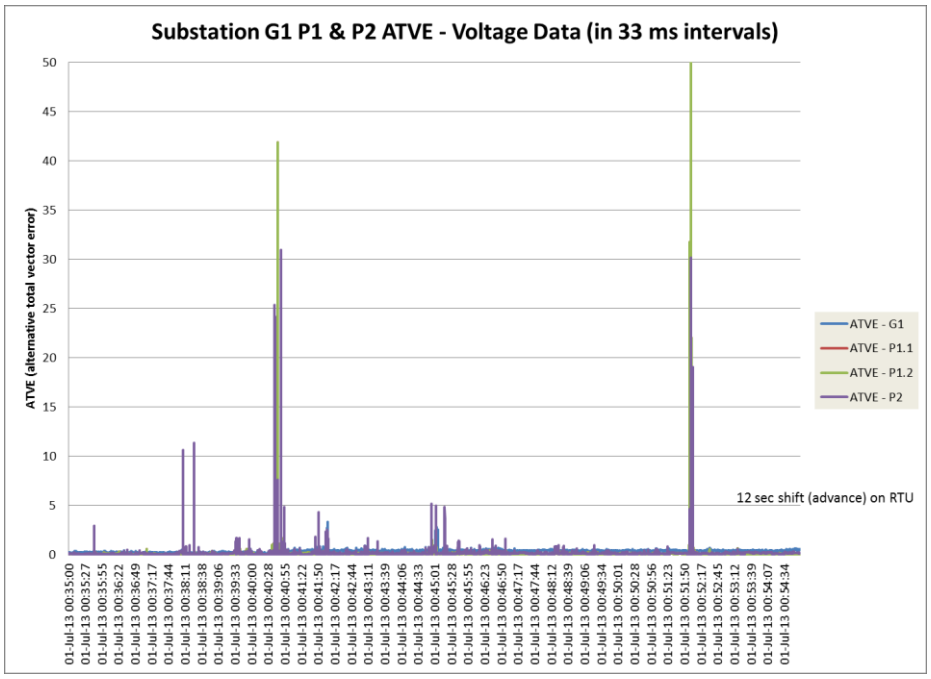

Figure 80. Alternative Total Vector Error of Voltage Measurement during a Generation Outage.

CHAPTER V

DISCUSSION

Faults and Outages

Synchrophasor measurements differ from conventional measurement in two particular areas: the availability of phase angle measurement and data resolution. These two aspects are particularly beneficial for monitoring and analyzing dynamic events. Synchrophasor technology provides a more comprehensive collection of measurements at higher resolution. This faster, more detailed information is beneficial to earlier assessment of faults and outages. In the case of system awareness, the higher resolution cuts down on the utilities exposure to system "blindness" during unique events. Frequency swings and voltage dips (or spikes) are more easily monitored with a higher data sampling rate.

As described in the events in Chapter II and IV, the frequency data from synchrophasors provides much more insight than the information from conventional measurement. This information is more easily correlated to the power flow information. In that aspect, the stages of frequency response can provide supporting information to the inertia response, governor response, and AGC response of the power system. Even if the system appears to have compensated for the loss of a facility, there are instances of instability that can be monitored with more information.

Power Quality

This faster, more detailed information is beneficial to earlier assessment of power quality issues as well. In the case of system awareness, the higher resolution cuts down on the utilities exposure to system "blindness" during unique events. Occasionally, natural events cause some significant impacts to the bulk electric power system. Interference and harmonic noise can result from these events. Although these issues may not result in the loss of a facility, the issues can result in the degradation of power quality. Frequency swings and voltage dips (or spikes) are more easily monitored with a higher data sampling rate.

As described by the significant storm event in Chapter II, the voltage data from synchrophasors provides much more insight than the information from conventional measurements. This information is more easily correlated to problems with power quality. The satisfaction of a utility's customers is important, and this information has the potential to improve that service. Even if the system appears to be performing well, the impacts of voltage instability can be profound on the end-use equipment.

Equipment Failure

This faster, more detailed information is beneficial to earlier assessment of equipment failure in some situations. Some equipment failures are not an immediate event, and the fault will "hang" until the equipment is destroyed. Interference and harmonic noise can result from these events. Depending on the implementation of some devices, voltage magnitude measurements are not sufficient in diagnosing the corrective actions for an event. Phasor measurements may improve system awareness during these events, and these measurements are available with synchrophasors.

As described by the catastrophic outage event in Chapter II, the voltage data from synchrophasors provides insight that conventional measurement does not. This information shows the voltage drop and the phase angle difference issues throughout the transformer fault, and the phasor data could have provided an earlier diagnosis.

Physical and Simulated System Demonstrations

The laboratory demonstration revealed some interesting discoveries. After the acquisition of the synchrophasor equipment, a couple of issues came to surface in the early stages of implementation. First, the communication link between the GPS clock and the satellites created some issues. The entire system relies on the timestamp information, as well as the consistent correction of that information. To do that, the GPS clock needs its antenna to have sufficient reception. In the laboratory scheme that was utilized in this demonstration, some non-typical methods had to be employed to acquire a sufficient signal with consistency. Second, the communication link between the PMU and the computer interface took some deeper understanding. The communication ports have limits to which they can transmit information, and that impacted the amount of data that could be transmitted in each message. It also dictated the rate at which the messages could be transmitted.

In the simulation investigation, it was discovered that the correct equipment would be required to allow such a system to be created and used for demonstration. The dSPACE system is incapable of this operation in its current form. The standard method for creating a power system model in Simulink is incompatible with the dSP board, and the voltages of the dSPACE outputs are incompatible with the requirements of the PMU measurement inputs. The alternate model method shows promise for

bypassing the Simulink model issues, but the output of the dSPACE system would require some more electronics to support the measurement requirements for the PMUs. The PMUs perform quite well when a physical model is available, and future projects to create a laboratory power system would be more suitable for this application.

Improvements to State Estimation and Visualization

In the conventional measurement schemes, state estimation is dependent on magnitude measurements, power metering, low resolution data, and physical estimates of grid facilities, such as transmission lines. The bulk electric power system is composed of 211,000 miles of transmission and over 10,000 power plants. It is not difficult to see that physical estimates of this expansive system can dramatically impact the accuracy of system monitoring. With synchrophasor measurement schemes, phase angle information is made available to the state estimator and resolution is improved. Physical estimates can be improved as well. Synchrophasor measurements can be used to correct and verify system parameters (transmission line impedances and transformer impedances).

In terms of visualization, the data could be used to monitor frequency response, total vector error, and interference. Frequency response can be directly linked to fault events, as demonstrated by the Fourier analysis. It can also be used to identify generation loss under some situations when the power flow information is not available. If the synchrophasor state estimator is available, TVE is another tool for correction and verification. However, many utilities do not have a state estimator available for the early stages of implementation. In this research, an alternative approach was used. In this alternative, the synchrophasor data was compared with

conventional measurements. In most cases, this information is strictly relational. If it corresponds to the conventional measurements, the synchrophasor measurements are accurate with the measurements being used. It may very well be even more accurate. From that stage, investment toward the appropriate state estimator may be more acceptable. Once it is in place, the technology can be calibrated toward the compliant level of 1% for sufficient error tolerance.

Lastly, interference can also been analyzed. Significant disturbances are easily observed with the use of high resolution data. These quick, detailed grid measurements could alleviate issues that have resulted from growing power system complexity.

Coordination between Industry and Academia

Measurements that represent the bulk power system are not readily available to the common researcher. That has encouraged many researchers to create representative systems within a laboratory setting. Representative systems are being built in many universities, but this requires some high level understanding of the representative system and its limitations compared to the full-scale power system. The alternative is to investigate measurements from the bulk electric power system, however, recovery of those measurements requires some high levels of access. The bulk power system is regulated by many compliance standards, and these compliance standards are developed to protect the reliability, security, and economic standing of the bulk power system. One specific part of compliance involves confidentiality of vital information.

In most cases, power system information is subject to non-disclosure agreements that are established between participating entities. This provides some security to the bulk power system and its customers, but it adds a layer of difficulty to

the research efforts that are needed for technological advancement. The individuals that have access to the information are extremely qualified in the tasks of advancing technology, but the regular tasks of operation, planning, and reliability force limitations on their resources and time. In the area of academics, researchers have the potential to aid in this task, but the regulated access creates a profound limitation.

To solve this problem, a form of representative data was created. To do this, some plot points were masked by an anonymous entity. Real measurements were assigned a random name and timestamp that were not associated with the point of measurement or measurement timeframe, respectively. In essence, some real plot points were provided, but the data was not attributed to a real location or time. This pseudonym and non-representative timestamp has little impact to the functional analytics being performed, but it opens the opportunity for outside entities to evaluate and report on the functionality of one data type versus the other (PMU data versus RTU data).

Conclusion and Future Work

Through the methods outlined, authentic power measurement data from the electric power system has been analyzed for different events. Although these different approaches to analysis are not profound, the characteristics are clearly observed, and the differences are not easily dismissed. Frequency response data has been observed, and the exercise has demonstrated some instances where synchrophasor technology displays the system governor response seconds before the conventional measurements. Depending on the frequency level that one references, it can be approximated up to 4

seconds (roughly two data samples, or 120 cycles). The primary reason for this comes from the lower resolution of conventional measurement using RTUs.

Error measurements are usually dependent on a full implementation of the synchrophasor equipment and a state estimator for the synchrophasor-based measurements. However, this can be an expensive and timely burden. If it is assumed that the conventional state estimator based on RTU measurements is a reasonable test case, a basis for comparison can be made by total vector error (TVE) calculations. In performing this analysis, it was found that the ATVE was within reasonable range of the industry standard. In the past, the standard was 5% (IEEE C37.118 2005), but it was recently made 1% (IEEE C37.118.1a-2014) [3]. The analysis did not satisfy that limit, but the method was simply meant for validation.

Additionally, interference identification is more feasible with some high resolution data as well. In the analysis of events that are a product of atmospheric changes, it was shown that synchrophasor data presents information that is lost in conventional measurements.

In this thesis, there were many contributions toward the identification of synchrophasor technology benefits. Synchrophasor technology and the measurements it produces were compared with conventional technology and its corresponding measurements. Some beneficial processes and data analyses were proposed, and all were performed on authentic power system data. Then, some equipment was made available for configuration and manipulation through some donations to the university. That allowed this research to provide some deeper insight on the process that's involved in implementing synchrophasor technology in a power system. The idea of

performing a cost-benefit analysis has been considered, however, it would be impossible without more access to the utility information (energy costs, customer rates, equipment costs, etc…). As a result, this thesis was directed toward the identification of some applications for synchrophasor measurements that could provide some helpful information and guidance that conventional measurements fail to produce. These applications don't require all of the effort required for full integration (as shown by this analysis), but it provides some information for power system operation. These aspects describe the contributions of this thesis.

In some future work, it seems that later researchers could investigate some new methods of working with the equipment at the university. Some more elaborate test beds could be developed, as mentioned in Chapter III. Also, some more extensive research agreements could be proposed to utility partners. There are some aspects that can be investigated without non-disclosure agreements, as it was done in this thesis. However, greater access could allow the researcher to do more detailed benefit analysis and state estimation development. For that level of work, non-disclosure agreements would probably be necessary.

REFERENCES

[1] ABB Group, *Wide Area Monitoring Systems: Portfolio, applications and experience*, http://www05.abb.com/global/scot/scot221.nsf/veritydisplay/3d85757b8c7f3bb6c125784d0056a586/$file/1KHL501042%20PSGuard%20WAMS%20Overview%202012-04.pdf.

[2] A. Abur and A. G. Expósito, *Power System State Estimation: Theory and Implementation*, *Marcel Dekker, Inc., New York, 2004*.

[3] A. Goldstein, National Institute of Standards and Technology, *Time Synchronization in Electrical Power Transmission and Distribution Systems*, http://www.atis.org/WSTS/papers/1-3_NIST_Goldstein_Time%20Sync%20in%20Electrical%20Power.pdf.

[4] A. Massoud, University of Strathclyde, *Flexible AC Transmission System*, http://people.qatar.tamu.edu/shehab.ahmed/ecen_459/FACTS.pdf.

[5] A. Rajapakse, University of Manitoba, *Wide Area Monitoring, Control and Protection Applications Using Synchrophasors*, IEEE Canada, Electrical Power and Energy Conference, October 2011.

[6] B.J. Kirby, Oak Ridge National Laboratory, Frequency Control Concerns in the North American Electric Power System, US Department of Energy, December 2002.

[7] H. A. Hadidi, B. Archer, and T. Weekes, Manitoba Hydro, *Manitoba Hydro's Experience with Synchrophasor Implementation*, IEEE Canada, Electrical Power and Energy Conference, October 2011.

[8] K. Narendra, ERLPhase Power Technologies Ltd., *Wide Area Monitoring Systems (WAMS) using Phasor Measurement Units (PMU)*, IEEE Canada, Electrical Power and Energy Conference, October 2011.

[9] R. Moxley, G. Zweigle, and B. Flerchinger, Schweitzer Engineering Laboratories, Inc., *Turning Synchrophasor Data Into Actionable Information*, https://www.selinc.com/literature/TechnicalPapers/ > [Search Article Title].

[10] Schweitzer Engineering Laboratories, Inc., *Synchrophasors and their Applications*, SEL_Synchrophasors[1].pdf > [Email Response from David Bisel from Schweitzer].

[11] State Load Dispatch Centre, *Remote Terminal Unit (RTU) Specifications*, http://www.sldcguj.com/compdoc/RTU_specifications.pdf.

[12] University of Tennessee, Knoxville, *Synchrophasor*, http://web.eecs.utk.edu/~kaisun/ECE421/Group1_Projectv1.3.pdf.
*** Other References (Picture Only):

[13] Wikipedia, *IEC 60870-5*, http://en.wikipedia.org/wiki/IEC_60870-5.